PLASMA MEMBRANE LIPID THERAPY:

DISRUPTION OF ONCOGENIC RAS DRIVEN PHENOTYPES BY MEMBRANE TARGETED DIETARY BIOACTIVES (MTDBS)

A Dissertation

by

NATIVIDAD ROBERTO FUENTES

Submitted to the Office of Graduate and Professional Studies of
Texas A&M University
in partial fulfillment of the requirements for the degree of

DOCTOR OF PHILOSOPHY

Chair of Committee,	Robert S. Chapkin
Committee Members,	Robert Burghardt
	Gonzalo Rivera
	Yanan Tian
Intercollegiate Faculty Chair,	Ivan Rusyn

December 2017

Major Subject: Toxicology

ABSTRACT

Approximately 30-50% of colorectal cancers contain KRas mutations, which confer resistance to standard therapy. A diet high in long-chain n-3 polyunsaturated fatty acids (n-3 PUFA) is generally considered chemoprotective in regard to colon cancer. However, the molecular mechanisms by which n-3 PUFA suppresses tumorigenesis remain to be determined. Therefore, our overall goal is to define the role of n-3 PUFA in the modulation of oncogenic KRas-driven colon cancer.

We hypothesized that n-3 PUFA would modify the biophysical properties of the plasma membrane though its incorporation into plasma membrane phospholipids. Utilizing quantitative fluorescence microscopy, we determined that n-3 PUFA reduce the rigidity of the plasma membrane of young adult mouse colonocytes (YAMC), CD3/CD28 activated $CD4^+$ T cells, and colonic crypts derived from transgenic *Fat-1* mice, which synthesize n-3 PUFA *de novo*. Interestingly, n-3 PUFA increased the rigidity of cytoskeletal free giant plasma membrane vesicles (GPMVs), derived from the aforementioned samples.

Oncogenic Ras signaling is dependent on the formation of specific plasma membrane localized proteolipid complexes. Thus, it is noteworthy in YAMC cells and *Drosophila* midguts we documented for the first time that n-3 PUFA generates mix clusters of H- and K-Ras isoforms, which signal through ERK less efficiently. This resulted in a reduction of Ras driven colonic phenotypes in mice and *Drosophila* models.

We then assessed the ability of n-3 PUFA to disrupt macropinocytosis, a cellular process in which extra cellular proteins are internalized through dynamic changes in plasma membrane lipids and cytoskeletal proteins. This process provides energy substrates that support the unique metabolic needs of Ras expressing cells. We determined that Ras expression mediates an increase in plasma membrane free cholesterol, which rigidifies the plasma membrane. Attenuating this rigidification by incorporating n-3 PUFA into the plasma membrane disrupted Ras driven macropinocytosis.

Overall, we have demonstrated that n-3 PUFA ameliorate oncogenic Ras driven phenotypes through modification of plasma membrane biophysical properties leading to a disruption of Ras signaling. This reduces the ability of tumor cells to acquire energy substrate necessary to maintain its unique metabolic needs. These data contribute to the mechanistic understanding of how n-3 PUFA protect against colon cancer.

DEDICATION

To my parents Rosa & Jesse Hernandez, and Robert & Rose Fuentes.

ACKNOWLEDGEMENTS

I would like to start by thanking my mentor, Robert Chapkin. He has been an inexhaustible source of knowledge, encouragement, and support. I will always be grateful for his guidance. I would likewise like to thank my committee members: Robert Burghardt, Gonzalo Rivera, and Yanan Tian. Their insight and direction was indispensable in developing this body of work.

Additionally, I could not have completed by PhD studies without Dr. Rola Barhoumi, who was instrumental in teaching me firsthand the skills necessary for acquiring quantitative microscopy images.

I am also thankful for the aid of all of the members of the Chapkin lab. They were always willing to provide a helping hand when it was most needed.

I would also like to thank my wife, Megan Fuentes. I can never thank her enough for her love and understanding throughout this process. Her assistance both in the lab and at home was integral in my success.

Lastly, I appreciate the love and support of my family. My parents have always inspired and encouraged me. I know that none of this would have been possible without them.

CONTRIBUTORS AND FUNDING SOURCES

Contributors

This work was supervised by a dissertation committee consisting of Dr. Robert S. Chapkin of the Department of Nutrition and Food Science and Dr. Robert Burghardt of the Department of Veterinary Integrative Biosciences and Dr. Gonzalo Rivera of the Department of Veterinary Pathobiology and Dr. Yanan Tian of the Department of Veterinary Physiology & Pharmacology.

The data analyses involving *Drosophila* depicted in Chapter 2 was conducted in part by Dr. Mohamed Mlih of the Department of Molecular and Cellular Medicine.

All other work conducted for the dissertation was completed by the student independently.

Funding Sources

Graduate study was supported by a fellowship from Texas A&M University System Louis Stokes Alliance for Minority Participation (TAMUS-LSAMP) Bridge-to-the Doctorate (BTD) and a pre-doctoral research fellowship from the Pharmaceutical Research and Manufacturers of America (PhRMA) Foundation.

This work was made possible in part by the National Institutes of Health (NIH) under Grant Number R35CA197707. Its contents are solely the responsibility of the authors and do not necessarily represent the official views of the National Institutes of Health (NIH).

TABLE OF CONTENTS

Page

ABSTRACT ii

DEDICATION iv

ACKNOWLEDGEMENTS v

CONTRIBUTORS AND FUNDING SOURCES vi

TABLE OF CONTENTS vii

LIST OF FIGURES ix

LIST OF TABLES xi

CHAPTER I INTRODUCTION AND LITERATURE REVIEW 1

1.1 Risk for Colorectal Cancer (CRC) 1
1.2 n-3 PUFA and CRC 1
1.3 Cellular lipid classes 3
1.4 Composition of cellular membranes 5
1.5 Structural and cellular function of membrane cholesterol 5
1.6 Plasma membrane nanoclusters and fluidity 6
1.7 Impact of dietary fatty acids on plasma membrane composition and structure 9
1.8 A novel role for MTDB's in modulating oncogenic KRas 12
1.9 Ras-dependent macropinocytosis 14
1.10 Clinical impact of n-3 PUFA 15
1.11 Summary of research goals 16

CHAPTER II LONG CHAIN N-3 FATTY ACIDS MODIFY PLASMA MEMBRANE BIOPHYSCIAL PROPERTIES 18

2.1 Introduction 18
2.2 Results 19
2.3 Discussion 28
2.4 Materials and methods 31

CHAPTER III LONG CHAIN N-3 FATTY ACIDS ATTENUATE ONCOGENIC RAS DRIVEN PROLIFERATION BY ALTERING PLASMA MEMBRANE PROTEIN NANOCLUSTERING....35

3.1 Introduction....35
3.2 Results....37
3.3 Discussion....50
3.4 Materials and methods....58

CHAPTER IV LONG CHAIN N-3 FATTY ACIDS DISRUPT COLINIC CELL MACROPOINOCYTOSIS....65

4.1 Introduction....65
4.2 Results....66
4.3 Discussion....75
4.4 Materials and methods....77

CHAPTER V SUMMARY AND CONCLUSIONS....80

5.1 Summary....80
5.2 Future directions....82
5.3 Conclusion....87

REFERENCES....88

LIST OF FIGURES

FIGURE		Page
1.1	Synthesis of cellular lipids	4
1.2	Pathway involved with enrichment of dietary n-3 PUFA into cellular plasma membranes	11
2.1	Determining membrane organization using Di-4-ANEPPDHQ	20
2.2	Long chain n-3 PUFA reduces plasma membrane rigidity in live cells	21
2.3	Plasma membrane rigidity of isolated crypts determined by FLIM	22
2.4	Isolated GPMVs are devoid of filamentous actin	22
2.5	Long chain n-3 PUFA increase GPMV rigidity	23
2.6	Exogenous fatty acids dose-dependently alter human CD4+ T cell membrane order and GPMV phase separation	26
3.1	Dietary n-3 PUFA ameliorates oncogenic KRasG12D mediated colonic phenotypes	38
3.2	Long chain n-3 PUFA disrupts Ras spatiotemporal dynamics	42
3.3	Long chain n-3 PUFA attenuated Ras mediated ERK signaling	44
3.4	Dietary n-3 PUFA disrupts Ras spatiotemporal dynamics, suppresses oncogenic Ras driven hyperproliferation phenotype and signaling in *Drosophila* midguts	46
3.5	Dietary corn oil does not disrupt Ras spatiotemporal dynamics in *Drosophila* midguts	50
3.6	Summary diagram highlighting n-3 PUFA suppression of oncogenic Ras mediated hyperproliferation and signaling through disruption of Ras spatiotemporal dynamics	53
3.7	Quantitative image based analysis of pERK	64
4.1	Macropinocytosis is attenuated by n-3 PUFA	67

4.2 Long chain n-3 PUFA attenuation of macropinocytosis is independent of EGF-mediated Ras activation status 68

4.3 Methyl-β-cyclodextrins depletes cholesterol, reduces membrane order and attenuates macropinocytosis in YAMC cells..... 69

4.4 Oncogenic KRasG12D expressing SW48 cells exhibit increased macropinocytosis 70

4.5 Oncogenic KRasG12D expressing SW48 cells exhibit increased membrane order 71

4.6 Oncogenic KRasG12D expressing SW48 cells exhibit increased cholesterol 72

4.7 Dietary fish oil ameliorates oncogenic KRas mediated macropinocytosis in isolated colonic crypts 73

4.8 Dietary fish oil ameliorates oncogenic KRas mediated membrane order in isolated colonic crypts..... 73

4.9 Dietary fish oil ameliorates oncogenic KRas mediated increase of free cholesterol in isolated colonic crypts 74

4.10 Dietary fish oil ameliorates oncogenic KRas mediated increase in membrane order and cholesterol in single cells from isolated colonic crypts..... 75

5.1 Putative model for the effect of DHA on membrane order 83

5.2 Putative mechanism by which bioactive dietary molecules interact with the plasma membrane 86

LIST OF TABLES

TABLE		Page
2.1	Incorporation of exogenous fatty acids into activated CD4+ T cell membrane phospholipids	24
2.2	Incorporation of exogenous fatty acids into activated CD4+ T cell neutral lipids	25
3.1	Mouse diet composition	39
3.2	Mouse diet fatty acid composition	40
3.3	Incorporation of exogenous fatty acids into murine colonic crypt membrane phospholipids	40
3.4	*Drosophila* diet fatty acid composition	47
3.5	Incorporation of exogenous fatty acids into *Drosophila* gut membrane phospholipids	48
3.6	Incorporation of exogenous fatty acids from corn oil into *Drosophila* gut membrane phospholipids	49

CHAPTER I

INTRODUCTION AND LITERATURE REVIEW

1.1 Risk for Colorectal Cancer (CRC)

CRC is the third most common type of cancer in the U.S. and is estimated to account for roughly 9% of new cancer cases and 9% of cancer deaths in 2017 (Siegel et al., 2017). Overall, CRC incidence and mortality rates have decreased in the past 20 years, attributed largely to use of CRC screening and polypectomy in adults over 50 years. However, among adults younger than 50 years, for whom screening is not recommended if at average risk, CRC incidence rates have been increasing by ~2% per year since 1994 in both men and women (American Cancer Society, 2015). While genetic factors account for some of the CRC risk, environmental factors, such as diet, obesity, tobacco use, or environmental pollutants, account for the majority of risk (Coussens et al., 2013).

1.2 n-3 PUFA and CRC

CRC risk could be greatly reduced through dietary modification, including increased dietary fiber intake and reduced fat intake (Vargas and Thompson, 2012). The long-chain PUFA, eicosapentaenoic acid (EPA) and docosahexaenoic acid (DHA) are found in fish oils (Strobel et al., 2012). In general, n-6 PUFA are considered pro-inflammatory whereas n-3 PUFA are considered anti-inflammatory (Chapkin et al., 2009; Spite et al., 2014). Given the strong association between inflammation and CRC

(Elinav et al., 2013), higher intakes of n-3 PUFA provide biological plausibility for a chemoprotective effect (Chapkin et al., 2007; Cockbain et al., 2012). Research using preclinical models consistently show reduced CRC risk with n-3 PUFA (Chang et al., 1997; Chapkin et al., 2008a; Piazzi et al., 2014; Reddy et al., 1991, 2005); however, epidemiologic data are inconsistent and the majority of studies did not include PUFA intake from supplemental fish oil (Beresford et al., 2006; Gerber, 2012; Henderson, 1992; Prentice and Sheppard, 1990; Watson and Collins, 2011). Two meta-analyses have concluded that fish intake is associated with decreased risk of CRC (Pot et al., 2009; Wu et al., 2012); however, two systematic reviews of n-3 PUFA on cancer risk qualitatively concluded that there is inadequate (MacLean et al., 2006) or limited (Gerber, 2012) evidence to suggest an association between long-chain n-3 PUFA intake and CRC risk. In contrast to the epidemiologic literature, in an endoscopy-based case-control study on colorectal adenomas, serum n-3 PUFA were inversely associated with colorectal adenoma risk (0.67; 95% CI: 0.46, 0.96) (Pot et al., 2008). Recently, in the VITamins And Lifestyle (VITAL) cohort, it was noted that persons using fish oil supplements on 4+ days/wk for 3+yr experienced 49% lower CRC risk than nonusers (hazard ratio = 0.51, 95% CI = 0.26–1.00; P trend = 0.06) (Kantor et al., 2014). Interestingly, the same study showed no association of dark fish and total EPA + DHA intake with CRC risk overall (Kantor et al., 2014).

With respect to clinical studies, mounting evidence suggests that the consumption of fish oil may reduce colon cancer risk in humans (Anti et al., 1992, 1994; Bartram et al., 1993; Caygill et al., 1996; Cheng et al., 2003; Courtney et al., 2007; Hall

et al., 2008). EPA and DHA appear to be ideally suited to work either alone or in combination with chemoprotective drugs (Vaughan et al., 2013), e.g., NSAIDs, whose long-term use is contraindicated (Baron et al., 2008; Graham, 2006). Recently, it was demonstrated that EPA reduced rectal polyp number and size in patients with familial adenomatous polyposis (FAP) (Cockbain et al., 2012; West et al., 2010). Most impressive was the fact that fish oil derived n-3 PUFA suppressed FAP to a degree similar to the selective COX-2 inhibitor celecoxib. Ongoing clinical trials (Clinical Trials.gov) are currently examining the effects of EPA on subjects at high risk of CRC (NCT02069561); the combinatory role of EPA and DHA in reducing rectal cancer risk (NCT02534389), and the combinatory role of EPA and NSAIDs on polyp recurrence in the colon (NCT01070355; ISRCTN05926847) (Cockbain et al., 2014; Hull et al., 2013). Collectively, these data indicate that n-3 PUFA hold promise as chemoprevention agents.

1.3 Cellular lipid classes

Lipids can be divided into the following classes: (1) fatty acids (FAs) that mainly serve as intermediates in lipid biosynthesis; (2) free sterols, e.g., cholesterol, that serve as structural components in membranes; (3) sterol esters that are formed from FAs and sterols and serve as lipid storage compounds, mainly as lipid bodies; (4) triacylglycerols (TAG) that are formed from glycerol and FAs that serve as lipid storage, mainly in lipid bodies; (5) phospholipids/phosphoglycerides (PLs) that are formed from FAs, glycerol and an alcohol moiety, e.g., inositol, choline or ethanolamine, that serve as structural

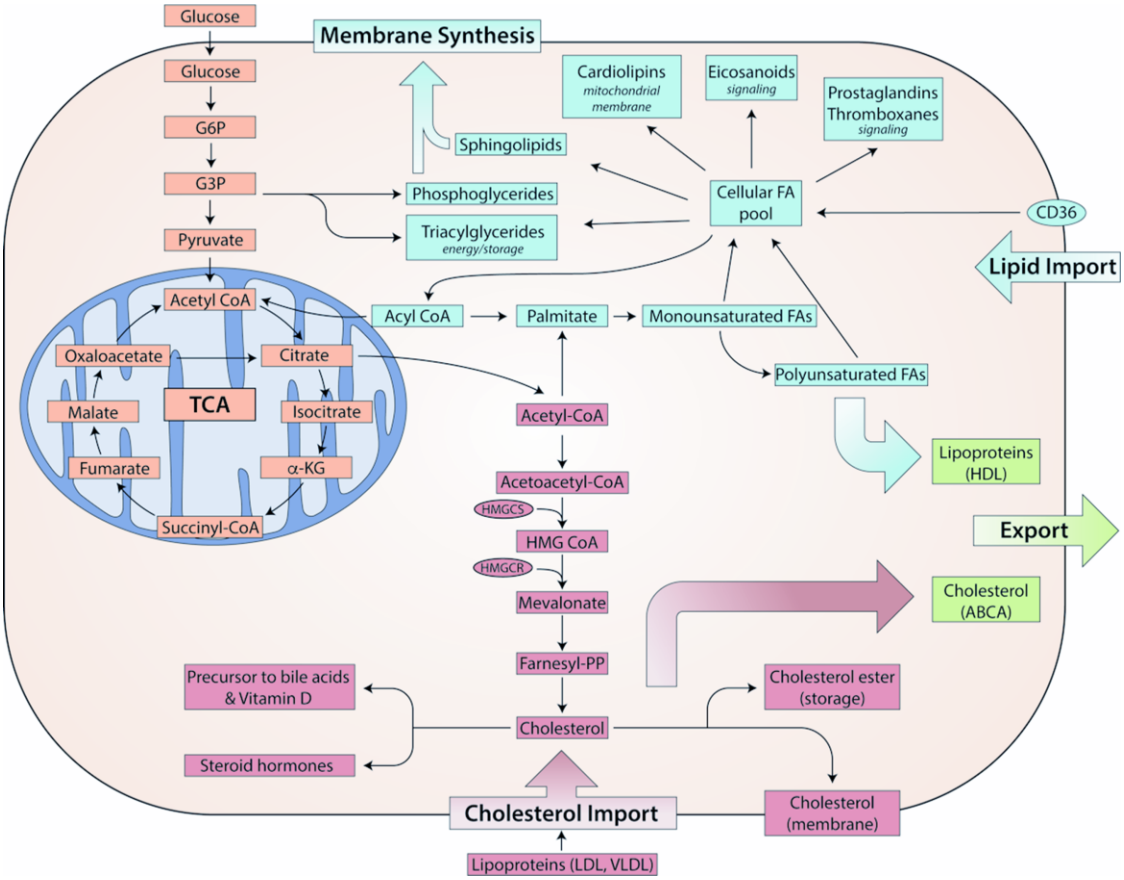

Figure 1.1. Synthesis of cellular lipids. Fatty acid building blocks are derived from exogenous and endogenous (de novo) sources.

components of membranes; and (6) sphingolipids that contain a sphingosine backbone and a very long chain FA. These phospholipids serve as structural components of cell membranes as well as play key signaling roles, e.g., regulation of endocytosis, ubiquitin dependent proteolysis and cell cycle control (Nielsen, 2009; Rohrig and Schulze, 2016). Despite the large chemical variety of lipids, they all have the same key carbon precursor, namely acetyl-CoA, and all initial steps of lipid/cholesterol biosynthesis occur in the cytosol (Rohrig and Schulze, 2016). As illustrated in **Figure 1.1**, lipid biosynthesis involves two branches from acetyl-CoA, one leading to sterols and the other leading to

FAs that serve as building blocks for biosynthesis of TAG, phospholipids, sterol esters and sphingolipids.

1.4 Composition of cellular membranes

Eukaryotic cells contain different types of membranes, including the plasma, endosomal, nuclear and mitochondrial membranes. The specific lipid composition of these membranes influences function, and since these membranes carry out vastly different functions, inherently their composition is extremely diverse (Spector and Yorek, 1985). Their heterogeneous composition is the result of *de novo* lipid synthesis (Kennedy pathway), exogenous substrate availability (Lands' cycle) and vesicular trafficking events (Spector and Yorek, 1985). Unlike proteins that are directly encoded in the genome, lipid composition is the result of an indirect influence of biosynthetic enzymes and exogenous substrate availability.

1.5 Structural and cellular function of membrane cholesterol

Cholesterol is an essential component of higher eukaryotic membranes and plays an important role in cell membrane organization, dynamics and function (Bloch, 1983). It is the end product of a sterol biosynthetic pathway involving more than 20 enzymes (Singh et al., 2013). According to the 'Bloch hypothesis', the sterol biosynthetic pathway parallels sterol evolution. In other words, the cholesterol biosynthetic pathway has evolved by the process of natural selection to optimize properties of eukaryotic cell membranes for specific biological functions (Hedlund et al., 2011). As an important

membrane component, cholesterol helps to generate a semi-permeable barrier between cellular compartments and to regulate membrane fluidity. Cholesterol favors the formation of highly packed and ordered rigid domains. A common term used for the ordered domains is “lipid-rafts” (Levental and Veatch, 2016; Sezgin et al., 2017). From a functional perspective, the cholesterol / phospholipid composition of cellular membranes is known to influence lipid raft formation and the ability of plasma membrane receptors / signaling proteins to function properly (Griffié et al., 2015; Hou et al., 2016; Phillips et al., 2009).

1.6 Plasma membrane nanoclusters and fluidity

The plasma membrane is composed of a heterogeneous mixture of lipids/cholesterol and proteins whose distinct organization maintains efficient signal transduction. Lipid rafts, enriched in sphingolipids, cholesterol and associated proteins, are special plasma membrane microdomains with an increased structural order, and are designated liquid ordered domains of plasma membranes (Sezgin et al., 2017). These lipid rafts are believed to be dynamic and small (5–200 nm) membrane microdomains, which play a critical role as sorting platforms for many membrane-associated proteins (Frisz et al., 2013; Hancock, 2006; Kraft, 2013; Levental and Veatch, 2016; Lingwood and Simons, 2010). Importantly, these domains are generally below the resolution of light microscopy (~200 nm). However, using techniques like fluorescence lifetime imaging microscopy combined with fluorescence resonance energy transfer (FLIM-FRET) or photo-activated localization microscopy (PALM), it is now possible to

directly observe nanoscale dynamics of membrane lipids in living cells (Eggeling et al., 2009; Sahl et al., 2014). For example, the increased accessibility of super-resolution microscopy techniques has shed new light on the nanoscale organization of membrane proteins (Sezgin, 2017; Wang et al., 2014).

According to the emerging membrane biology picture, protein and lipid nanoclusters can be organized to form domains that are capable of facilitating signaling events (Ariotti et al., 2014; Garcia-Parajo et al., 2014; Zhou and Hancock, 2015). The formation of these nanoclusters is believed to be driven by cortical actin and/or proximal transmembrane proteins (Garcia-Parajo et al., 2014). Currently, protein-protein, lipid-lipid and protein-lipid nanoclusters are considered a predominant feature of the plasma membrane and appear to mediate critical signaling processes (Ariotti et al., 2014), including signal integration and cross talk of the transduction of oncogenic Ras and the epidermal growth factor receptor (EGFR) (Ariotti et al., 2014; Janosi et al., 2012; Zhou et al., 2012) regulated pathways. This is noteworthy, because there is emerging evidence that drugs and select membrane active dietary components, which we term membrane targeted dietary bioactives (MTDBs), e.g., n-3 PUFA, can attenuate Ras and EGFR (Ariotti et al., 2014; Chapkin et al., 2008b; Nussinov et al., 2014) activity by modulating nanocluster organization. It also has been suggested that disrupting clustering/dimerization of membrane associated proteins can lead to attenuation of downstream oncogenic signaling and the suppression of tumor growth (Fuentes et al., 2017).

Approximately 90% of cellular cholesterol resides in the plasma membrane (Kim et al., 1991; Lange et al., 1989; Ueland et al., 1986), and increases in cholesterol promote plasma membrane order (Montero et al., 2008). This is significant, because highly ordered/rigid lipid rafts are increased in many types of cancer (Li et al., 2006; Patra, 2008) and some multidrug-resistant cancers (Yang et al., 2009; Yi et al., 2013). The term 'rigidity' refers to the packing of the lipids in the membrane, and cholesterol favors the production of more tightly pack "rigid" domains. This increased rigidity associated with increased lipid rafts typically facilitates efficient cellular signaling. Interestingly, multidrug-resistant cells have remodelled their membranes to be in a state that is more rigid and thus receptive to activation (Li et al., 2015; Raghavan et al., 2015). This increase in rigidity, may explain why lung cancer cells have more clustered and highly activated epidermal growth factor receptor (EGFR), compared to normal lung epithelium (Wang et al., 2014).

There is evidence suggesting that disruption of lipid rafts in cancer can lead to increased responsiveness to anti-cancer therapies (Fedida-Metula et al., 2012; Irwin et al., 2011). Additionally, some anti-cancer drugs have beneficial effects through alteration of the protein content of lipid rafts (George and Wu, 2012; Hryniewicz-Jankowska et al., 2014). In colon cancer, lipid rafts have been shown to function in cell death (apoptosis)-mediated signaling (Lacour et al., 2004; Rebillard et al., 2007), cell entry/bioavailability of bioactive compounds (Adachi et al., 2007) and localization of key proteins involved in immune response (Bene et al., 2004). These findings indicate that lipids can no longer be ignored in the structures of membrane complexes, due to

their ability to fine-tune and stabilize different signaling interfaces (Barrera et al., 2013; Levental et al., 2016; Lin et al., 2016). For several viruses linked to cancer risk, a dependence on cholesterol for virus entry and/or morphogenesis has also been shown. Cholesterol depletion of virus-infected cells affects integrity of the virus envelope, causes disruption of the viral envelope and adversely affects virus infectivity (Barman and Nayak, 2007; Imhoff et al., 2007). For this reason, there is considerable interest in identifying alternative strategies for lowering cholesterol, micronutrient supplementation and pharmaceutical development.

1.7 Impact of dietary fatty acids on plasma membrane composition and structure

Diet can play an impactful role in modifying the plasma membrane. The idea that dietary lipids can influence membrane structure is intuitive, since the plasma membrane itself is composed of phospholipids. Phospholipids are amphiphilic molecules composed of two hydrophobic fatty acid tails and a hydrophilic head. In general, dietary lipids are transported as circulating lipoproteins containing triglycerides and phospholipids. Cells subsequently take up circulating lipids and use them for energy or the synthesis and remodeling of membranes. Animal and plant fats and oils are composed of fatty acids of different chain lengths (14-24 carbons), which contain different amounts of unsaturation (1-6 double bonds). Not only the chain length and amount of unsaturation, but also the position of the double bonds in relation to the methyl end of the FA (n-9 vs n-6 vs n-3) impact its biophysical properties. Mammalian cells can endogenously produce most

fatty acids, however, they lack the desaturase enzymes necessary to produce n-6 or n-3 fatty acids de novo (Chapkin, 2007). Therefore, these lipids must be obtained via the diet and are considered essential. For example, linoleic acid (LA), an n-6 PUFA is highly enriched in a common staple of the western-diet, corn oil. In comparison, n-3 PUFA, e.g., alpha-linoleic acid (ALA), eicosapentaenoic acid (EPA, $20:5^{\Delta 5,8,11,14,17}$) and docosahexaenoic acid (DHA, $22:6^{\Delta 4,7,10,13,16,19}$), are less prevalent in the western-diet.

With respect to the molecular mechanism of n-3 PUFA action, there is a growing body of *in vitro* and *in vivo* evidence indicating that n-3 PUFA reshape plasma membrane domains. For example, EPA and DHA, whose membrane phospholipid levels are readily influenced by diet in general (Katan et al., 1997), are rapidly incorporated into cells, primarily into membrane phospholipids at the *sn*-2 position (**Figure 1.2**) (Chapkin et al., 1991; Hou et al., 2016; Williams et al., 2012). The presence of long chain n-3 PUFA in membrane phospholipids imparts unique biophysical properties which have been linked to alterations in plasma membrane structure and function (Levental et al., 2016; Ma et al., 2004b; Seo et al., 2006; Williams et al., 2012). For example, DHA is known to influence membrane fluidity, ion permeability, fatty acid exchange, and resident protein function (Hou et al., 2015, 2016; Stillwell and Wassall, 2003), including the inhibition of epidermal growth factor receptor (EGFR) signaling in

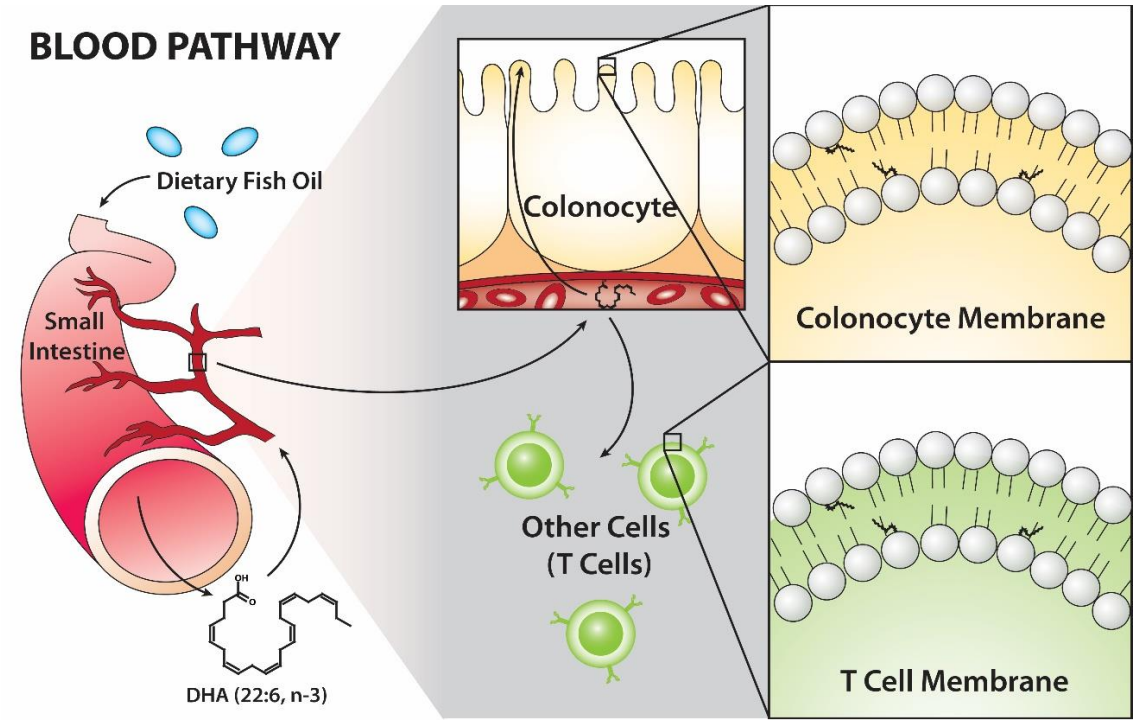

Figure 1.2. Pathway involved with enrichment of dietary n-3 PUFA into cellular plasma membranes. Polyunsaturated fatty acids are delivered to colonocytes and other cells types, such as T-cells, through the bloodstream after digestion and absorption from the small intestine into the portal vein. Once in the cell the n-3 PUFA are esterified to phospholipids. Abbreviation: DHA, docosahexaenoic acid reprinted from (Hou et al., 2016).

tumor bearing mice by disassociating EGFR from lipid rafts (Turk et al., 2012). Interestingly, n-3 PUFA are also known to modulate differences in membrane rigidity between raft and non-raft domains (Levental et al., 2016; Lin et al., 2016), likely driven by repulsive forces between n-3 PUFA and cholesterol (Wang et al., 2017). From a systemic perspective, membrane order is also increased in T cell plasma membranes from fish oil fed mice or transgenic mice that produce n-3 PUFA (Kim et al., 2008, 2014). Similarly, B cells isolated from mice fed n-3 PUFA-enriched diet exhibit an increase in membrane order in cross-linked cells relative to non-cross-linked (Rockett et

al., 2012). This is in contrast to the decrease in membrane order reported in Jurkat cells treated with EPA and DHA (Kim et al., 2010; Zech et al., 2009). A possible explanation for the differences reported in these studies is that malignant transformed Jurkat cell lines may be inherently distinct from primary T-cells with respect to specific plasma membrane properties. Precisely how these diet modulated changes in cell membrane order influence cell function remains to be determined.

Diet can also impact plasma membrane structure in a less intuitive manner. Specifically, many foods contain amphiphilic molecules that can directly interact with the plasma membrane (Fuentes et al., 2017). For example, turmeric (*Curcuma longa Linn*) extracts, including curcumin (diferuloylmethane), a yellow color pigment of turmeric, inserts deep into the membrane in a trans-bilayer orientation, anchored by hydrogen bonding to the phosphate group of lipids in a manner analogous to cholesterol (Hung et al., 2008; Ingolfsson et al., 2007). The combinatorial membrane interactions of n-3 PUFA and curcumin may explain the beneficial synergism observed in various studies (Altenburg et al., 2011; Kim et al., 2016; Saw et al., 2010; Siddiqui et al., 2013).

1.8 A novel role for MTDB's in modulating oncogenic KRas

Ras proteins are GTPases, which are targeted to the membrane by farnesylation coupled to either palmitoylation, N, H and K(A), or a polybasic motif, K(B) (Eisenberg et al., 2013). Approximately 30-50% of colorectal cancers contain KRas mutations, which confer resistance to standard therapy (Stephen et al., 2014), thereby reducing survival (Phipps et al., 2013). Unfortunately, attempts to directly target Ras have

repeatedly failed (Phipps et al., 2013). Ras proteins are important mediators of cell signaling. There are a large number of Ras effector proteins, notably Raf (MAP kinase pathway), PI3K (Akt/mTOR pathway), and RalGDS (Ral pathway). These effectors are highly complex with numerous redundancies and interactions between pathways (Downward, 2003). Dysregulated (oncogenic) Ras signaling results in increased proliferation, decreased apoptosis, disrupted cellular metabolism and increased angiogenesis, all seminal hallmarks of cancer (Downward, 2003; Vasan et al., 2014). Since no curative treatments for KRas driven colon cancer are available, there is a critical need to develop toxicologically innocuous KRas therapeutic approaches that are free of safety problems intrinsic to drugs administered over long periods of time. High efficiency signaling of KRas is dependent on its spatial organization into defined nanoclusters in inner leaflet of the plasma membrane (Tian et al., 2007). Recently, it was demonstrated that select amphiphilic agents, through direct modulation of the biophysical properties of the plasma membrane, compromise oncogenic KRas nanoclustering to modulate signal transduction (Zhou and Hancock, 2015; Zhou et al., 2012). These findings suggest that Ras nanoclusters could be a novel new therapeutic target (Cho and Hancock, 2013). This is consistent with a growing body of evidence indicating that n-3 PUFA suppress oncogenic Ras signaling (Collett et al., 2001; Ma et al., 2004b; Rogers et al., 2010; Seo et al., 2006; Turk et al., 2012).

1.9 Ras-dependent macropinocytosis

Macropinocytosis is the cellular process in which membrane ruffling leads to the engulfment of extracellular components driven by dynamic changes in plasma membrane lipids and cytoskeletal proteins (Bohdanowicz and Grinstein, 2013; Levin et al., 2015; Lim and Gleeson, 2011). Recently, macropinocytosis has been identified as a dependency of "undruggable" Ras driven cancers, and is being targeted as an alternate strategy for cancer therapy (Commisso et al., 2013; Salloum et al., 2014). Plasma membrane components such as cholesterol (Grimmer et al., 2002) are required for membrane ruffling. Furthermore, phosphoinositide signaling (Maekawa et al., 2014) linked to Rac1 activation (Fujii et al., 2013) underlies the action of membrane ruffling which is essential for macropinocytosis. The effects of cholesterol depletion on Rac1 activation vary (Grimmer et al., 2002; Iliev et al., 2007), however, macropinocytosis is consistently inhibited. This is likely a result of altering Rac1 membrane location (Grimmer et al., 2002) and lateral organization into specific membrane domains (Moissoglu et al., 2014). The ability of Rac1 to stabilize cytoskeletal mesh networks ultimately influences the organization of the plasma membrane (Navarro-Lérida et al., 2012). Similarly, cholesterol plays a crucial role in stabilizing membrane organization (Lingwood and Simons, 2010) and cytoskeletal connections (Kwik et al., 2003). However, precisely how the cytoskeleton and membrane interact to mediate macropinocytosis remains to be determined. Thus, we seek to determine how MTDB's that alter plasma membrane organization in a cytoskeletal-dependent process attenuate macropinocytosis.

1.10 Clinical impact of n-3 PUFA

There are more than 550 clinical trials registered in the ClinicalTrials.gov investigating the effect of fish oil on various chronic diseases, implying the potential clinical impact of n-3 PUFA in human health. For example, EPA (2 g/d for 3 mo) has been shown to reduce colonic crypt cell proliferation and increase apoptosis in normal colonic mucosa in subjects with a history of colorectal adenomas (Courtney et al., 2007). No tolerable upper limit has been set for EPA and DHA, although the US Food and Drug Administration recognizes doses of up to 3 g/day as safe and the European Safety Union up to 5 g/day as safe (Azzi et al., 2005). Side effects of fish oil supplements or EPA + DHA ethyl esters include fishy burps, dyspepsia, gas, and diarrhea (Browning et al., 2012; Yates et al., 2014). Importantly, human studies using doses as high as 17.6 g/day EPA+DHA have been performed with no serious side effects (Skarke et al., 2015). n-3 PUFA emulsion-based parenteral nutrition alleviates the inflammatory reactions and reduces the rate of inflammatory complications for patients recovering from surgical resection of gastric tumors (Wei et al., 2014). EPA is incorporated rapidly into colonic mucosa and the colonic muscular layer in patients given 3 g of n-3 PUFA daily for 7 days before surgery for colorectal cancer (Sorensen et al., 2014), which supports claims related to the clinical benefits of n-3 PUFA. Additional clinical studies are needed to assess the effect of EPA and/or DHA dose and duration on key molecular targets, e.g., cell plasma membranes, and related phenotypic outcomes.

1.11 Summary of research goals

Establishing a causal role for cancer dietary chemoprevention approaches that are generally free of safety problems intrinsic to drugs administered over long periods of time would have a major translational impact in cancer prevention and patient survivorship (Ford et al., 2009; Lien, 2009). In view of this need, our long-term goal is to better understand the molecular mechanisms modulating intestinal epithelial cell responses to MTDB's. Therefore, our overall goal is to define the role of n-3 PUFA in the suppression of oncogenic KRas-driven colon cancer. Initially, we focused on elucidating the mechanisms underlying the ability of MTDB's to modulate plasma membrane architecture. (Aim 1). Secondly, we elucidated the mechanisms underlying the ability of MTDB's to modulate Ras signaling through disruption of nanocluster complexes (Aim 2). Lastly, (Aim 3) we characterized the suppressive effects of n-3 PUFA on macropinocytosis, a recently identified oncogenic KRas driven dependency (Commisso et al., 2013), in the colon. This is both appropriate and timely, because the NCI has identified the "Ras Challenge" as a major initiative (Stephen et al., 2014). In terms of future application, since oncogenic KRas signaling is the primary driver in the progression of pancreatic ductal adenocarcinoma (PDAC) (Bryant et al., 2014), select MTDB's may also reduce cancer development and delay progression at multiple sites (Mohammed et al., 2012; Strouch et al., 2011).

We propose a mechanistic hypothesis to generally explain the function of n-3 PUFA bioactives. We propose that n-3 PUFA fall into a unique class of plasma membrane-targeted dietary bioactives (MTDB's) which, because of their unique

amphiphilic properties, are capable of modulating plasma membrane hierarchical organization. By characterizing the effects of MTDB's on plasma membrane protein/protein interactions, this dissertation addresses the utility of MTDB's as a novel class of innocuous dietary bioactives for membrane targeted colon cancer prevention and therapy.

CHAPTER II

LONG CHAIN n-3 FATTY ACIDS MODIFY PLASMA MEMBRANE BIOPHYSCIAL PROPERTIES

2.1 Introduction

Long chain docosahexaenoic acid (DHA, $22:6^{\Delta 4,7,10,13,16,19}$) and eicosapentaenoic acid (EPA, $20:5^{\Delta 5,8,11,14,17}$), found in cold water fish, are generally thought to be beneficial for human health. Dietary intake of these compounds results in physical incorporation of these fatty acids into cellular plasma membrane phospholipids. The plasma membrane (PM) is a dynamic cellular structure composed of a myriad of lipids and proteins (Barrera et al., 2013). These membrane components are exquisitely organized, through various forms of interactions (Garcia-Parajo et al., 2014; Nussinov et al., 2014). The nomenclature used to describe these interactions varies (Sevcsik and Schütz, 2015), however, what is known is that perturbations to this organization can lead to disruption of cellular events (Kim et al., 2008; Zhou et al., 2013). Long chain PUFAs impart unique biophysical properties to the phospholipids they form (Shaikh et al., 2004, 2009), which results in alterations to the spatiotemporal organization of the plasma membrane (Kim et al., 2008, 2014; Levental et al., 2016; Lin et al., 2016). In this study, we examined the mechanism and consequences of n-3 PUFA phospholipid incorporation on the biophysical properties of colonocyte plasma membranes. Using the membrane order sensitive probe Di-4-ANEPPDHQ, we demonstrate that in live cells, n-3 PUFA reduced the rigidity of the plasma membrane. However, in cytoskeletal-free isolated

giant plasma membrane vesicles (GPMVs), we observed an increase in the rigidity of the membrane. This suggests that n-3 PUFA indirectly alters plasma membrane-cytoskeletal interactions.

2.2 Results

2.2.1 Long chain n-3 PUFA reduce murine colonocyte membrane rigidity

To explore the effects of n-3 PUFA on plasma membrane rigidity, we utilized immortalized young adult mouse colonocyte (YAMC) cells (Whitehead and Robinson, 2009), since this model faithfully recapitulates n-3 PUFA *in vivo* effects (Ma et al., 2004b; Turk et al., 2012, 2013) and allows for lipidomic and proteomic studies under well-controlled conditions (Seo et al., 2006). Cells were treated with a physiologically relevant level (50 μM) (Conquer and Holub, 1998) of albumin-complexed n-3 PUFA (DHA, EPA) or control long-chain n-6 PUFA linoleic acid (LA) for 72 h. BSA-complexed fatty acids are used to represent the non-esterified fatty acids that are bound to albumin *in vivo*. We subsequently determined plasma membrane rigidity by fluorescence imaging of the membrane order sensitive probe Di-4-ANEPPDHQ (Di4) (Owen et al., 2012a). This probe has an advantage over another commonly used probe, laurdan, as it is minimally internalized in live cells (Sezgin et al., 2014). Di4 excites at 488 nm and shifts its emission spectrum from 565 nm to 605 nm in ordered and disordered membranes, respectively (Owen et al., 2012a; Sezgin et al., 2014). This shift in emission profile between the ordered and disordered domains allows for a quantitative assessment of membrane order by calculating a ratio of the fluorescent intensity in each

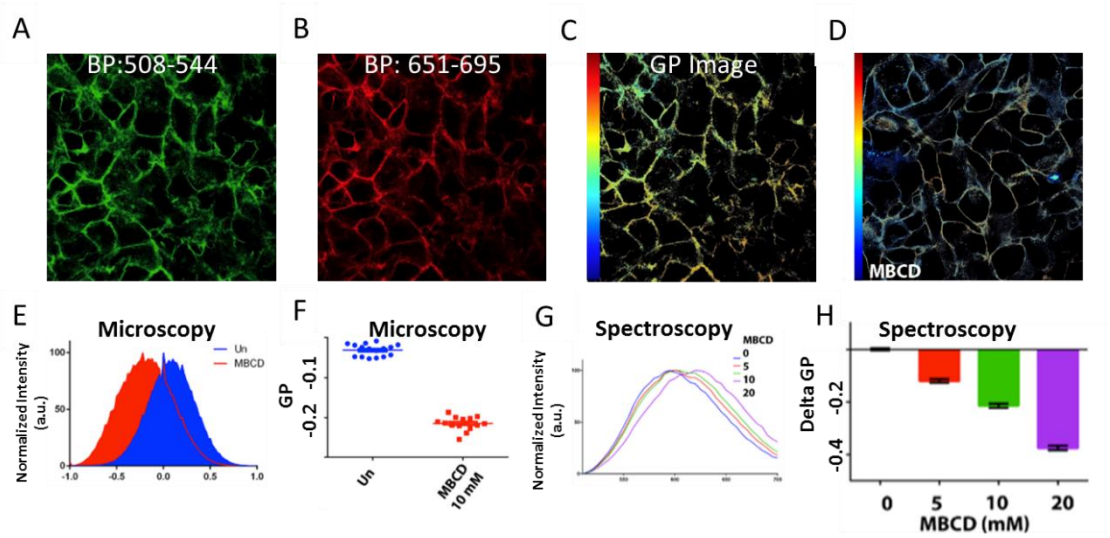

Figure 2.1. Determining membrane organization using Di-4-ANEPPDHQ. Membrane rigidity was determined by fluorescence microscopy or fluorescence spectroscopy. Methyl-β-cyclodextrins (MβCD) reduced membrane rigidity in a dose dependent manner. YAMC cells were incubated with Di-4-ANEPPDHQ (2.5 uM) and immediately imaged to prevent internalization. Dye was excited at 488 nm and emission was collected from (A) 508-544 nm and (B) 651-695. These two images were used to generate a (C) GP image as described in methods and materials. YAMC cells were treated with indicated doses of MBCD for 30 minutes. (E) Histogram and (F) mean GP values derived from (C) control or (D) MBCD (10 uM) treated YAMC cells. (G) Fluorescence spectrum and (H) mean GP from YAMC cells pre-incubated with indicated dose of MBCD for 30 min determined by fluorescence spectroscopy.

channel, known as a generalized polarization (GP) value (**Figure 2.1A-D)**. We validated our methodology by decreasing plasma membrane cholesterol levels with methyl-β-cyclodextrins (MβCD) (Zidovetzki and Levitan, 2007), which resulted in decreased GP values determined by microscopy (**Figure 2.1A-F**) and fluorescence spectroscopy (**Figure 2.1G & H**).

We also utilized the *fat-1* transgenic mouse model which produces n-3 PUFA endogenously through elongation of n-6 fatty acids (Hudert et al., 2006; Kang; Kang et al., 2004). We have previously shown that the mole% of EPA and DHA in the colonic

mucosa of *fat-1* mice is 2.13% and 2.28%, respectively, vs a control mouse with undetectable levels of EPA and 0.81% DHA (Jia et al., 2008). We sought to determine how this incorporation would affect the rigidity of the plasma membrane *in vivo*. Overall, the plasma membrane of isolated colonic crypts from *fat-1* mice was less rigid than control mice (**Figure 2.2A&B**). We further validated this observation by fluorescence lifetime imaging (FLIM) of Di4 (Owen et al., 2006), in which a lower lifetime value reflects a more fluid membrane (**Figure 2.3**). Exogenous supplementation of immortalized YAMC cells (Whitehead and Robinson, 2009) with a physiologically relevant (Conquer and Holub, 1998; Seo et al., 2006) dose of 50 µM bovine serum albumin (BSA) complexed fatty acids corroborated our *in vivo* findings (**Figure 2.2C&D**). The n-6 polyunsaturated fatty acid linoleic acid (LA) was used as an additional control for assessing the general effects of fatty acid polyunsaturation.

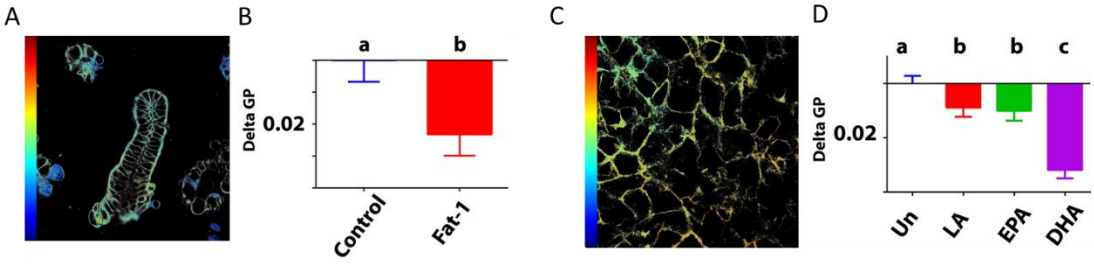

Figure 2.2. Long chain n-3 PUFA reduces plasma membrane rigidity in live cells. Isolated primary crypts or YAMC cells were incubated with 2.5 uM Di-4-ANEPPDHQ and imaged with a confocal microscope. Representative general polarization (GP) images of live (A) isolated primary crypts and (C) YAMC cells. Mean and SEM of (B) primary crypt, (D) YAMC cells. All values are expressed as delta GP (sample – control). Data represent mean +/- SEM for (B) ~30 crypts from 4 mice per genotype, and (D) at least 10 field of views containing at least 100 cells from 2 independent experiments. Statistical significance between treatments as indicated by different letters ($P<0.05$) was examined using one-way ANOVA and uncorrected Fisher's LSD tests.

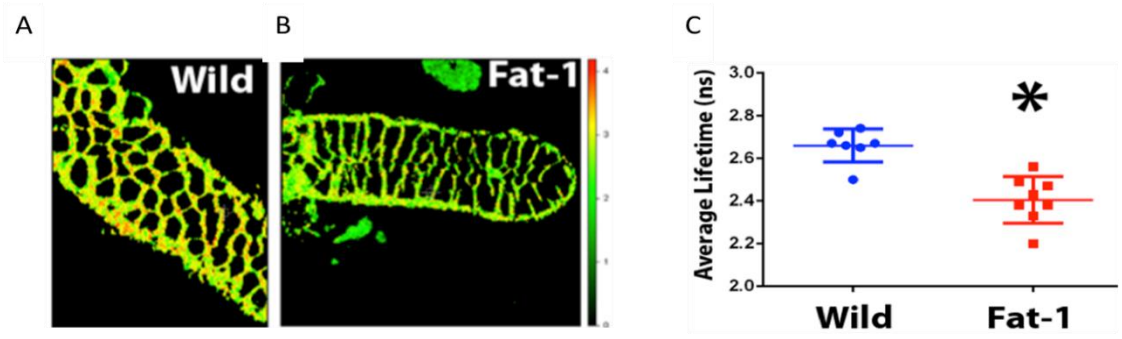

Figure 2.3. Plasma membrane rigidity of isolated crypts determined by FLIM. Isolated primary crypts, were incubated with 2.5 uM Di-4-ANEPPDHQ and average lifetime (ns) was determined by FLIM as described in the materials and methods. Representative lifetime images of live (A) wild type or (B) Fat-1 isolated primary crypts. (C) Mean ± SEM of primary crypt lifetime. Data represents mean ± SEM from Wild type=7 and Fat-1=8 crypts from 1 animal per genotype.

Since the actin cytoskeleton plays a role in stabilizing certain membrane domains (Delos Santos et al., 2015; Dinic et al., 2013; Plowman et al., 2005), we sought to determine the effect of n-3 PUFA in a cytoskeletal free model. For this purpose, we used giant plasma membrane vesicles (GPMVs) which maintain much of the lipid and protein

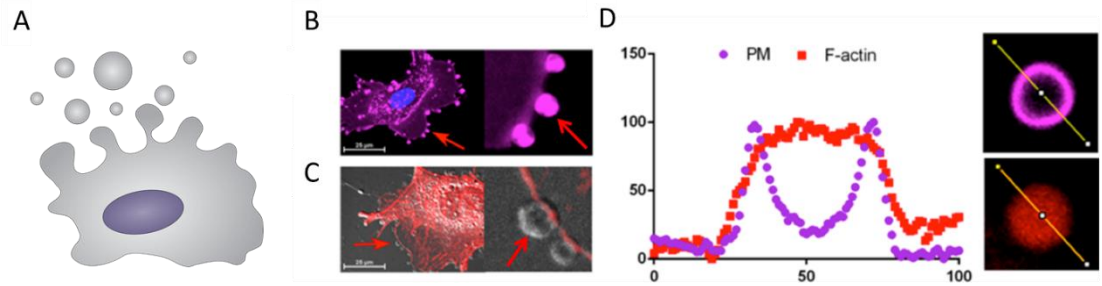

Figure 2.4. Isolated GPMVs are devoid of filamentous actin. GPMVs were generated from YAMC cells as described in the materials and methods. (A) Representative actively blebbing GPMVs from YAMC cells. (B) Membrane stained with deep red plasma membrane stain; (C) filamentous actin visualized by LifeAct-mCherry. (D) Line scans of normalized intensity profile of GPMVs derived from (A) plasma membrane (PM) or (B) f-actin.

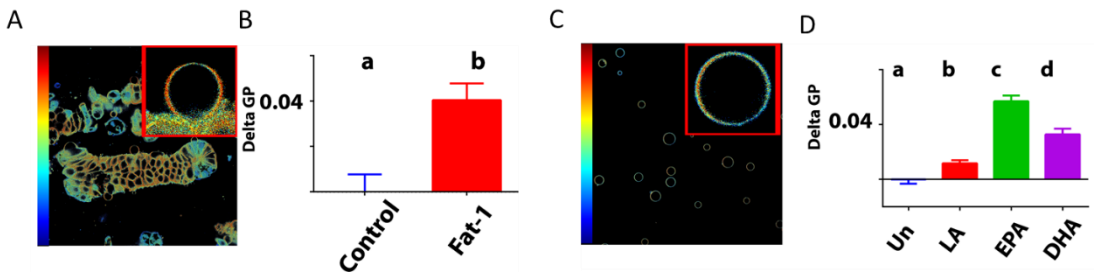

Figure 2.5. Long chain n-3 PUFA increase GPMV rigidity. GPMVs from isolated primary crypts and YAMC cells were incubated with 2.5 uM Di-4-ANEPPDHQ and imaged with a confocal microscope. Representative general polarization (GP) images of GPMVs from (A) isolated primary crypts, or (C) YAMC cells. Mean ± SEM of GPMVs derived from (B) crypts or (D) YAMC cells. All values are expressed as delta GP (sample – control). Data represent mean ± SEM for (B) ~150 GPMVs from 3 mice per genotype, and (D) at least 10 field of views containing at least 100 GPMVs from 2 independent experiments. Statistical significance between treatments as indicated by different letters ($P<0.05$) was examined using one-way ANOVA and uncorrected Fisher's LSD tests.

diversity and content of the cells from which they are derived (Sezgin et al., 2012). As expected, GPMVs derived from YAMC cells exhibited no structured filamentous actin (**Figure 2.4**).

Interestingly, long chain n-3 PUFA increased the rigidity of GPMVs *in vivo* and *in vitro* (**Figure 2.5**). The opposite effects on membrane rigidity in live cells vs. GPMVs indirectly implicate an effect of n-3 PUFA on the actin cytoskeleton. Interestingly, the effect of EPA on the rigidification of the GPMV membranes was larger than DHA, while LA had only a modest effect. Further work will be necessary to elucidate the precise mechanism underlying n-3 PUFA's ability to modulate cytoskeletal mediated plasma membrane rigidity.

2.4.1 Long chain n-33 PUFA reduce human T-cell membrane rigidity ex vivo

We next sought to determine if a different cell type would show similar effects to plasma membrane rigidity in comparison to colonocytes. For this we utilized $CD4^+$ T cells.

Following a 5 d incubation period, albumin bound linoleic acid (LA, C18:2n6), EPA and DHA were dose-dependently incorporated into human $CD4^+$ T cell membrane phospholipids, as shown in **Table 2.1**. Compared to the control untreated (UT) group, exogenous LA (n-6 PUFA control) significantly ($p < 0.05$) elevated membrane bound LA levels from 1.8 mole % to 8.1-22.7 mole%, while exogenous EPA and DHA

FA[1]	UT	L12.5	L25	L50	E12.5	E25	E50	D12.5	D25	D50
(mole%)										
14:0	5.4±0.2^{a}	5.3±0.1^{a}	4.5±0.3^{a}	4.0±0.3^{a}	5.4±0.2^{a}	5.1±0.3^{a}	5.3±0.4^{a}	5.7±0.1^{ab}	4.8±0.3^{a}	7.7±1.3^{b}
16:0	42.2±1.5^{a}	45.9±1.5^{b}	45.0±1.1^{b}	46.0±1.8^{b}	54.6±0.7^{cd}	53.6±1.3^{c}	53.6±1.9^{c}	56.3±1.2^{d}	55.2±2.0^{cd}	58.5±2.0^{e}
16:1n7	6.7±0.4^{b}	2.6±0.2^{a}	1.1±0.1^{a}	0.8±0.1^{a}	1.8±0.1^{a}	1.4±0.1^{a}	0.5±0.2^{a}	1.1±0.1^{a}	1.1±0.2^{a}	0.5±0.2^{a}
18:0	18.9±0.4^{c}	18.9±0.5^{c}	17.5±1.0^{c}	13.1±0.9^{a}	18.0±0.1^{c}	15.0±0.3^{b}	14.5±0.8^{ab}	18.3±0.6^{c}	15.0±0.3^{b}	11.7±1.5^{a}
18:1n9	15.6±0.3^{e}	10.9±0.6^{d}	6.3±0.5^{bc}	4.4±0.2^{a}	8.4±0.2^{cd}	7.4±0.1^{c}	5.4±0.5^{ab}	6.9±0.5^{bc}	6.8±0.6^{bc}	5.5±0.4^{ab}
18:1n7	5.5±0.4^{c}	3.9±0.2^{bc}	2.9±0.2^{b}	2.0±0.2^{ab}	2.6±0.1^{ab}	2.4±0.1^{ab}	1.8±0.3^{ab}	2.1±0.2^{ab}	2.4±0.3^{ab}	1.1±0.4^{a}
18:2n6	1.8±0.2^{a}	8.1±0.4^{b}	15.3±1.8^{c}	22.7±2.7^{d}	0.9±0.2^{a}	0.9±0.1^{a}	0.6±0.3^{a}	0.9±0.1^{a}	1.3±0.2^{a}	0.8±0.3^{a}
20:2n6	nd^{a}	nd^{a}	1.7±0.4^{ab}	2.9±0.5^{b}	nd^{a}	nd^{a}	nd^{a}	nd^{a}	nd^{a}	nd^{a}
20:3n6	nd^{a}	1.7±0.1^{ab}	2.8±0.1^{b}	2.5±0.3^{b}	nd^{a}	nd^{a}	nd^{a}	nd^{a}	nd^{a}	nd^{a}
20:4n6	3.9±0.5^{b}	2.8±0.1^{ab}	3.2±0.2^{b}	2.2±0.1^{ab}	2.1±0.1^{ab}	2.3±0.3^{ab}	0.8±0.4^{a}	1.9±0.1^{ab}	3.0±0.4^{b}	1.7±0.6^{a}
20:5n3	nd^{a}	nd^{a}	nd^{a}	nd^{a}	2.8±0.2^{b}	5.3±0.5^{c}	10.1±0.9^{d}	nd^{a}	nd^{a}	nd^{a}
22:5n3	nd^{a}	nd^{a}	nd^{a}	nd^{a}	3.6±0.2^{b}	6.7±0.4^{c}	7.5±0.3^{c}	nd^{a}	nd^{a}	nd^{a}
22:6n3	nd^{a}	nd^{a}	nd^{a}	nd^{a}	nd^{a}	nd^{a}	nd^{a}	6.9±1.0^{b}	10.2±0.8^{c}	12.7±0.5^{d}

Table 2.1. Incorporation of exogenous fatty acids into activated $CD4^+$ T cell membrane phospholipids.
[1]Values represent mean ± SE (n = 3-7).
[2]Superscript with different letters are significantly difference ($P < 0.05$).
[3]Only selected fatty acids (> 1 mol%) are reported.
[4]Abbreviations: nd, not detectable; UT, no exogenous FA treated; L12.5, LA [12.5 µM]; L25, LA [25 µM]; L50, LA [50 µM]; E12.5, EPA [12.5 µM]; E25, EPA [25 µM]; E50, EPA [50 µM]; D12.5, DHA [12.5 µM]; D25, DHA [25 µM]; D50, DHA [50 µM].

significantly ($p < 0.05$) elevated membrane n-3 PUFA from an undetectable level to 2.8 – 10.1 mole% for EPA, and 6.9 -12.7 mole% for DHA. In addition, upon incorporation into the membrane, exogenous EPA was further elongated to docosapentaenoic acid (DPA, C22:5n3). Interestingly, exogenous LA did not alter arachidonic acid (AA, 20:4n6) levels, while only the highest dose of exogenous n-3 PUFA produced a compensatory reduction in AA. Overall, the combined phospholipid levels of EPA and DPA (6.4 – 17.6 mol%) were comparable to DHA levels. In addition, incubation with high doses of exogenous PUFA (25 and 50 µM) resulted in the incorporation of EPA, DPA and DHA into neutral lipid fractions as shown in **Table 2.2**.

FA[1]	UT	L12.5	L25	L50	E12.5	E25	E50	D12.5	D25	D50
(mole%)										
14:0	11.0±1.1	10.6±0.7	8.2±1.1	6.3±1.2	9.9±1.5	10.2±0.5	7.8±0.9	10.9±1.4	7.5±0.9	8.6±1.3
16:0	77.1±2.5^{d}	83.7±0.8^{e}	70.5±4.7^{c}	52.7±7.0^{a}	83.8±2.1^{e}	71.8±3.8^{cd}	58.6±4.0^{b}	85.3±1.8^{e}	72.2±4.0^{d}	67.1±5.9^{c}
18:0	6.7±1.3	5.7±0.3	5.7±0.3	3.3±0.5	6.4±0.6	6.0±1.1	4.0±0.4	3.4±0.5	4.5±0.6	2.5±0.8
18:1n9	3.2±1.2	nd	3.0±1.1	3.0±0.3	nd	4.1±1.3	4.0±0.6	0.4±0.4	3.7±1.0	2.9±1.1
18:2n6	nd^{a}	nd^{a}	9.0±3.3^{b}	30.0±6.9^{c}	nd^{a}	nd^{a}	nd^{a}	nd^{a}	nd^{a}	nd^{a}
20:2n6	nd	nd	nd	1.2±0.6	nd	nd	nd	nd	nd	nd
20:3n6	nd	nd	2.2±1.1	3.4±0.7	nd	nd	nd	nd	nd	nd
20:5n3	nd^{a}	nd^{a}	nd^{a}	nd^{a}	nd^{a}	2.2±0.8^{a}	12.4±2.2^{b}	nd^{a}	nd^{a}	nd^{a}
22:5n3	nd^{a}	nd^{a}	nd^{a}	nd^{a}	nd^{a}	5.7±1.4^{b}	13.4±2.2^{c}	nd^{a}	nd^{a}	nd^{a}
22:6n3	nd^{a}	nd^{a}	nd^{a}	nd^{a}	nd^{a}	nd^{a}	nd^{a}	nd^{a}	11.1±2.2^{b}	17.3±4.9^{c}

Table 2.2. Incorporation of exogenous fatty acids into activated $CD4^{+}$ T cell neutral lipids.
[1]Values represent mean ± SE (n = 3-7).
[2]Superscript with different letters are significantly difference ($P < 0.05$).
[3]Only selected fatty acids (> 1 mol%) are reported.
[4]Abbreviations: nd, not detectable; UT, no exogenous FA treated; L12.5, LA [12.5 µM]; L25, LA [25 µM]; L50, LA [50 µM]; E12.5, EPA [12.5 µM]; E25, EPA [25 µM]; E50, EPA [50 µM]; D12.5, DHA [12.5 µM]; D25, DHA [25 µM]; D50, DHA [50 µM].

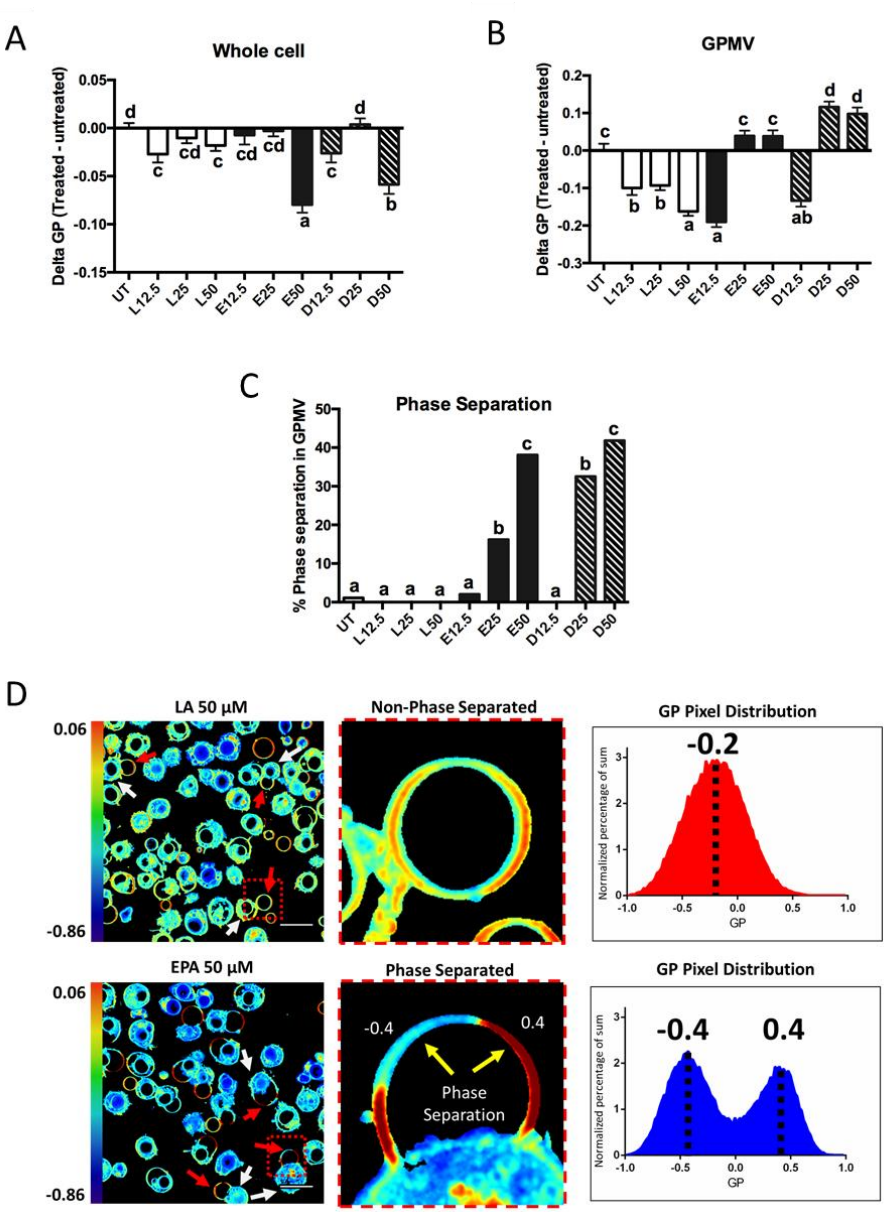

Figure 2.6. Exogenous fatty acids dose-dependently alter human CD4⁺ T cell membrane order and GPMV phase separation. Human pan CD4⁺ T cells isolated from buffy-coat leukocytes were incubated with various doses (0 – 50 µM) of LA, EPA and DHA conjugated with BSA for 2 days. Cultures were further stimulated for 3 days with Dynabeads Human T-Activator CD3/CD28 at a bead-to-cell ratio of 1:1, in the presence of their respective FA. Membrane order was measured following 5 days of total incubation. Data are expressed as the change in generalized polarization (delta GP) compared to the untreated (UT) group in (A) whole cells and (B) GPMVs. (C) n-3 PUFA significantly increased the amount of GPMVs that show phase separation. Phase separation was scored as present or absent. (D) Representative field of view GP images of GPMV's (red arrows) blebbing from cells (white arrows), with a zoomed image clearly showing non vs phase separated GPMVs and their corresponding pixel distribution. Note that GPMV's rarely detach fully from cells. Scale bar equal 20 µm. Data are reported as mean ± SE (n = 50-183), pooled from 3 separate experiments. Mean values not sharing a common letter are significantly different ($P < 0.05$).

Following a 5 d fatty acid incubation period in the presence of CD3/CD28 ab stimulation (for 3 d), all 3 PUFA treatments resulted in a decrease in whole cell membrane order, relative to UT cells. However, n-3 PUFA (EPA and DHA) exhibited significantly ($p < 0.05$) lower GP values compared to n-6 PUFA (LA) at the highest dose (50 μM) only (**Figure 2.6A**). In order to determine if PUFA can directly modulate plasma membrane biophysical properties without the contribution of a cytoskeleton, T cells were incubated with a membrane order sensitive dye Di-4-ANEPPDHQ for 30 min prior to generation of GPMVs. Interestingly, n-3 PUFA treated cells exhibited a significant ($p < 0.05$) elevation in membrane order compared to n-6 PUFA (LA) at 25 and 50 μM doses (**Figure 2.6B**). The striking inversion in EPA and DHA-induced membrane order was associated with a phase separation of the GPMV bilayer (**Figure 2.6C**). Representative images and histograms (**Figure 2.6D**) highlight how phase separation was uniquely imposed by n-3 PUFA in disordered domains that are more disordered, and ordered domains that are more ordered. This is apparent in the histogram generated from the pixels of the LA treated GPMVs display a Gaussian distribution centered around -0.2, while the EPA treated GPMVs display a two Gaussian distribution with the most fluid centered around -0.4 and the most ridged centered around 0.4 (**Figure 2.6D**). Interestingly, GPMV phase separation was only associated with the membrane level of n-3 PUFA, not the ratio of n-3/n-6 PUFA, as shown in **Table 2.1**.

2.3 Discussion

The plasma membrane is an essential cellular structure composed of a phospholipid bilayer and a myriad of proteins, which constitute the outer boundary of the cell. Not only does the cell membrane control molecular transport, it also regulates communication between the cell and its environment by transducing signals. Recent studies have documented important functions for plasma membrane lipids in regulating cellular signaling (Turk et al., 2012). One method that the cell utilizes to organize the membrane relies on cholesterol, which generates biophysical interactions that generate highly packed and ordered, rigid domains commonly referred to as "lipid-rafts" (Levental and Veatch, 2016; Sezgin et al., 2017). From a functional perspective, the cholesterol / phospholipid composition of cellular membranes is known to influence lipid raft formation and the ability of plasma membrane receptors / signaling proteins to function properly (Griffié et al., 2015; Hou et al., 2016; Phillips et al., 2009). Recently the biophysical properties of the plasma membrane have been linked to various cellular processes, such as EMT (Tisza et al., 2014), cell cycle progression (Gray et al., 2015), insulin secretion (Sezgin et al., 2015) and various chronic disease processes (McDonald et al., 2014; Miguel et al., 2011). Since some of the biophysical properties of the plasma membrane result from cytoskeletal driven interactions (Alvarez-Guaita et al., 2015; Dinic et al., 2013), we sought to compare and contrast the effect of n-3 PUFAs in both live cells and cytoskeletal free GPMVs.

Interestingly, long chain n-3 PUFA reduced membrane rigidity in live cells (Fig 2), while elevating membrane order in isolated GPMVs (Fig 3), implicating an indirect

effect of the cytoskeleton. This is not surprising given that fact that n-3 PUFA are known to suppress phosphatidylinositol 4,5-bisphosphate (PIP_2)-dependent actin remodeling during $CD4^+$ T-cell activation (Hou et al., 2012) and attenuate activation of the cytoskeletal remodeling proteins Rac1 and Cdc42 (Turk et al., 2013) in colonocytes. In addition, similar effects of DHA on phase separation stability in GPMVs derived from rat basophilic leukemia (RBL) cells have been reported (Levental et al., 2016).

With respect to T-cells, fatty acid composition has been linked to immune (Hou et al., 2012, 2015; Kim et al., 2008; Yog et al., 2010) and inflammatory homeostatic responses (Calder, 2015; Monk et al., 2014). Therefore, we isolated highly purified, viable, primary human $CD4^+$ T cells (> 96% viability) from buffy-coat leukocytes and demonstrated the dose-dependent in vitro incorporation and elongation of exogenous PUFA into cell membrane phospholipids (**Table 2.1**). We observed that exogenous EPA was extensively elongated to DPA (22:5n-3), a process that is common to other cell types (Chapkin and Carmichael, 1990; Chapkin et al., 1991).

Since changes in membrane lipid order have been associated with immune cell function and inflammatory disease status (McDonald et al., 2014; Miguel et al., 2011), it is noteworthy that EPA or DHA differentially dose-dependently modulated membrane lipid order in whole $CD4^+$ T cells vs GPMVs as compared to UT or n-6 PUFA control treatments (**Figures 2.6A&B**). Interestingly, at higher doses of n-3 PUFA in vitro, a profound induction of phase transition was induced which contributed to an increase in GPMV membrane rigidity (**Figure 2.6**).

Recently, GPMVs have attracted great attention in studies focusing on cell membrane biophysical properties, due to the fact that they are comprised of the membrane bilayer without the contribution of the cytoskeleton (Sezgin et al., 2012). Thus, by contrasting *in vitro* effects of n-3 PUFA on membrane order in live cells vs GPMV, our findings suggest the involvement of the cytoskeleton in the modulation of membrane lipid order. The striking membrane phase separation in $CD4^+$ T cell derived GPMVs is consistent with previous studies examining polyunsaturated lipids (Levental et al., 2016), cholesterol (Levental et al., 2009), bile acids (Zhou et al., 2013), anesthetics (Gray et al., 2013; Machta et al., 2016), chemotherapeutics (Raghunathan et al., 2015), cell cycle progression (Gray et al., 2015), epithelial-mesenchymal transition (Tisza et al., 2014), and protein lipid interaction (Podkalicka et al., 2015). The ability of n-3 PUFA to induce phase separation at room temperature in GPMVs has been linked to suppression of Snail function and the inhibition of lung metastasis (Tisza et al., 2014). Therefore, the unique phase separation in human $CD4^+$ T cell GPMVs by high dose n-3 PUFA may be a biomarker for predicting the potential of n-3 PUFA to suppress chronic disease progression.

In conclusion, we have demonstrated that n-3 PUFA *in vitro* and *in vivo* increase mouse colonocyte and human $CD4^+$ T cell membrane fluidity by reducing lipid order and promote phase separation in GPMVs.

2.4 Materials and methods

2.4.1 Materials

RPMI 1640 medium, Leibovitz medium, FBS, Glutamax, penicillin, streptomycin and Dynabeads Human T-Activator CD3/CD28 were purchased from Gibco (Gaithersburg, MD). Leucosep tubes were obtained from Greiner Bio One (Monroe, NC). Ficoll-Paque medium was purchased from GE (Pittsburgh, PA). RBC lysis buffer was obtained from BioLegend (San Diego, CA). EasySep human $CD4^+$ T cell isolation kits were purchased from StemCell technologies (Cambridge, MA). Poly-L-lysine was purchased from Sigma (St. Louis, MO). Di-4-ANEPPDHQ was obtained from Invitrogen (Carlsbad, CA). Glass bottom 35-mm dishes were purchased from MatTek Corporation (Ashland, MA). CellTiter-Blue cell viability assay was obtained from Promega (Madison, WI). Silica gel 60 G plates and all organic solvents were purchased from EM Science (Gibbstown, NJ). Free fatty acids and fatty acid methyl ester standards were purchased from NuChek Prep (Elysian, MN).

2.4.2 YAMC Cell Culture

Conditionally immortalized Young Adult Mouse Colonic (YAMC) cells and YAMC-HRasG12V were originally obtained from R.H. Whitehead, Ludwig Cancer Institute (Melbourne, Australia). YAMC cells (passages 14–19) were cultured under permissive conditions, 33°C and 5% CO_2 in RPMI 1640 media (Mediatech, Manassas, VA) supplemented with 5% fetal bovine serum (FBS; Hyclone, Logan, UT), 2 mM GlutaMax (Gibco, Grand Island, NY), 5 μg/mL insulin, 5 μg/ml transferrin, 5 ng/ml

selenious acid (Collaborative Bio-medical Products, Bedford, MA), and 5 IU/mL of murine interferon-γ (Roche, Mannheim, Germany). Isogenic SW48 parental and KRasG12D cells (Horizon Discovery) were maintained at 33°C and 5% CO_2 in McCoy's 5A medium supplemented with 10% FBS. Select cultures were treated for 72 h with 50 μM fatty acid [linoleic acid (LA, 18:2n6), arachidonic acid (AA, 20:4n6), eicosapentaenoic acid (EPA, 20:5n3) or docosahexaenoic acid (DHA, 22:6n3); NuChek, Elysian, MN] complexed with fatty acid free bovine serum albumin (BSA).

2.4.3 CD4+ T cell isolation and culture

Buffy-coat leukocyte source from Gulf Coast Regional Blood Center (Houston, TX) or freshly collected whole blood was layered onto Leucosep tube containing Ficoll-Paque medium followed by 800 x g centrifugation for 15 min. Peripheral blood mononuclear cells (PBMC) were collected from the interphase and washed once with PBS (Rees et al., 2006). Red blood cell (RBC) contamination was removed by incubating cell pellets in 1X RBC Lysis buffer on ice for 5 min, followed by PBS washing. $CD4^+$ T cells from PBMC were purified by negative selection using an EasySep human $CD4^+$ T cell isolation kit following the manufacture's protocol. The purity of viable $CD4^+$ T cell population as analyzed by flow cytometry was 96.5 ± 1.2 % (n=3).

$CD4^+$ T cells isolated from the buffy-coat leukocyte source were incubated with various doses (0 – 50 μM) of linoleic acid (LA, 18:2n6), eicosapentaenoic acid (EPA, 20:5n3) or DHA conjugated with BSA for 2 days (basal state). Basal T cell bioenergetic profiles were measured at the end of the first 2 days of incubation. In addition, select

cultures were stimulated for an additional 3 day period with Dynabeads Human T-Activator CD3/CD28 at a bead-to-cell ratio of 1:1 in the presence of exogenous FA (0 – 50 μM LA, EPA or DHA) (activated state). FA incorporation, membrane order, cell proliferation and bioenergetic profiles were subsequently determined.

2.4.4 GPMV generation and membrane order measurement

Giant plasma membrane vesicle (GPMV) generation was performed as described previously (Sezgin et al., 2012). Briefly, basal or activated $CD4^+$ T cells were pelleted and re-suspended in GPMV vesiculation buffer (10 mM HEPES, 150 mM NaCl, 2 mM $CaCl_2$, pH 7.4, 25 mM PFA, 2 mM dithiothreitol) for at least 1 h at 37°C. GPMVs were then spun down at 2000 x g for 3.5 min and pellets were re-suspended in serum-free Leibovitz medium containing Di-4-ANEPPDHQ (5 μM), transferred to a 35-mm glass bottom dish, and immediately imaged. For Adherent YAMC cells GPMVs were generated similarly, however, attachment of cells allowed collection of GPMV enriched supernatant without the need for centrifugation. GPMV rich supernatant was then used for imaging.

2.4.5 Membrane order imaging and quantification

Basal or activated whole $CD4^+$ T cells were stained with Di-4-ANEPPDHQ for membrane order determination as previously described (Owen et al., 2011; Chapkin et al., 2014). Briefly, T-cells were gently pelleted at 200 x g for 5 min, re-suspended in serum-free Leibovitz medium containing Di-4-ANEPPDHQ (5 μM), transferred to a 35-mm glass bottom dish, and immediately imaged to avoid dye internalization. YAMC cells were

washed with Leibowitz, followed by incubation in serum-free Leibovitz medium containing Di-4-ANEPPDHQ (5 μM), and immediately imaged to avoid dye internalization.

Imaging experiments were conducted on a Zeiss 510 or a Zeiss 780 confocal microscope equipped with a 32-channel GaAsP line-array spectral detector. YAMC cells and crypts were imaged with a 1.4 numerical aperture 40× Plan Apochromat oil objective, while T-cells and GPMVs were imaged with a 1.4 numerical aperture 63× Plan Apochromat oil objective at room temperature. Laser light at 488 nm was used to excite Di-4-ANEPPDHQ and emission wavelengths were collected in two channels representing order (O: 508-544) and disordered (D: 651-695).

Generalized polarization (GP) was calculated using the equation below:

$GP= (I_{(O)}-I_{(D)})/(I_{(O)}+I_{(D)})$. The same laser power and settings were used for every experiment. Image processing was conducted using Fiji/ImageJ (NIH) software, with a GP-plugin and a custom-built macro. Briefly, images were converted to 8-bit tiffs, combined into RBG images, thresholded to exclude background pixels, and converted into GP images. Average GP was determined from region of interest (ROI) of cells or GPMVs.

CHAPTER III

LONG CHAIN n-3 FATTY ACIDS ATTENUATE ONCOGENIC RAS DRIVEN PROLIFERATION BY ALTERING PLASMA MEMBRANE PROTEIN NANOCLUSTERING

3.1 Introduction

Ras GTPase proteins are targeted to the cytoplasmic face of the plasma membrane by farnesylation coupled to either palmitoylation, N, H and K(A) or a polybasic motif, K(B) (Eisenberg et al., 2013). Approximately 30-50% of colorectal cancers (CRCs) harbor KRas mutations, and KRas-mutant CRCs exhibit resistance to standard therapy (Stephen et al., 2014), thereby reducing survival (Phipps et al., 2013). Moreover, to date, targeting of mutant RAS proteins in cancers has not been possible (Phipps et al., 2013). A number of Ras effector proteins and cell signaling pathways have been defined, including the Raf and the MAP kinase pathway, the PI3K and the Akt/mTOR pathway, and the RalGDS and Ral pathway. RAS effector proteins physically associate with RAS proteins to propagate signal transduction (Herrmann, 2003; Wittinghofer and Herrmann, 1995). These effectors are highly complex with numerous redundancies and interactions between pathways (Downward, 2003). Dysregulated (oncogenic) Ras signaling results in increased proliferation, decreased apoptosis, disrupted cellular metabolism, and increased angiogenesis, all seminal hallmarks of cancer (Downward, 2003; Vasan et al., 2014). Thus, there is a critical need to develop new KRas targeted therapeutic approaches with reduced toxicities in the setting of acute or chronic administration.

High fidelity signaling of K-Ras is dependent on its spatial organization into defined dimers (Muratcioglu et al., 2015; Nan et al., 2015) or nanoclusters containing ~6-7 Ras molecules, measuring ~9 nm in radius in the inner leaflet of the plasma membrane (Henis et al., 2009; Tian et al., 2007). Recently, it was demonstrated that select amphiphilic agents, through direct modulation of the biophysical properties of the plasma membrane, compromise oncogenic K-Ras nanoclustering to modulate signal transduction (Zhou and Hancock, 2015; Zhou et al., 2012). These findings suggest that Ras nanoclusters could be a novel therapeutic target (Cho and Hancock, 2013; Zhou et al., 2010). From this perspective, there is a growing body of evidence indicating that n-3 PUFA, found in cold water fish and over the counter supplements and prescription therapeutics, e.g., Lovaza, can attenuate oncogenic Ras signaling (Collett et al., 2001; Ma et al., 2004b; Rogers et al., 2010; Seo et al., 2006; Turk et al., 2012).

With respect to the molecular mechanism of action, there is a growing body of *in vitro* and *in vivo* evidence indicating that n-3 PUFA reshape plasma membrane domains. For example, EPA and DHA, whose membrane phospholipid levels are readily influenced by diet in general (Katan et al., 1997), are rapidly incorporated into cells, primarily into membrane phospholipids at the *sn*-2 position (Chapkin et al., 1991; Williams et al., 2012). The presence of long chain n-3 PUFA in membrane phospholipids imparts unique biophysical properties which have been linked to alterations in plasma membrane structure and function (Chapkin et al., 2008b; Levental et al., 2016; Ma et al., 2004a, 2004b; Seo et al., 2006; Williams et al., 2012). For example, DHA is known to influence membrane fluidity, ion permeability, fatty acid

exchange, and resident protein function (Hou et al., 2016; Stillwell and Wassall, 2003), including the inhibition of epidermal growth factor receptor (EGFR) signaling in tumor bearing mice by disassociating EGFR from lipid rafts (Turk et al., 2012). Since changes in the biophysical properties of the plasma membrane have been linked to alterations in Ras signal transmission (Zhou and Hancock, 2015; Zhou et al., 2012), we hypothesized that select amphiphilic membrane targeted dietary bioactives (MTDBs) modulate Ras nanocluster formation. Herein, we report DHA and EPA (i) modify Ras nanocluster formation, (ii) disrupt oncogenic Ras driven signaling (pERK), and (iii) suppress phenotype (hyperproliferation) *in vitro* and *in vivo*. Together, these results suggest a unique role for MTDBs in the modulation of Ras nanoscale spatial organization and signaling.

3.2 Results

3.2.1 Dietary n-3 PUFA ameliorate oncogenic KRasG12D mediated colonic phenotypes in vivo.

We previously demonstrated that n-3 PUFA suppress intestinal wild type H- and KRas activation *in vitro* and *in vivo*, leading to a reduction in downstream signaling (Ma et al., 2004b; Turk et al., 2012). Interestingly, the effects of n-3 PUFA are not limited to wild type Ras, as DHA also attenuates activation of ERK and reduces the growth of mouse colonocytes expressing oncogenic HRas (Collett et al., 2001; Turk et al., 2012). This is consistent with studies documenting the ability of n-3 PUFA to reduce cell proliferation, signaling, and anchorage independent growth in

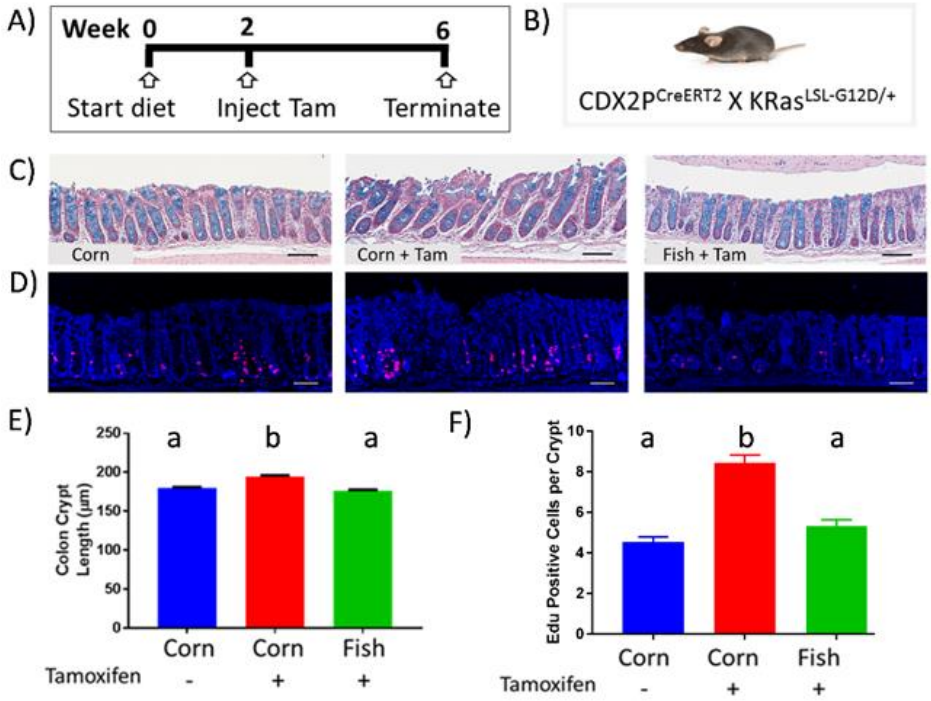

Figure 3.1. Dietary n-3 PUFA ameliorates oncogenic KRasG12D mediated colonic phenotypes. (A) Experimental design to determine the efficacy of dietary intervention on a (B) genetic mouse model of oncogenic KRasG12D driven hyper-proliferation in the colon, (C) alcian blue-staining of colonic crypts, (D) Nuclei (blue) and edu-labeled (red) proliferating colonocytes in mice 4 weeks post tamoxifen (Tam, 200 mg/kg) fed corn or fish oil-containing diets. Quantitative analysis of (E) crypt length and (F) cell proliferation. Scale bar = 50 µM. Statistical significance between treatments as indicated by different letters ($P<0.05$) was examined using one-way ANOVA and uncorrected Fisher's LSD tests (Panel E; n = 4 mice per group and at least 508 crypts counted; Panel F; n = 4 mice per group and 200 crypts counted).

colon cancer cell lines (HCT116, SW480, SW620) and pancreatic ductal adenocarcinoma models harboring KRas mutations G12V and G13D (Dunn et al., 2011; Fasano et al., 2012; Liu et al., 2016; Mohammed et al., 2012; Rogers et al., 2010; Schonberg et al., 2006; Strouch et al., 2011). To determine if dietary n-3 PUFA can suppress oncogenic Ras mediated phenotypes, we utilized an inducible genetic model of oncogenic KRas driven colonic hyperproliferation. (Feng et al., 2011,

2013)(**Figures 3.1A & B**). Mice were fed a diet containing corn (n-6 PUFA control) or fish oil (**Tables 3.1 & 3.2**) for 2 wks prior to tamoxifen induction of oncogenic KRas, and maintained for an additional 4 weeks (**Figure 3.1A**). This dose is comparable to a diet containing approximately 8.6 g/day n-3 PUFA in humans (Fuentes et al., 2017). As expected, mice fed a diet containing n-3 PUFA exhibited an enrichment of DHA and EPA in membrane phospholipids (**Table 3.3**). Dietary n-3 PUFA treatment substantially reduced colonic hyperproliferation as indicated by the significant ($P<0.05$) reduction of crypt length (**Figures 3.1C & E**) and number of Edu positive proliferative cells per crypt (**Figures 3.1D & F**). Collectively, these findings suggest that dietary fish oil containing EPA and DHA can attenuate oncogenic KRas driven phenotypes *in vivo*.

Ingredients	Diet (g/100 g)	
	Corn Oil	Fish Oil
Sucrose	42	42
Casein	20	20
DL-methionine	0.3	0.3
AIN-76 Mineral mix	3.5	3.5
AIN-76 Vitamin mix	1	1
Choline Chloride	0.2	0.2
Corn Starch	22	22
Cellulose	6	6
Fish Oil	0	4
Corn oil	5	1
Total	100	100

Table 3.1. Mouse diet composition.

Fatty Acid	Corn Oil (5%)	Fish Oil (4%)
(mole%)	(mole%)	(mole%)
14:0	0.00	10.23
16:0	13.94	22.46
16:1n-7	0.00	10.13
18:0	1.85	3.80
18:1n-9	27.63	11.12
18:1n-7	0.00	2.61
18:2n-6 (LA)	55.63	10.71
18:3n-3	0.94	1.24
18:4n-3	0.00	2.65
20:0	0.00	0.00
20:3n-6	0.00	0.00
20:4n-6	0.00	0.00
20:5n-3 (EPA)	0.00	12.07
22:0	0.00	0.00
22:5n-3	0.00	1.47
22:6n-3 (DHA)	0.00	11.51

Table 3.2. Mouse diet fatty acid composition.
[1]Values represent means from lipids extracted from ~ 1g of experimental diet.
[2]Only selected fatty acids in which at least one observation was > 0.2 mol% are reported.

Fatty Acid	Corn Oil Control		Corn Oil + Tamoxifen		Fish Oil + Tamoxifen	
(mole%)	Mean	SEM	Mean	SEM	Mean	SEM
14:0	8.41	1.65	7.67	1.31	9.43	2.25
16:0	32.39^{ab}	0.57	29.99^{a}	1.44	33.35^{b}	0.97
16:1n-7	2.62	0.24	2.98	0.38	5.05	0.14
18:0	18.25	0.57	17.80	0.79	16.78	0.53
18:1n-9	13.74^{a}	0.90	15.78^{ab}	1.98	18.34^{b}	1.54
18:1n-7	5.18	0.32	4.63	0.55	5.47	0.22
18:2n-6 (LA)	6.96^{a}	0.63	7.67^{a}	1.07	2.52^{b}	0.32
20:0	0.36	0.03	0.48	0.06	0.53	0.07
20:3n-6	2.54	0.13	2.13	0.25	0.37	0.07
20:4n-6	9.15^{a}	0.42	5.94^{b}	0.68	0.95^{c}	0.12
20:5n-3 (EPA)	0.00^{a}	0.00	0.00^{a}	0.00	3.50^{b}	0.88
22:0	0.42	0.02	0.47	0.06	0.68	0.03
22:5n-3	0.00	0.00	0.00	0.00	0.17	0.17
22:6n-3 (DHA)	0.00^{a}	0.00	0.00^{a}	0.00	2.87^{b}	0.51

Table 3.3. Incorporation of exogenous fatty acids into murine colonic crypt membrane phospholipids.
[1]Values represent mean ± SEM (n = 4 mice per treatment).
[2]Statistical significance between treatments as indicated by different letters ($P<0.05$) was examined using one-way ANOVA and uncorrected Fisher's LSD tests.
[3]Only selected fatty acids in which at least one observation was > 0.2 mol% are reported.

3.2.2 Long chain n-3 PUFA disrupt Ras spatiotemporal dynamics.

Previous experiments conducted by our lab using immuno-gold electron microscopy of plasma membrane sheets, suggest that plasma membrane organization of inner leaflets is fundamentally altered by EPA and DHA (Chapkin et al., 2008b; Kim et al., 2010). Specifically, n-3 PUFA treatment altered the nanoclustering of truncated forms of wild type H- and KRas in cervical adenocarcinoma (HeLa) and colorectal carcinoma (HCT-116) cells (Chapkin et al., 2008b; Kim et al., 2010). Nanoclustering of Ras isoforms is primarily controlled by distinct C-terminal hypervariable regions (HVR) which share ~20% homology among Ras protein species (Prior and Hancock, 2001, 2012). As a tool to study Ras nanoclustering, fluorescent GFP and RFP proteins are attached to the minimal membrane anchoring domain of H- or K-Ras (Prior et al., 2003). When the technique of fluorescence lifetime imaging microscopy combined with fluorescence resonance energy transfer (FLIM-FRET) is applied to cells transiently expressing these probes it allows for the quantification of the nanoscale organization of these proteins (Najumudeen et al., 2016; Zhou and Hancock, 2017; Zhou et al., 2012, 2015). Importantly, transient expression of these probes faithfully reports on the nanoscale interactions of Ras, as the clustered fraction of Ras proteins remains constant over a multi-log range of expression levels (Plowman et al., 2005; Tian et al., 2007; Zhou and Hancock, 2015). A reduction of GFP lifetime is indicative of more extensive FRET as a result of a smaller distance between GFP and RFP, which is correlated with more extensive nanoclustering. Lifetime values are then converted to apparent FRET efficiency %, where an increase is indicative of enhanced nanoclustering (Guzman et

al., 2014). To further explore the effects of n-3 PUFA on Ras spatiotemporal dynamics, we utilized immortalized young adult mouse colonocyte (YAMC) cells (Whitehead and Robinson, 2009), since this model faithfully recapitulates n-3 PUFA *in vivo* effects (Ma et al., 2004b; Turk et al., 2012, 2013) and allows for lipidomic and proteomic studies under well-controlled conditions (Seo et al., 2006). Cells were treated with a physiologically relevant level (50 uM) (Conquer and Holub, 1998) of albumin-complexed n-3 PUFA (DHA, EPA) or control long-chain n-6 PUFA linoleic acid (LA) for 72 h. In addition, mevastatin, an HMG-CoA inhibitor was used as a positive control

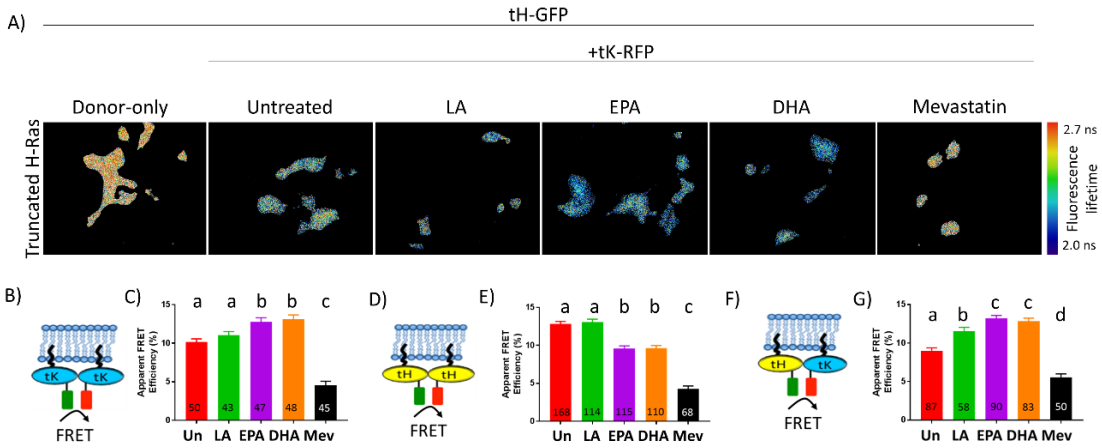

Figure 3.2. Long chain n-3 PUFA disrupts Ras spatiotemporal dynamics. Nanoclustering-FRET analysis (illustrated in schemes) in (A) YAMC cells co-expressing GFP- and RFP-tagged (B) truncated K-Ras (tK), (D) truncated H-Ras (tH) or (F) tH-GFP and tK-RFP. (A) Representative examples of FLIM-FRET images of YAMC cells from the different FRET samples as indicated. (C, E, G) YAMC cells were treated with mevastatin (Mev, 5 uM) or indicated fatty acids (50 uM) for 24 or 72 h, respectively. Cells were transfected 48 h prior to imaging. In all graphs (C, E and G), the apparent FRET efficiency was calculated from FLIM data (mean ± SEM, n= 2-3 and independent experiments). Values in the bars indicate the number of cells examined. Statistical significance between treatments as indicated by different letters ($P<0.05$) was examined using one-way ANOVA and uncorrected Fisher's LSD tests. Un – untreated cells, LA – linoleic acid, EPA – eicosapentaenoic acid, DHA – docosahexaenoic acid.

to reduce nanoclustering of Ras and FRET efficiency by blocking farnesylation and thus membrane anchorage of Ras (Kohnke et al., 2012). Surprisingly, n-3 PUFA significantly increased ($P<0.05$) the clustering of truncated KRas (tK) (**Figures 3.2A - C**) while truncated HRas (tH) (**Figures 3.2D & E**) clustering was reduced ($P<0.05$) compared to untreated control. Since n-3 PUFA are known to modulate differences in membrane rigidity between raft and non-raft domains (Levental et al., 2016; Lin et al., 2016), we sought to determine if this would result in the formation of mixed heterotypic nanoclusters of tH and tK, as observed with certain nonsteroidal anti-inflammatory drugs (Zhou et al., 2012). DHA and EPA significantly increased ($P<0.05$) the formation of heterotypic clustering, as well as LA to a lesser extent (**Figures 3.2F & G**). Polyunsaturation of lipids in general, may have a minor effect on the lateral segregation of H- and K-Ras since, LA did increase heterotypic clustering but had no effect on homotypic clustering. This suggests that incorporation of long chain n-3 PUFA into plasma membrane phospholipids alters the precise nanometer spatial organization of H- and KRas, thereby enhancing heterotypic mixed clusters.

3.2.3 Long chain n-3 PUFA attenuate oncogenic Ras mediated ERK signaling.

We next sought to determine if the nanoscale alterations to Ras organization imposed by n-3 PUFA attenuate oncogenic Ras signaling defects. We initially tested YAMC cells expressing oncogenic HRasG12V (D'Abaco et al., 1996) as a representation of normal colonocytes en route to malignancy (Smith et al., 2002). Since physiological expression of oncogenic KRas does not result in large increases in

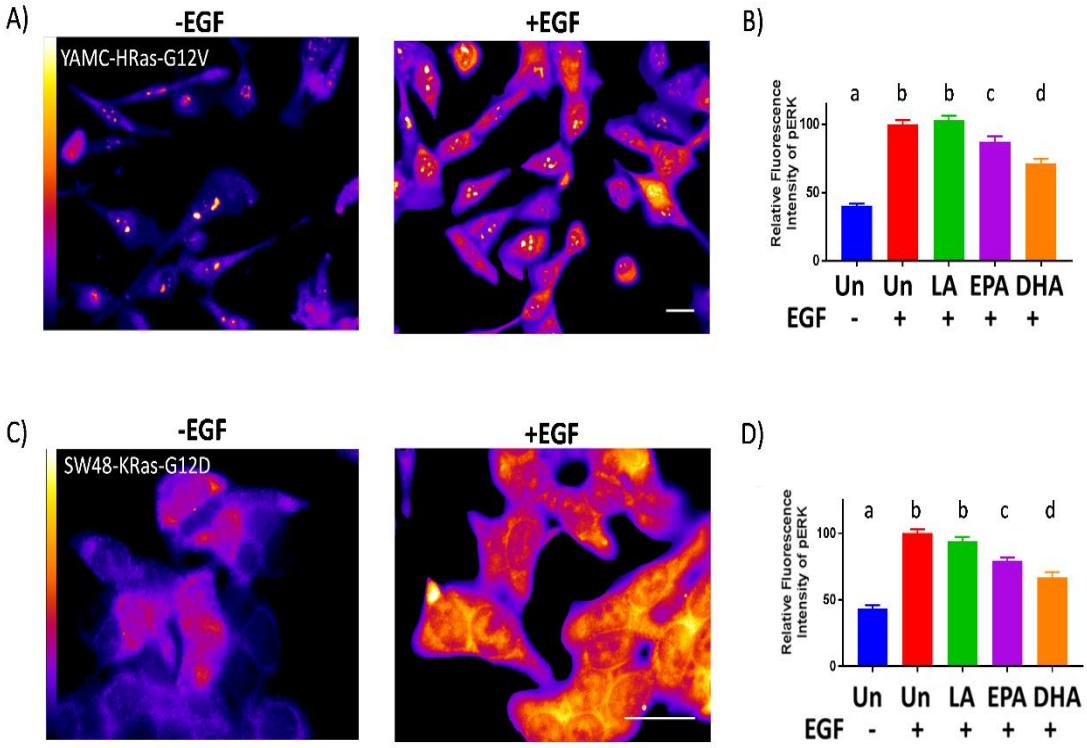

Figure 3.3. Long chain n-3 PUFA attenuated Ras mediated ERK signaling. (A) YAMC-HRasG12V or (C) SW48-KRasG12D cells grown in 8-well glass bottom dishes and treated with 50 uM indicated fatty acid for 72 h. Cells were starved (0.5% FBS) over the final 18 hours in the presence of fatty acid and stimulated with EGF (25 ng/ml) for 5 min, then immediately fixed in ice cold 100% methanol. (A, C) Representative masked images of cells immunostained for pERK +/- EGF. Color scale represents relative fluorescence intensity. Scale bar = 20 µM. (B and D) Average fluorescence intensity for pERK. Data represent average fluorescence intensity ± SEM from at least 15 fields of view with ~20-30 cells per field, from 3 independent experiments. Statistical significance between treatments as indicated by different letters ($P<0.05$) was examined using one-way ANOVA and uncorrected Fisher's LSD tests.

phosphorylation of ERK, we therefore stimulated cells with EGF (Stolze et al., 2015; Vartanian et al., 2013). As detected by immunofluorescence staining of phosphorylated ERK, EPA and DHA reduced ($P<0.05$) EGF induced ERK phosphorylation by ~13 and 29%, respectively (**Figures 3.3A & B**). In contrast, the n-6 PUFA control (LA) had no

effect compared to untreated control (**Figure 3.3B**). Since oncogenic HRas is not commonly mutated in colon cancer (Prior et al., 2012), we subsequently utilized a human colon cancer SW48 cell line expressing mutated KRas (Hammond et al., 2015; Modest et al., 2013; Vartanian et al., 2013). This cell line model was generated using adeno-associated virus (AAV) somatic homologous recombination-based technology to directly modify endogenous Ras genes via introduction of activating mutations (Inoue et al., 2001; Russell et al., 2002). To limit the confounding effects associated with over-expression of oncogenic Ras, these cells were designed to express mutated KRas variant G12D from the endogenous KRas locus (Stolze et al., 2015). This particular KRas variant was chosen because one third of colorectal tumors harbor KRas mutations and ~80% of these mutations are at codon 12, while the remaining mutations are at codon 13 (Prior et al., 2012). Consistent with treatment effects on mutant HRas, DHA and EPA also reduced ($P<0.05$) EGF stimulated ERK phosphorylation in SW48-KRasG12D cells relative to the n-6 PUFA (LA) and untreated controls (**Figures 3.3C & D**).

3.2.4 Dietary n-3 PUFA disrupt Ras spatiotemporal dynamics and suppress oncogenic Ras-mediated hyperproliferation in Drosophila intestinal stem cells.

In order to assay n-3 PUFA-mediated changes of Ras nanoclustering *in vivo*, we turned to the *Drosophila* intestinal (midgut) epithelium. The presence of somatic intestinal stem cells (ISCs) within the fly midgut allows for the use of a wide range of genetic tools to assay signalling events that govern proliferative homeostasis *in vivo* (Biteau et al., 2011; Buchon et al., 2013; Micchelli and Perrimon, 2006; Ohlstein and Spradling, 2006). This

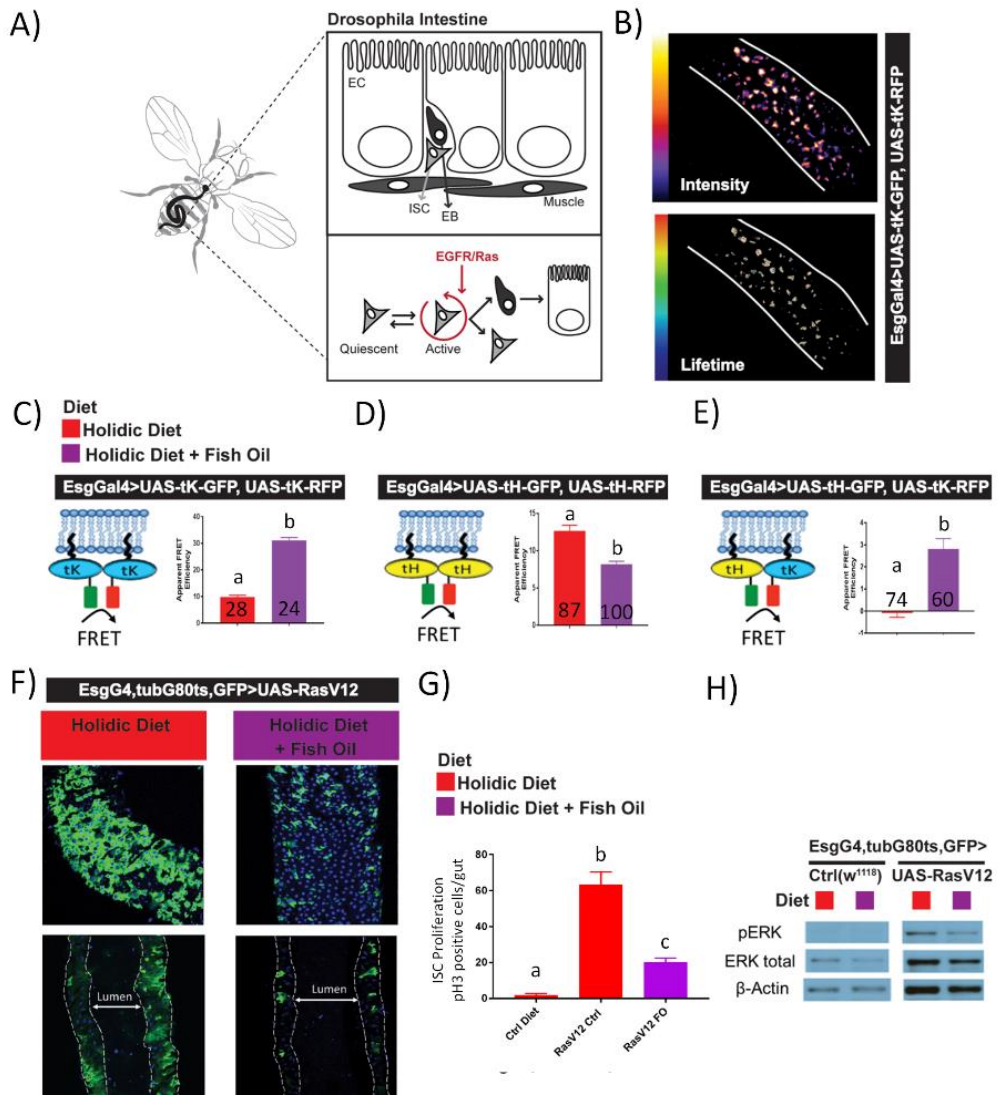

Figure 3.4. Dietary n-3 PUFA disrupts Ras spatiotemporal dynamics, suppresses oncogenic Ras driven hyperproliferation phenotype and signaling in *Drosophila* midguts. (A) Schematic diagram of drosophila intestine. (B) Representative intensity and lifetime field of view (FOV) images of Drosophila midguts. Nanoclustering-FRET analysis (illustrated in schemes) in Drosophila midgut stem cells co-expressing GFP- and RFP-tagged (C) truncated K-Ras (tK), (D) truncated H-Ras (tH) or (E) tH-GFP and tK-RFP. (C, D, and E) 1-2 d old Drosophila were placed on holidic diet containing no lipid (red) or fish oil (purple) for 5 d prior to dissection and mounting of midguts for microscopy. In all graphs (C, D and E), the apparent FRET efficiency was calculated from FLIM data (mean ± SEM, n=2 independent experiments). Values in the bars indicate the number of analyzed FOVs. Induction of oncogenic RasV12 in Drosophila midgut stem cells resulted in (F) hyperproliferation at 24 hours and luminal thickening at 48 hours. Drosophila fed a fish oil vs control holidic diet for 5 d prior to induction of oncogenic RasV12 in midgut stem cells exhibited reduced hyperproliferation and midgut luminal thickening. (G) Quantitative analysis of proliferation as assed by pH3 at 48 hours post RasV12 induction. (H) After 24 hour RasV12 induction, guts were harvested and used to assess pERK by western blot. Statistical significance between treatments as indicated by different letters ($P<0.05$) was examined using an unpaired t-test.

barrier epithelia, with functional and morphological similarities to the mammalian small intestine and mouse airway epithelia (Biteau et al., 2011), contains ISCs that can asymmetrically divide, forming an enteroblast (EB) that directly differentiates into functional enterocytes (**Figure 3.4A**). Thus, the *Drosophila* ISC lineage provides an excellent model to study signaling mechanisms regulating stem cell maintenance and dysfunction, including EGFR/Ras-mediated proliferative signaling (Biteau et al., 2011; Jiang and Edgar, 2009).

To extend our findings in YAMC cells *in vivo,* we assessed n-3 PUFA-dependent effects on Ras nanoclustering in *Drosophila* utilizing transgenic flies that express Ras FRET pair constructs (UAS-GFP/RFP-truncated KRas and/or UAS-GFP/RFP-truncated

Fatty Acid	Holidic Diet	Fish Oil (1.79%)	Corn Oil (1.79%)
(mole%)	(mole%)	(mole%)	(mole%)
14:0	0.00	12.89	0.00
16:0	0.00	23.27	13.33
16:1n-7	0.00	14.61	0.00
18:0	0.00	3.77	1.87
18:1n-9	0.00	6.82	28.40
18:1n-7	0.00	3.27	0.00
18:2n-6 (LA)	0.00	1.67	55.69
18:3n-3	0.00	1.32	0.71
18:4n-3	0.00	3.40	0.00
20:0	0.00	0.00	0.00
20:3n-6	0.00	0.00	0.00
20:4n-6	0.00	0.00	0.00
20:5n-3 (EPA)	0.00	15.74	0.00
22:0	0.00	0.00	0.00
22:5n-3	0.00	1.60	0.00
22:6n-3 (DHA)	0.00	11.62	0.00

Table 3.4. *Drosophila* diet fatty acid composition.
[1]Values represent means from lipids extracted from ~ 1g of experimental diet.
[2]Only selected fatty acids in which at least one observation was > 0.2 mol% are reported.

HRas) (Zhou et al., 2015) specifically within ISCs/EBs (using the EsgGal4 driver). Control flies expressing only the UAS-GFP-truncated KRas/esgGal4 stem cell driver (lacking the FRET pair; establishes baseline lifetime of GFP with no FRET interaction) or UAS-GFP/RFP truncated HRas/esgGal4 (used to comparatively determine treatment effects on clustering of HRas) were also assessed. Flies were fed a chemically defined holidic diet (Piper et al., 2014) that allowed for precise control over all ingredients. The experimental diet differed from the control diet only in its lipid profile – fish oil presented at 1.79% (w/w) (**Tables 3.4**). t-BHQ was added to the diet to prevent oxidative deterioration of EPA/DHA (Fritsche and Johnston, 1988). Phospholipid analysis of the midgut indicated that EPA, and to a lesser extent DHA, was enriched in

Fatty Acid	Holidic Control	Fish Oil
(mole%)	(mole%)	(mole%)
14:0	4.62	3.07
16:0	11.62	22.79
16:1n-7	35.68	20.71
18:0	3.36	3.47
18:1n-9	36.77	32.19
18:1n-7	0.00	1.94
18:2n-6 (LA)	3.60	4.73
20:0	3.28	1.77
20:3n-6	0.00	0.00
20:4n-6	0.46	0.00
20:5n-3 (EPA)	0.00	5.47
22:0	0.62	0.80
22:5n-3	0.00	0.00
22:6n-3 (DHA)	0.00	1.12

Table 3.5. Incorporation of exogenous fatty acids into *Drosophila* gut membrane phospholipids.
[1]Values represent means from pooled *Drosophila* guts (n= Control 51, and Fish Oil 46), grown in two separate vials.
[2]Only selected fatty acids in which at least one observation was > 0.2 mol% are reported.

flies feeding on the n-3 PUFA-enriched diet (**Table 3.5**). Utilizing these dietary and genetic conditions, we then performed FLIM-FRET to monitor truncated H- and KRas nanoclustering in *Drosophila* intestinal stem cells/enteroblasts. Consistent with our *in vitro* nanoclustering data (**Figures 3.2B-G**), flies on the fish oil diet had increased tK clustering, reduced tH clustering and increased formation of heterotypic clustering (**Figure 3.4B-E**). In a complementary set of experiments, flies were fed an additional n-6 PUFA control diet containing equal amounts of lipid (corn oil) (**Tables 3.4**). This resulted in a dramatic increase in LA-containing phospholipids (**Table 3.6**), however no effect on tK or tH clustering was observed (**Figure 3.5**). Finally, we examined the effect of dietary n-3 PUFA on oncogenic Ras-mediated phenotypes originating from stem cells in the *Drosophila* midgut. For this purpose, the expression of oncogenic RasV12 was

Fatty Acid	Corn Oil
(mole%)	(mole%)
14:0	2.11
16:0	21.24
16:1n-7	4.44
18:0	3.92
18:1n-9	23.67
18:1n-7	0.00
18:2n-6 (LA)	40.78
20:0	2.09
20:3n-6	0.00
20:4n-6	1.75
20:5n-3 (EPA)	0.00
22:0	0.00
22:5n-3	0.00
22:6n-3 (DHA)	0.00

Table 3.6. Incorporation of exogenous fatty acids from corn oil into *Drosophila* gut membrane phospholipids.
[1]Values represent means from pooled Drosophila guts (n= Corn Oil 28), grown in two separate vials.
[2]Only selected fatty acids in which at least one observation was > 0.2 mol% are reported.

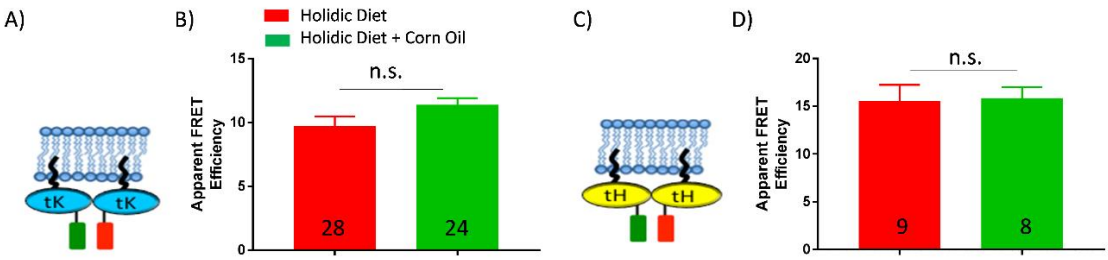

Figure 3.5. Dietary corn oil does not disrupt Ras spatiotemporal dynamics in Drosophila midguts. Nanoclustering-FRET analysis (illustrated in schemes) in Drosophila midgut stem cells co-expressing GFP- and RFP-tagged (A) truncated KRas (tK) or (B) truncated HRas (tH). (B and D) 1-2 d old Drosophila were placed on holidic diet containing no lipid (red) or corn oil (green) for 5 d prior to dissection and mounting of midguts for microscopy. In all graphs (B and D), the apparent FRET efficiency was calculated from FLIM data (mean ± SEM, n= (B) 2 or (D) 1 independent experiment(s)). Values in the bars indicate the number of analyzed FOVs. Statistical significance between treatments as indicated by different letters ($P<0.05$) was examined using an unpaired t-test.

targeted to ISCs in the adult fly, which leads to stem cell hyperproliferation and intestinal dysplasia (**Figure 3.4F**) (Jiang and Edgar, 2009). Strikingly, flies fed n-3 PUFA vs control exhibited a drastic reduction in stem cell hyperproliferation, luminal thickening/tissue dysplasia (**Figures 3.4F-G**) and ERK activation (**Figure 3.4H**). Collectively, these data demonstrate that dietary fish oil results in the incorporation of n-3 PUFA into plasma membrane phospholipids in *Drosophila* ISCs, which is associated with the disruption of Ras nanoscale organization, and the amelioration of oncogenic Ras-dependent signaling and hyperproliferation *in vivo*.

3.3 Discussion

Here we provide evidence that a diet containing long chain n-3 PUFA, e.g., EPA and DHA, attenuate oncogenic Ras signaling by altering its precise nanoscale spatial

organization. To our knowledge, this is the first *in vivo* evidence that dietary bioactives can fundamentally alter Ras membrane organization and signaling in the intestine. This is highly relevant since no curative treatments for KRas-driven colon cancer are available. From a translational and feasibility perspective, these findings lay the foundation for the development of toxicologically innocuous KRas therapeutic approaches. Our data suggest that membrane therapy as a strategy likely requires the long term shaping of cellular phospholipids and hence their resident proteins (Escriba et al., 2015). The use of a prolonged regimen as a therapeutic strategy would ideally need to exhibit little or no adverse effects. From a human dose perspective, EPA and DHA administration as high as 17.6 g/day has been shown to be safe and well tolerated (Skarke et al., 2015). This is opposed to traditional therapeutic approaches which often exhibit off target effects and unwanted toxicological ramifications (Muller and Milton, 2012).

With respect to membrane structure, the plasma membrane is composed of a heterogeneous mixture of lipids and proteins, whose distinct order maintains efficient signal transduction. Membrane lipids typically undergo phase separations and interact selectively with membrane proteins and sub-membrane cytoskeletal elements (Horejsi and Hrdinka, 2014). Accumulating evidence suggests that lipid rafts are highly dynamic and small (5-200 nm) membrane microdomains enriched in sphingolipids and/or cholesterol, which function as sorting platforms for many membrane-associated proteins (Frisz et al., 2013; Hancock, 2006; Kraft, 2013; Levental and Veatch, 2016; Lingwood and Simons, 2010). Stabilization of these domains is generally thought to be maintained by lipid and cytoskeletal influences (Head et al., 2014). This is noteworthy from a cancer perspective

because lipid rafts may modulate the malignant transformation process. For example, the levels of lipid rafts are increased in many types of cancer (Jahn et al., 2011; Li et al., 2006; Patra, 2008) and the modulation of raft properties by DHA may impact epithelial-mesenchymal transition (EMT) (Tisza et al., 2014). There is also evidence suggesting that disruption of lipid rafts in cancer can lead to increased responsiveness to anti-cancer therapies (Fedida-Metula et al., 2012; Irwin et al., 2011). Additionally, some anti-cancer drugs have beneficial effects through alteration of the protein content of lipid rafts (George and Wu, 2012; Hryniewicz-Jankowska et al., 2014). In colon cancer, lipid rafts have been shown to function in cell death-mediated signaling (Lacour et al., 2004; Rebillard et al., 2007), cell entry/bioavailability of bioactive compounds (Adachi et al., 2007) and the localization of key proteins involved in immune response (Bene et al., 2004). These findings indicate that exogenous lipids can no longer be ignored in the structures of membrane complexes, due to their ability to fine-tune and stabilize different signaling interfaces (Barrera et al., 2013; Levental et al., 2016; Lin et al., 2016). According to this emerging picture, protein and lipid nanoclusters can be organized to form domains that are capable of facilitating Ras signaling events (Ariotti et al., 2014; Garcia-Parajo et al., 2014; Zhou and Hancock, 2015). For example, the formation of Ras dimers/nanoclusters is believed to be driven by cortical actin and/or proximal transmembrane proteins (Garcia-Parajo et al., 2014). This is noteworthy, because there is emerging evidence that drugs

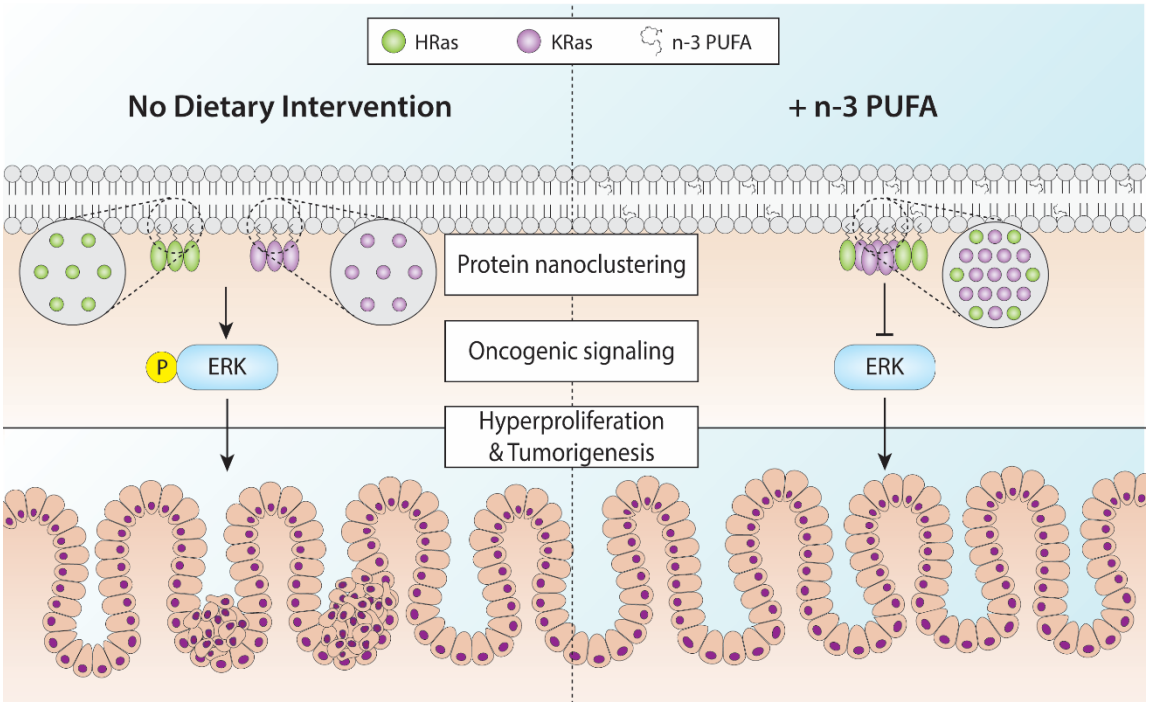

Figure 3.6. Summary diagram highlighting n-3 PUFA suppression of oncogenic Ras mediated hyperproliferation and signaling through disruption of Ras spatiotemporal dynamics. Incorporation of long chain n-3 PUFA into plasma membrane phospholipids generates heterotypic mixed clusters of H- and KRas proteins, disrupting their ability as nanoswitches to regulate ERK signaling. This results in the suppression of oncogenic Ras driven phenotypes in the colon.

and MTDB's can attenuate Ras and EGFR activity by modulating nanocluster organization (Ariotti et al., 2014; Nussinov et al., 2014). Thus, we were interested in documenting the ability of n-3 PUFA to modulate clustering of membrane associated Ras proteins and the resultant attenuation of downstream oncogenic signaling in the intestine (**Figure 3.6).**

The spatial organization of Ras isoforms into non-overlapping nanometer scale domains on the plasma membrane facilitates the recruitment of Raf leading to ERK

activation (Tian et al., 2007), creating a novel drug target (Cho and Hancock, 2013). We observed that long chain n-3 PUFA selectively generate mixed clusters of K- and HRas (**Figure 3.2G and Figure 3.4N**), which ultimately attenuate ERK signaling (**Figure 3.3B&D and Figure 3.4E**) and ameliorate Ras-driven phenotypes (**Figure 3.1C-F and Figure 3.4A-D**). This is consistent with the ability of nonsteroidal anti-inflammatory drugs (Zhou et al., 2012) or actin disruption (Plowman et al., 2005; Zhou and Hancock, 2015) to generate heterotypic mixed clusters, which compromise Ras signaling by reducing the physical engagement of downstream effectors. Interestingly, DHA is known to affect actin dynamics which may partially explain the mechanism underlying the formation of heterotypic clusters (Hou et al., 2012; Kim et al., 2008; Turk et al., 2013). Furthermore the lipid composition of caveolae, which also regulate Ras lateral segregation (Ariotti et al., 2014), is modified by long chain n-3 PUFA (Ma et al., 2004b). Specific lipid pools such as phosphatidylserine (PS), phosphatidic acid (PA), and phosphatidylinositol-4,5-bisphosphate (PIP_2) are key structural components of Ras nanoclusters (Zhou and Hancock, 2017; Zhou et al., 2014). Specifically, the lateral segregation and heterotypic mixing of H- and KRas is dependent on PS levels in the PM, where only optimal levels produce segregated clusters (Zhou et al., 2014). Interestingly, we have previously demonstrated that dietary fish oil results in the incorporation of EPA and DHA into the acyl chains of PS and to a lesser extent PIP_2 (Fan et al., 2003; Hou et al., 2012; Ma et al., 2004b). This is noteworthy, because KRas plasma membrane localization and nanoclustering requires specific PS acyl chain species (Zhou et al., 2017),

raising the possibility that the altered PS acyl chain profile generated by dietary fish oil may underlie its effects on Ras nanoclustering.

The *Drosophila* genome encodes three members of Ras (Ras1, Ras2 and Ras3), of which Ras1 and Ras2 appear to share similarity with the carboxy terminus region of exon 4B of human KRas (Shira Neuman-Silberberg et al., 1984). Thus, we utilized a mutated form of Ras1 (RasV12) for our *in vivo Drosophila* functional studies. Interestingly, long chain n-3 PUFA suppressed Ras1-dependent oncogenic signaling and phenotypes in the fly, similar to the murine model. We therefore posit that long-chain n-3 PUFA may also generate heterotypic mixed clusters of *Drosophila* Ras isoforms (**Figure 3.6**). However, further work is needed to address this possibility.

A common criticism facing the primary chemoprevention field is the fact the dietary bioactives, i.e., constituents in foods or dietary supplements other than those needed to meet basic human nutritional needs (Wallace et al., 2015), appear to be pleiotropic and affect diverse physiological processes including cell membrane structure/function (Turk et al., 2012), eicosanoid signaling (Fan et al., 2014; Serhan, 2014), nuclear receptor activation (Pegorier et al., 2004), and inflammatory responses (Hou et al., 2015; Kim et al., 2010). Our view is that this pleiotropic response of n-3 PUFA in regard to cancer treatment is a benefit that counteracts the cellular heterogeneity of cancer. From a chemoprevention perspective, we speculate that in addition to n-3 PUFA, other diet-derived amphiphilic compounds which accumulate in the colonic lumen, e.g., curcuminoids and polyphenols, may also alter plasma membrane organization and protein clustering (Chapkin et al., 2014; Fuentes et al., 2017; Hou et

al., 2016). This may in part explain the chemoprotective effects attributed to the consumption of high levels of fruits and vegetables in the Mediterranean diet (Fazio and Ricciardiello, 2014). Some supporting evidence documenting the interactive effects of membrane targeting bioactive compounds is provided by studies that demonstrate the combinatorial activity of curcumin and n-3 PUFA in gut stem cells during cancer initiation (Kim et al., 2016).

The complexity of cancer begins with the biological reprograming that occurs at the cellular level, but then scales exponentially with interactions taking place at the multi-cellular (McGranahan et al., 2015) and micro-environmental levels (Quail and Joyce, 2013). Cancer stem cells (CSCs) maintain intratumor complexity and heterogeneity, making it an ideal therapeutic target (Dragu et al., 2015). Importantly, n-3 PUFA modulation of Ras nanoscale organization may be useful in targeting CSCs, since salinomycin, a recently established CSC inhibitor, targets KRas signaling and suppresses stemness (Najumudeen et al., 2016). It is noteworthy, that DHA in part by altering lipid raft properties, has proven utility in inhibiting stem like properties that occur during epithelial mesenchymal transition (Tisza et al., 2014).

The differential effects of Ras isoforms on proliferation and tumor progression have largely been attributed to the HVR (Eisenberg et al., 2013). As such, colonic epithelial expression of oncogenic NRas, which lacks a polybasic repeat region but contains a palmitoylation site, fails to reproduce the growth properties imparted by oncogenic KRas (Haigis et al., 2008). This in part explains why colonic tumors predominantly contain KRas mutations (Prior et al., 2012) and therefore most strategies

are geared toward targeting this isoform. However, the KRas transcript is alternately spliced and two products are produced, i.e., K(B)-Ras, the form normally identified as KRas, and K(A)-Ras (Plowman et al., 2006). Recent work has demonstrated that both KRas isoforms are expressed in human tumor cells (Tsai et al., 2015), creating a need to therapeutically target both. The K(A)-Ras isoform contains a dual targeting motif distinct from K(B)-Ras, that has a small polybasic domain and is palmitoylated (Eisenberg et al., 2013; Tsai et al., 2015). Intriguingly, since n-3 PUFA can antagonize oncogenic HRas (**Figure 3.3B**) which is palmitoylated, it is possible that it would also inhibit K(A)-Ras signaling. Further studies are needed to address this question.

As the technology used to monitor plasma membrane dynamics evolves (Klymchenko and Kreder, 2014; Kwiatek et al., 2014; Stone et al., 2017), it is becoming increasingly apparent that the actions of endogenous (Sousa et al., 2015; Zhou et al., 2013) and exogenous (Machta et al., 2016; Zhang et al., 2016; Zhou et al., 2013) compounds are mediated in part through modifications of plasma membrane structure. In line with this, our novel observations support the feasibility of utilizing diet-related strategies that target plasma membrane organization to reduce oncogenic signaling and cancer risk (Escriba et al., 2015; Fuentes et al., 2017; Zalba and ten Hagen, 2017; Zhou et al., 2012).

3.4 Materials and methods

3.4.1 Cell Culture

Conditionally immortalized Young Adult Mouse Colonic (YAMC) cells and YAMC-HRasG12V were originally obtained from R.H. Whitehead, Ludwig Cancer Institute (Melbourne, Australia). YAMC cells (passages 14–19) were cultured under permissive conditions, 33°C and 5% CO_2 in RPMI 1640 media (Mediatech, Manassas, VA) supplemented with 5% fetal bovine serum (FBS; Hyclone, Logan, UT), 2 mM GlutaMax (Gibco, Grand Island, NY), 5 μg/mL insulin, 5 μg/ml transferrin, 5 ng/ml selenious acid (Collaborative Bio-medical Products, Bedford, MA), and 5 IU/mL of murine interferon-γ (Roche, Mannheim, Germany). Flies were fed a chemically defined holidic diet (Piper et al., 2014) that allowed for precise control over all ingredients.

3.4.2 Conditional Expression of UAS-Linked Transgenes

The esgGal4 driver was combined with a ubiquitously expressed temperature-sensitive Gal80 inhibitor (tubGal80ts). The escargot construct drives expression in stem cells using the EGFR-Ras axis to maintain stemness and suppress differentiation (Jiang et al., 2011; Korzelius et al., 2014). Crosses and flies were kept at 18°C (permissive temperature) and 5-day-old females were fed the test diets 5 days and then shifted to 29°C for 2 days to allow expression of the transgenes before analysis.

3.4.3 Immunostaining and microscopy

Intact fly guts were fixed at room temperature for 20 min in 100 mM glutamic acid, 25 mM KCl, 20 mM $MgSO_4$, 4 mM sodium phosphate, 1 mM $MgCl_2$, and 4% formaldehyde. All subsequent incubations were performed using PBS, 0.5% BSA, 0.1% Triton X-100 at 4°C. The following primary antibodies were used: anti-phospho-Histone H3 (Millipore; 1:1000), anti-armadello (1:250 dilution), obtained from the Developmental Studies Hybridoma Bank. Fluorescent secondary antibodies were obtained from Jackson Immunoresearch. Hoechst dye was used to stain DNA. Confocal microscopy images were collected using a Nikon Eclipse Ti confocal system and processed using Nikon software and Adobe Photoshop.

3.4.4 Western Blot Analysis of Intestinal Proteins

Intact female guts were dissected in cold PBS and proteins extracted in Laemmli buffer, separated on 10% acrylamide gel and transferred according to standard procedures (Karpac et al., 2013). Antibodies directed against phospho-ERK (Cell Signaling Technology; 1:1,000), ERK total (Cell Signaling Technology; 1:1,000), β-actin (Cell Signaling Technology; 1:5,000 dilution) were used. Total protein extracts were pooled from 4 guts.

3.4.5 Mouse genetics, diet and husbandry

The animal use protocol was approved by the University Animal Care Committee of Texas A&M University and conformed to NIH guidelines. To generate an inducible

colonic targeted oncogenic KRas mouse model, CDX2P-CreERT2 mice (Jackson Laboratory, Stock No: 022390) were crossed with LSL-K-ras G12D mice (Jackson Laboratory, Stock No: 008179). Mice were housed in cages in a temperature- and humidity-controlled animal facility with a 12 h light/dark cycle and fed lab chow. For *in vivo* diet studies, mice were fed experimental diets containing either n-6 (control) or n-3 PUFA for two weeks prior to tamoxifen injection (**Figure 3.1A**). Both diets contained 20% (w/w) casein, 42% sucrose, 22% cornstarch, 6% cellulose, 3.5% AIN-76 mineral mix, 1% AIN-76 vitamin mix, 0.3% methionine, 0.2% choline, and 0.02% t-butylhydroquinone (TBHQ). The n-6 diet contained 5% (w/w) corn oil (Dyets, Bethlehem, PA, #401150), and the n-3 diet contained 4% menhaden fish oil (Omega Pure, Houston, TX) and 1% corn oil. The diets were changed daily and contained TBHQ in order to prevent peroxidation (Fritsche and Johnston, 1988). Four weeks prior to termination, mice were injected once intraperitoneally (i.p.) with 200 mg/kg tamoxifen (Sigma-Aldrich, St. Louis, MO)(Feng et al., 2013) dissolved in corn oil or corn oil alone. For the purpose of measuring rates of colonic cell proliferation, mice were injected i.p. with 50 mg/kg EdU (Life Technologies, A10044) 2 h prior to termination. At the time of euthanasia, colon tissue was flushed with PBS and the colon was processed to generate Swiss-rolls (Kim et al., 2016). Swiss rolls were subsequently fixed in 4% paraformaldehyde and embedded in paraffin.

3.4.6 In vivo measurement of crypt length and proliferation

For crypt length, tissue sections were stained with Alcian blue and imaged with a Leica Aperio CS2 digital pathology scanner. Crypt measurement was performed using ImageScope software. For cell proliferation assays, formalin-fixed paraffin-embedded 4 μm colon sections were deparaffinized and rehydrated through graded ethanol washes. Cell proliferation in colonic crypts was measured using the Click-iT EdU Alexa Fluor 555 Imaging kit (Life Technologies) as per the manufacturer's instructions (Kim et al., 2016). Negative control slides were incubated without Click-iT Edu Alexa Fluor 555.

3.4.7 Fluorescence lifetime imaging microscopy combined with fluorescence resonance energy transfer (FLIM-FRET)

YAMC cells were seeded at a density of $1x10^4$ in cell imaging 8 chamber coverglass (Eppendorf, 0030742036) 24 h prior to fatty acid-BSA (50 uM) treatment. Following a 24 h incubation period, media without fatty acid was added and Lipofectamine 3000 was used to transiently transfect cells with plasmids of donor (GFP-tagged protein) alone or co-transfected with FRET acceptors (Zhou and Hancock, 2015; Zhou et al., 2015). FRET acceptors were RFP-tagged proteins of interest (GFP-: RFP-plasmid at 1:3 ratio, 0.25 μg total plasmid per well). After 8 h in transfection media, cells were gently washed with PBS and incubated with complete media plus fatty acids for 40 h. Subsequently, cells expressing GFP-tagged protein alone or co-expressing both GFP-tagged and RFP-tagged proteins were washed with PBS and fixed in 4% PFA for 15 min. After three washes in 1X PBS, HPBS was added to wells. Cells were imaged with a 1.3

numerical aperture 40x Plan-Fluor oil objective mounted on a wide field Nikon Eclipse microscope. GFP was sinusoidally excited by a modulating 3-Watt 497 nm light-emitting diode (LED) at 40 MHz and fluorescence lifetime measured using a Lambert Instrument (Roden, The Netherlands) FLIM unit. At least 40 individual cells were imaged and lifetime (phase) values were pooled and averaged. Each experiment was replicated 2 times. Statistical analysis was performed using one-way ANOVA.

For *Drosophila* FLIM experiments, adult flies expressing GFP/RFP constructs in gut stem cells were dissected in PBS and fixed 20 min in 4% PFA prior to mounting in Mowiol medium. Fields of view were scanned with an inverted LSM 780 microscope (Carl Zeiss Microimaging, Thornwood, NY) and a 1.4 numerical aperture 40× Plan Apochromat oil objective. Two-photon excitation was provided by a Chameleon (Coherent Inc.) Ti:sapphire laser tuned to 900 nm. Emission events were registered with FastFLIM system (ISS, Champaign, IL). Fluorescence lifetime images (256 × 256 pixels) were acquired with a pixel dwell time of 6.3 μs. Lifetime of the imaged samples was determined with the frequency domain technique using the ISS VistaVision Suite version 4.1. At least 10 images were collected per treatment. The percentage of the apparent FRET efficiency (E_{app}) was calculated using the measured lifetimes of each donor-acceptor pair (τ_{DA}) and the average lifetime of the donor only (τ_D) samples. The formula employed was Eapp = $(1-\tau_{DA}/\tau_D)$ x 100% (Posada et al., 2016).

3.4.8 Immunofluorescence

Cells were seeded in cell imaging 8 chamber coverglass slides (Eppendorf, 0030742036) and treated with select fatty acids (50 uM) for 72 h. Cells were subsequently starved (0.5% FBS, YAMC; 0% FBS, SW48) for 18 h in the presence of fatty acid, stimulated with EGF (25 ng/ml) (PeproTech, 315-09) for 5 min and immediately fixed in ice cold 100% methanol. Cells were incubated with primary phosphor-ERK (Cell Signaling Technology, #4370, dilution 1:200) antibody followed by Alexa Fluor 647-conjugated secondary antibody (Jackson, #711-605-152, dilution 1:400). CellMask™ Green Plasma Membrane Stain (ThermoFisher, #C37608, dilution 1:1000) was used to label the cells and Hoechst 33342 (ThermoFisher, #H3570, 5 ug/mL) to label the nucleus. Cells were imaged with a 1.3 numerical aperture 40x Plan-Fluor oil objective or 1.4 numerical aperture 100x Plan-Apo oil objective mounted on a wide field Nikon Eclipse microscope using identical settings between samples. For analysis, images were opened in ImageJ (NIH), converted to Tiff files and a custom macro was used to quantify average fluorescent intensity of pERK. Briefly, green membrane stain was used to define a binary cell mask that was applied to pERK images. Average fluorescent intensity of the mask images was subsequently recorded (**Figure 3.7**).

3.4.9 Lipid extraction and fatty acid analysis

For assessment of dietary lipid incorporation into membrane phospholipids, total lipids were extracted from isolated mouse crypts (Ma et al., 2004b) and at least 28 dissected drosophila guts per treatment with 2:1 (v/v) chloroform-methanol as previously

described (Fan et al., 2003). Total phospholipids were subsequently separated by thin-layer chromatography with 90:8:1:0.8 (v/v/v/v) chloroform-methanol-acetic acid-water. After transesterification using methanolic HCl, fatty acid methyl esters were quantified by capillary gas chromatography-mass spectrometry (Fan et al., 2003).

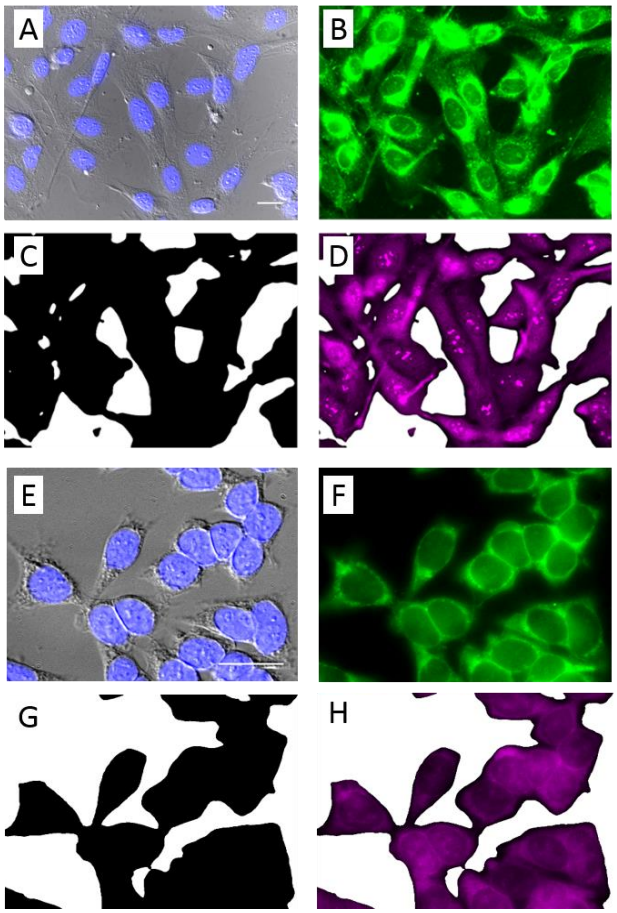

Figure 3.7. Quantitative image based analysis of pERK. (A) YAMC-HRasG12V or (E) Sw48-KRasG12D cells were grown in 8-well glass bottom dishes and treated with 50 uM indicated fatty acid for 72 h. Cells were starved (0.5% FBS, YAMC; 0% FBS, SW48) for 18 h in the presence of fatty acid and subsequently stimulated with EGF (25 ng/ml) for 5 min. Cells were then immediately fixed in ice cold 100% methanol. (A, B) merged DIC and DAPI images; (B, F) CellMaskTM Green Plasma Membrane Stain was used to define (C, G) binary whole cell masks, which was used to create (D, H) masked images of pERK. Scale bar = 20 µM.

CHAPTER IV

LONG CHAIN n-3 FATTY ACIDS DISRUPT COLINIC CELL MACROPOINOCYTOSIS

4.1 Introduction

n-3 PUFA (DHA and EPA) found in fish oil, are often described as chemoprotective with respect to colon cancer (Hall et al., 2008). The mechanism underlying this association is not well resolved. Approximately 30-50% of colorectal cancers contain KRas mutations, which confer resistance to standard therapy (Stephen et al., 2014), and reduce survival (Phipps et al., 2013). Unfortunately, attempts to directly target Ras have repeatedly failed (Phipps et al., 2013), leading to strategies developed that target identified dependencies such as unique metabolic requirements (Cox et al., 2014). Macropinocytosis is the cellular process of engulfment of extracellular components driven by dynamic changes in plasma membrane lipids and cytoskeletal proteins (Bohdanowicz and Grinstein, 2013; Levin et al., 2015; Lim and Gleeson, 2011), which has been identified as the delivery route for the fuel that feeds these cancers (Commisso et al., 2013; Salloum et al., 2014). Since we previously demonstrated that n-3 PUFA modify plasma membrane organization through a cytoskeletal mediated process (Chapkter II), we sought to determine if the clinically relevant, cytoskeletal mediated process of macropinocytosis would be inhibited.

By using colonic cell lines and *in vivo* transgenic models, we show that n-3 PUFA attenuate macropinocytosis. Furthermore, we elucidate a mechanism by which expression of oncogenic KRas results in an increase in plasma membrane rigidity which

is maintained by increased plasma membrane free cholesterol levels. Normalization of plasma membrane rigidity through incorporation of n-3 PUFA or cholesterol depletion results in an attenuation of macropinocytosis. These findings demonstrate how n-3 PUFA act as chemoprotective agents, and identify plasma membrane rigidity as a pharmacological target for oncogenic KRas driven colon cancers.

4.2 Results

4.2.1 Macropinocytosis is attenuated by n-3 PUFA

Previous experiments demonstrated that long chain n-3 PUFA reduced the rigidity of live cell plasma membranes (**Figure 2.2**), and disrupted membrane-cytoskeletal connections indirectly (**Figure 2.4**) or directly through attenuation of Rac1 and Cdc42 (Turk et al., 2013). Therefore we sought to determine the effect of n-3 PUFA on a cellular process which depends on plasma membrane-cytoskeletal interactions, i.e. macropinocytosis (Fujii et al., 2013; Grimmer et al., 2002; Maekawa et al., 2014).

Macropinocytosis was determined by an imaging based assay which relies on the identification and quantification of internalized fluorescently labeled dextrans (Commisso et al., 2014). When stimulated with epidermal growth factor (EGF), YAMC cells exhibit an increase in macropinocytosis which is attenuated by DHA and EPA (**Fig 4.1A & B**). Importantly, *fat-1* mouse derived crypts also exhibited reduced macropinocytosis (**Fig 4.1C & D**).

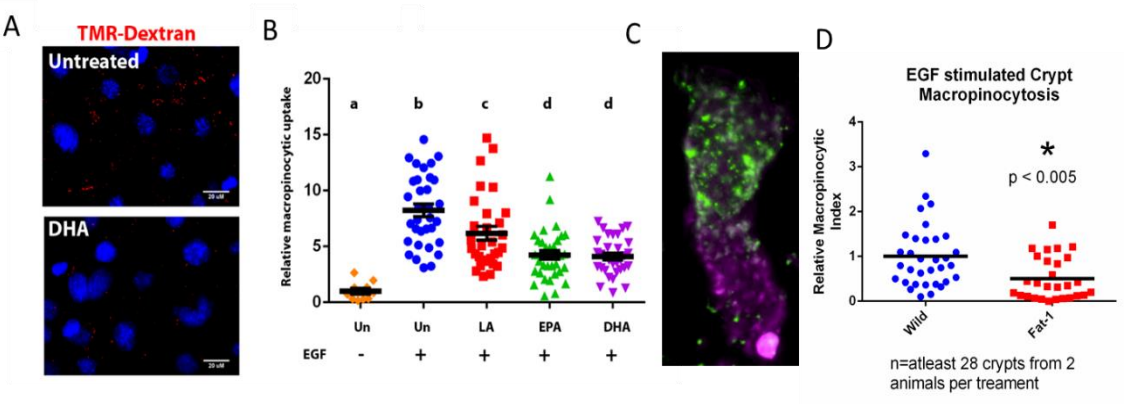

Figure 4.1. Macropinocytosis is attenuated by n-3 PUFA. Macropinocytosis uptake was determined by incubating (A) YAMC cells or (C) colonic crypts with fluorescently labeled dextrans for 15 minutes with or without the presence of EGF (100 ng/ml). (B) Quantification of relative macropinocytotic index of cells incubated with 50 uM FA for 72 hrs. Data represent mean macropinocytosis uptake from each field of view (FOV, n= Un –EGF 10, Un +EGF 33, LA 30, EPA 34 and DHA 32) from 2 independent experiments. (D) Colonic crypts isolated from fat-1 mice show reduced macropinocytosis. Data represent mean macropinocytosis per crypt from at least 28 crypts from 2 animals per genotype. Statistical significance between treatments as indicated by different letters ($P<0.05$) was examined using one-way ANOVA and uncorrected Fisher's LSD tests or indicated by (*$P < 0.005$) was determined using an unpaired t-test.

Since EGF mediated Ras activation is linked to macropinocytosis and DHA is known to disrupt the EGFR-Ras axis (Ma et al., 2004b; Rogers et al., 2010; Turk et al., 2012), we sought to determine if n-3 PUFA effects on macropinocytosis is independent of Ras activation. For this purpose, we utilized a genetically encoded biosensor that reports on Ras activation by surveying the temporal GEF/GAP activity in H- and K-Ras domains (Fukano et al., 2007; Mochizuki et al., 2001). These Ras-Raichu probes exhibit high FRET efficiency when in the GTP bound state (Mochizuki et al., 2001). Only

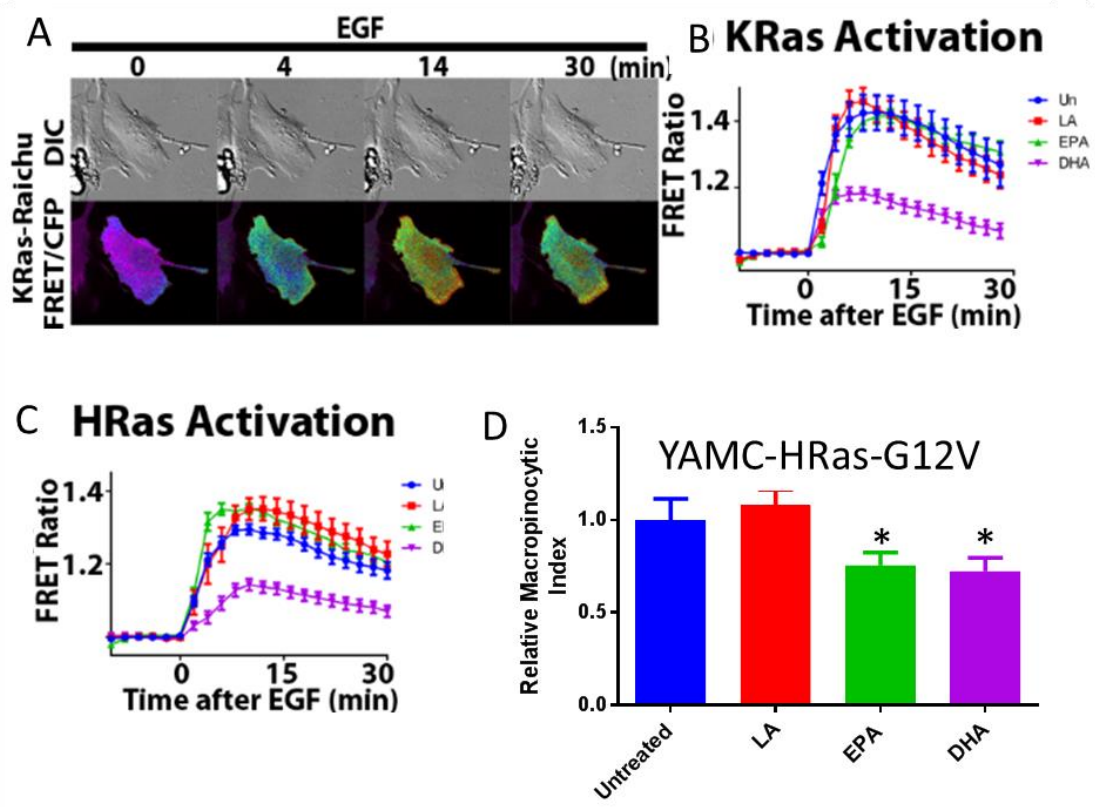

Figure 4.2. Long chain n-3 PUFA attenuation of macropinocytosis is independent of EGF-mediated Ras activation status. (A) Spatiotemporal activation of Ras was determined by monitoring activation of Ras-Raichu FRET biosensors targeted to (B) K- or (C) H-Ras domains. (D) Non-EGF stimulated oncogenic Ras driven macropinocytosis was determined in YAMC cells expressing oncogenic HRasG12V proteins incubated with 50 uM FA for 72 hrs. Data represent mean ± SEM FRET ratio for each cell, (B) n=Un 9, LA 11, EPA 11 and DHA 9 from 1 experiment, (C) n=Un 26, LA 10, EPA 10 and DHA 22 from 2 independent experiments. (D) Data represent mean macropinocytosis uptake from each field of view (FOV, n=Un 20, LA 15, EPA 18 and DHA 16). Statistical significance between treatments as indicated by different letters ($P<0.05$) was examined using one-way ANOVA and uncorrected Fisher's LSD tests.

DHA was able to attenuate Ras activation (**Figure 4.2A-C**) in both H- and K-Ras domains, indicating a Ras independent effect of EPA to attenuate EGF stimulated macropinocytosis. Furthermore, EGF independent constitutive macropinocytosis driven

by oncogenic HRasG12V (Commisso et al., 2013; D'Abaco et al., 1996) was attenuated by both EPA and DHA (**Figure 4.2D**).

4.2.2 Cholesterol depletion reduces membrane order and macropinocytosis

Since n-3 PUFA disrupt membrane order and macropinocytosis, we sought to determine if there is a relationship between membrane order and macropincoytosis. As a means of pharmacologically disrupting membrane order, YAMC cells were treated with several doses of MBCD to deplete cholesterol (**Figure 4.3A&B**), reduce membrane order (**Figure 2.1**), and subsequently attenuate macropincoytosis (**Figure 4.3C**).

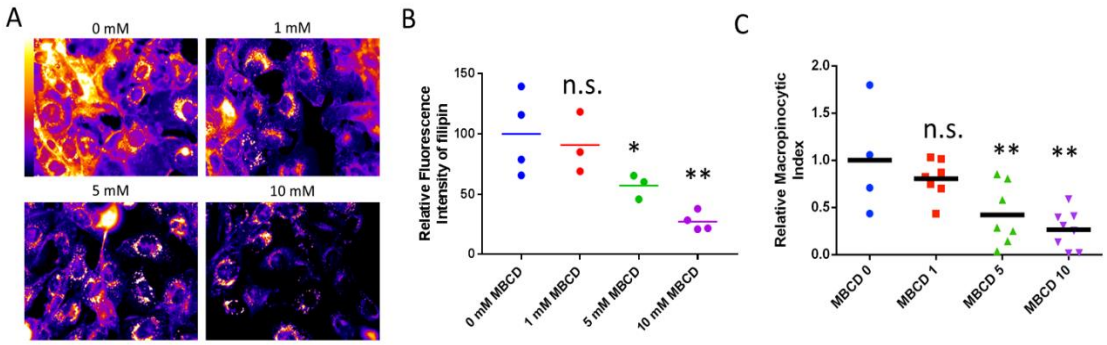

Figure 4.3. Methyl-β-cyclodextrins depletes cholesterol, reduces membrane order and attenuates macropinocytosis in YAMC cells. YAMC cells were pre-incubated with the indicated dose of MβCD (0-10 mM) for 30 min followed by (A) staining with filipin to determine (B) cholesterol, or incubated with EGF (100 ng/ml, 15min) and FITC-Dextran to determine macropinocytosis. (B) Data represent mean filipin intensity from each FOV from n= (MβCD 0mM 4, MβCD 1mM 3, MβCD 5mM 3, MβCD 10mM 4). (C) Relative macropinocytotic index from each FOV from n= MβCD 0 mM 4, MβCD 1 mM 7, MβCD 5 mM 7, MβCD 10 mM 8) with ~10 cells per FOV. Statistical significance of differences between untreated control and treated cells were examined using one-way ANOVA tests (n.s., not significant; *P < 0.05; **P < 0.01).

4.2.3 Oncogenic Ras increases membrane order through increased cholesterol which facilitates macropinocytosis

Oncogenic Ras expressing cells constitutively upregulate macropinocytosis to provide fuel necessary for metabolic reprogramming (Commisso et al., 2013; Salloum et

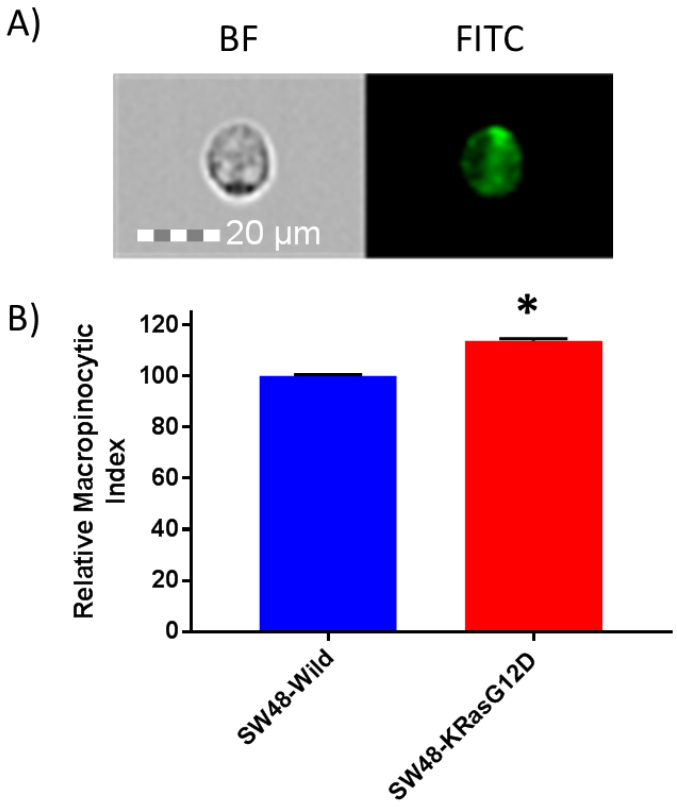

Figure 4.4. Oncogenic KRasG12D expressing SW48 cells exhibit increased macropinocytosis. SW48 wild type and KRasG12D expressing cells were incubated with fluorescently (FITC) labeled dextran (70 kDa, 1 mg/mL) for 30 minutes, trypsinized, fixed in PFA, and assayed using an imaged based flow cytometry system (Amnis FlowSight). (A) Representative bright field and FITC image. (B) Quantification of macropinocytosis normalized to wild type control. Data represent mean ± SEM for at least 1,000 cells. Statistical significance between wild type control and KRasG12D expressing cells (*P < 0.0001) was determined using an unpaired t-test.

al., 2014). Activation of PI3K, PLC, and Rac1 play a role in this process (Bar-Sagi and Feramisco, 1986; Porat-Shliom et al., 2007; Walsh and Bar-Sagi, 2001), however the contribution of plasma membrane organization to this process has not been established. Similarly, phagocytosis, although distinct from macropinocytosis, is a cellular internalization process which requires coordinated membrane-cytoskeletal dynamics and maintenance of rigid membrane domains (Magenau et al., 2011).

Isogenic cell lines expressing oncogenic H- or K-Ras showed increased macropinocytosis under basal conditions vs parental cells with wild type Ras (**Figure 4.4**). SW48 cells expressing oncogenic KRas exhibited increased PM rigidity (**Figure 4.5**), likely driven by an increase in plasma membrane free cholesterol (**Figure 4.6**). Importantly these results are not an artifact of overexpression as these cell lines are engineered to express endogenous levels of oncogenic KRas (Hammond et al., 2015).

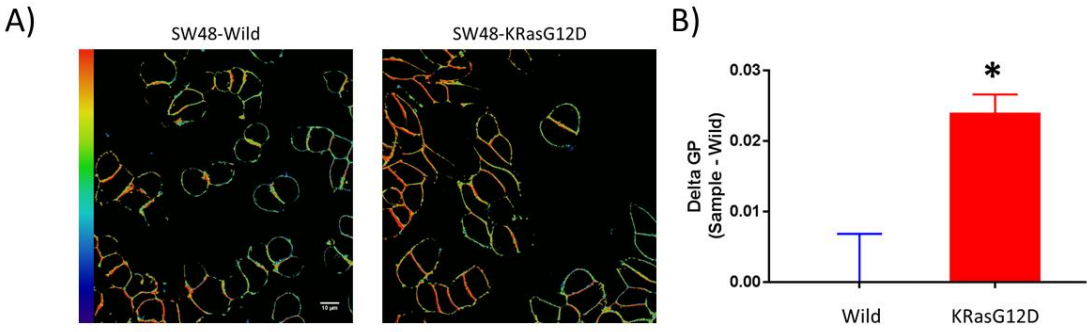

Figure 4.5. Oncogenic KRasG12D expressing SW48 cells exhibit increased membrane order. SW48 wild type and KRasG12D expressing cells were stained with Di-4-aneppdhq (5uM) and immediately imaged by confocal microscopy. (A) Representative GP images. (B) Quantification of membrane order. Values are expressed as delta GP (sample – control). Data represent mean ± SEM for at least 15 field of views containing at least 150 cells from 2 independent experiments. Statistical significance between wild type control and KRasG12D expressing cells (*P < 0.001) was determined using an unpaired t-test.

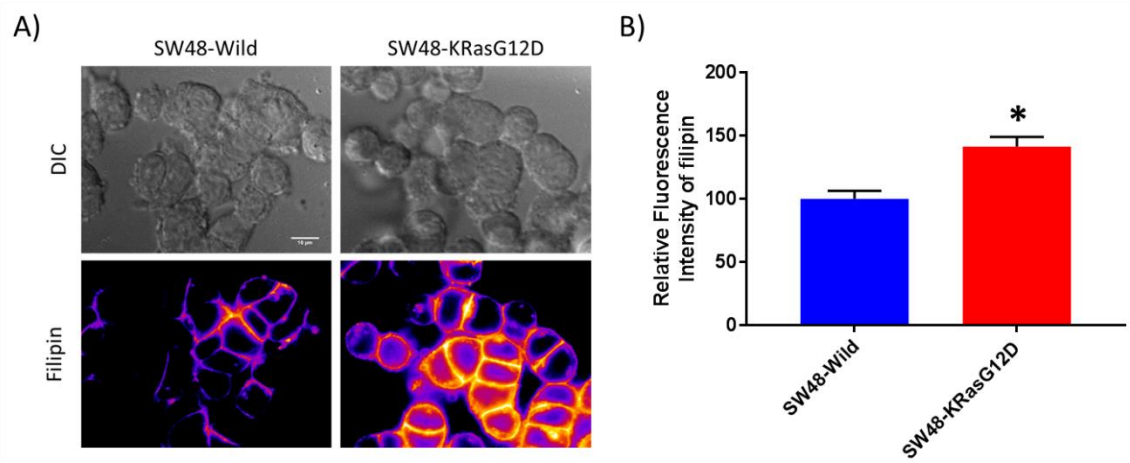

Figure 4.6. Oncogenic KRasG12D expressing SW48 cells exhibit increased cholesterol. SW48 wild type and KRasG12D expressing cells were stained with filipin III (50 ug/ml) for 45 minutes on ice in the dark, followed by imaging by wide filed microscopy. (A) Representative DIC and filipin intensity images. (B) Quantification of filipin intensity. Values are normalized to wild type control. Data represent mean ± SEM for at least 5 fields of views containing at least 60 cells. Statistical significance between wild type control and KRasG12D expressing cells (*$P < 0.01$) was determined using an unpaired t-test.

We subsequently confirmed our *in vitro* results (SW48 cells) utilizing an *in vivo* mouse model in which oncogenic KRas is inducibly targeted to the colon as described previously (Feng et al., 2011, 2013) (**Figure 3.1B**). Mice were fed a diet containing corn oil (n-6 PUFA control) or fish oil (**Tables 3.1 & 3.2**) for 2 wks prior to tamoxifen induction of oncogenic KRas and maintained for an additional 11-13 weeks. As we observed *in vitro*, primary oncogenic expressing colonic crypts from mice fed a corn oil diet exhibited increased macropinocytosis (**Figure 4.7**), membrane order (**Figure 4.8**) and cholesterol (**Figure 4.9**) vs corn oil injected wild type control crypts (**Figure 4.7-4.9**). Importantly, the macropinocytosis and membrane order phenotype was reversed to

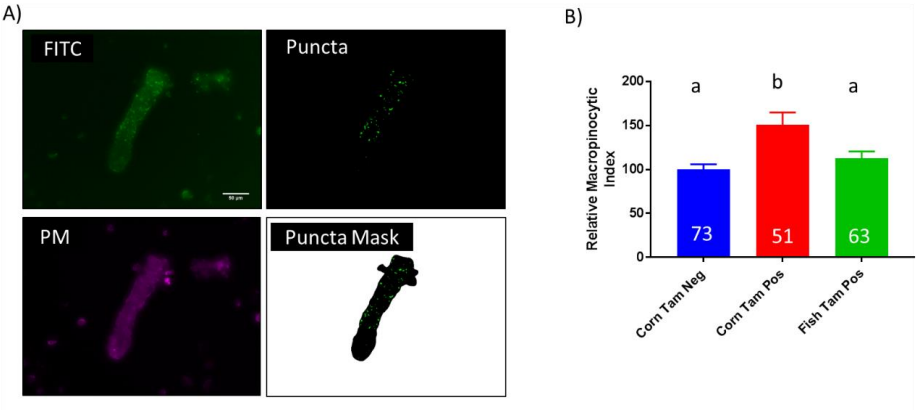

Figure 4.7. Dietary fish oil ameliorates oncogenic KRas mediated macropinocytosis in isolated colonic crypts. Mice were fed experimental diets for 2 weeks prior to induction of oncogenic KRasG12D in the colon by injection of tamoxifen (200 mg/kg, 1X). Isolated colonic crypts were incubated with FITC-Dextran (1mg/ml) and deep red plasma membrane stain for 30 minutes, fixed and imaged with a 20x oil objective. A) Representative crypt used to define regions of interest. B) Quantitative macropinocytosis data. Bars represent mean ± SEM from number of crypts indicated in each bar, from at least four mice in each group normalized to the corn oil, no Tamoxifen control. Statistical significance between treatments as indicated by different letters ($P<0.05$) was examined using Tukey's multiple comparisons test.

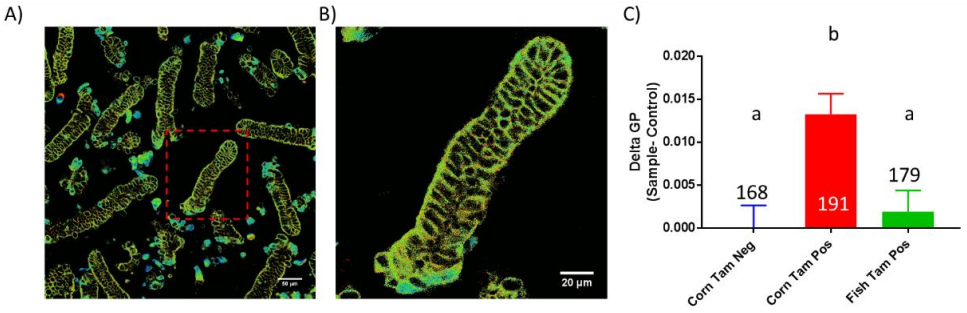

Figure 4.8. Dietary fish oil ameliorates oncogenic KRas mediated membrane order in isolated colonic crypts. Mice were fed experimental diets for 2 weeks prior to induction of oncogenic KRasG12D in the colon by injection of tamoxifen (200 mg/kg, 1X). After 10-12 weeks post tamoxifen injection, isolated colonic crypts were stained with Di-4-aneppdhq (5 uM) and immediately imaged with a 20x oil objective. A) Example field of view containing multiple crypts. B) Representative crypt used to define region of interest. C) Quantitative membrane order data. Bars represents mean ± SEM from the number of crypts indicated in each bar, from at least four mice in each group, normalized to corn oil no Tamoxifen control. Statistical significance determined by Tukey's multiple comparisons test.

basal wild type levels by the dietary administration of fish oil (**Figure 4.7 & 4.8**). Interestingly, although fish oil treatment reduced membrane order, it did not significantly reduce plasma membrane free cholesterol in the tamoxifen injected oncogenic KRas expressing group (**Figure 4.9**). In a subset of mice we further verified the increase in membrane order and membrane cholesterol at 20 weeks post oncogenic KRas induction. This analysis was performed using imaged based flow cytometry of isolated single cells from primary crypts (**Figure 4.10**). In this set of experiments, dietary fish oil treatment reduced membrane order and cholesterol levels relative to the oncogenic KRas expressing corn oil control (**Figure 4.10**).

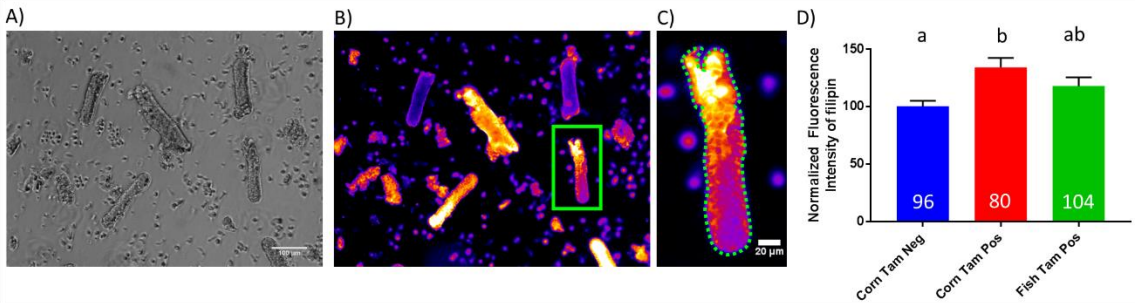

Figure 4.9. Dietary fish oil ameliorates oncogenic KRas mediated increase of free cholesterol in isolated colonic crypts. Mice were fed the experimental diets for 2 weeks prior to induction of oncogenic KRasG12D in the colon by injection of tamoxifen (200 mg/kg, 1X). After 11-13 weeks, isolated colonic crypts were fixed and stained with filipin III (50 ug/ml) for 45 minutes on ice in the dark, imaged with a 10x 0.3 NA phase objective. Representative (A) phase and (B) filipin field of view. (C) Representative region of interest (dashed green) defining crypts in filipin image. D) Quantitative free cholesterol data. Bars represent mean ± SEM from the number of crypts indicated in each bar in at least four mice per each group, normalized to corn oil, no Tamoxifen control. Statistical significance determined by Tukey's multiple comparisons test.

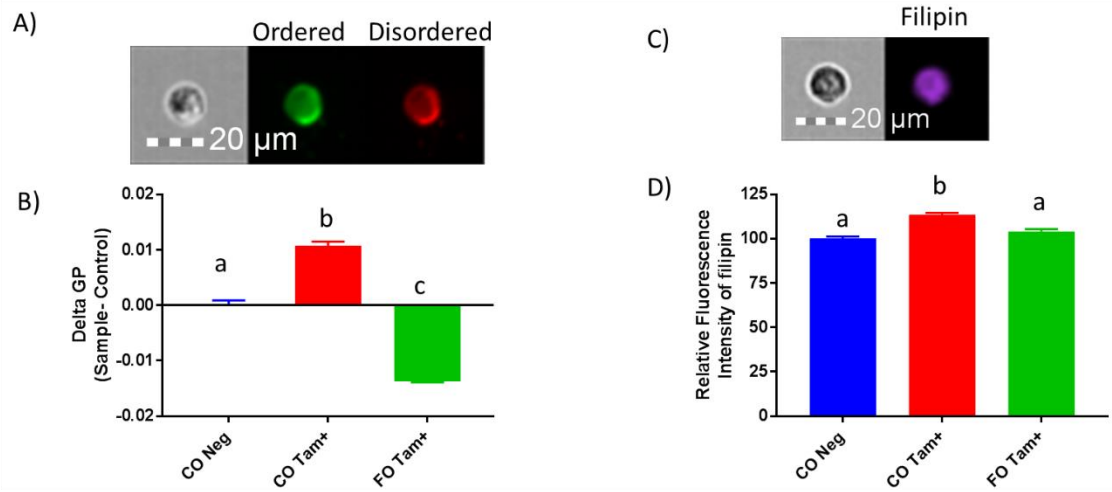

Figure 4.10. Dietary fish oil ameliorates oncogenic KRas mediated increase in membrane order and cholesterol in single cells from isolated colonic crypts. Mice were fed the treatment diets for 2 weeks prior to induction of oncogenic KRasG12D in the colon by injection of tamoxifen (200mg/kg, 1X). Single cells were generated from colonic crypts after 20 weeks and stained with Di-4-aneppdhq (1 uM) or fixed, stained with filipin (50 ug/ml, 45 min) and imaged on the Flowsight imaging system. A) Representative image and B) quantitative membrane order data. C) Representative images and D) quantitative free cholesterol (filipin) data. Bars represent mean ± SEM from at least 10,000 events from two mice in each group, normalized to corn oil, no Tamoxifen control. Statistical significance determined by Tukey's multiple comparisons test.

4.3 Discussion

In this work we investigated the relationship between plasma membrane rigidity and macropinocytosis during exogenous treatment with long chain n-3 PUFA and the induction of oncogenic KRas. We demonstrate for the first time live cell plasma membrane rigidity and macropinocytotic capacity are highly correlated.

Long chain n-3 PUFA attenuated EGF stimulated colonic cell macropinocytosis *in vitro* an *in vivo* (**Figure 4.1**). Importantly this was not a direct effect of DHA on EGF activation (Ma et al., 2004b; Rogers et al., 2010; Turk et al., 2012), since EPA which

does not affect EGF mediated Ras activation (**Figure 4.2**), also attenuated macropinocytosis (**Figure 4.1A**). Further evidence was provided by n-3 PUFAs attenuation on non-EGF stimulated macropinocytosis (**Figure 4.2D**) in YAMC cells expressing a HRasG12V mutation (Commisso et al., 2013; D'Abaco et al., 1996).

Oncogenic Ras expression *in vivo* and *in vitro* resulted in an increase of macropinocytosis (**Figure 4.4 & 4.7**) accompanied by an increase in membrane rigidity (**Figure 4.5 & 4.8**) triggered by plasma membrane free cholesterol accumulation (**Figure 4.6 & 4.9**). Reducing membrane rigidity through cholesterol depletion (**Figure 4.3**) or membrane incorporation with n-3 PUFA reduced macropinocytosis (**Figure 4.7 & 4.8**). Further work will be required to probe the exact mechanism underlying the ability of oncogenic KRas to upregulate free cholesterol. A possible explanation for the increase in cholesterol may involve the cholesterol transporter ABCA1, which is down regulated by oncogenic Ras (Smith and Land, 2012) and is known to alter plasma membrane biophysical properties (Zarubica et al., 2009), Rac1 activation (Pagler et al., 2011) and affect endocytosis (Zarubica et al., 2009).

Taken together, our data indicate that exogenous treatments that reduce plasma membrane rigidity may prove useful in attenuating oncogenic KRas mediated macropinocytosis. Establishing a role of long chain n-3 PUFA in colon cancer prevention would have a major translational impact because these dietary bioactives are safe, well tolerated, relatively inexpensive, and provide additional health benefits, such as reduction in mortality (Bell et al., 2014). In addition, the ingestion of long chain n-3

PUFA in combination with other agents with complementary anti-tumor action may improve their efficacy in colon cancer prevention/therapy.

4.4 Materials and methods

4.4.1 YAMC Cell Culture

Conditionally immortalized Young Adult Mouse Colonic (YAMC) cells and YAMC-HRasG12V were originally obtained from R.H. Whitehead, Ludwig Cancer Institute (Melbourne, Australia). YAMC cells (passages 14–19) were cultured under permissive conditions, 33°C and 5% CO_2 in RPMI 1640 media (Mediatech, Manassas, VA) supplemented with 5% fetal bovine serum (FBS; Hyclone, Logan, UT), 2 mM GlutaMax (Gibco, Grand Island, NY), 5 μg/mL insulin, 5 μg/ml transferrin, 5 ng/ml selenious acid (Collaborative Bio-medical Products, Bedford, MA), and 5 IU/mL of murine interferon-γ (Roche, Mannheim, Germany). Isogenic SW48 parental and KRasG12D cells (Horizon Discovery) were maintained at 33°C and 5% CO_2 in McCoy's 5A medium supplemented with 10% FBS. Select cultures were treated for 72 h with 50 μM fatty acid [linoleic acid (LA, 18:2n6), arachidonic acid (AA, 20:4n6), eicosapentaenoic acid (EPA, 20:5n3) or docosahexaenoic acid (DHA, 22:6n3); NuChek, Elysian, MN] complexed with fatty acid free bovine serum albumin (BSA).

4.4.2 Macropinocytosis Assay

Macropinocytosis assay was performed as described previously (Commisso et al., 2014). Briefly, YAMC cells were treated with FA were serum starved (0.5%, FBS)

for 12-18 hours, incubated with 0.5 mg/mL TMR-Dextran and stimulated with EGF (100 ng/ml) for 15 minutes at 33°C and fixed in 4% PFA, and mounted with ProLong Diamond with DAPI (Life Technologies).

4.4.3 Ras-Raichu FRET Biosensor Ratiometric Imaging and Quantification

YAMC cells were untreated or treated with indicated PUFA for 24 hours then transfected with plasmid encoding H-Ras (Raichu-141x) and K-Ras (Raichu-124x) targeted Ras-Raichu biosensors (Mochizuki, 2001). Cells were then treated an additional 48 hours and starved in Phenol free-RPMI (0.5%, FBS), 1% Glutamax, 1% Pen/Strep, with IFN-y, no ITS for 4 hours before stimulation with EGF (25 ng/ml). Images were acquired with a Nikon wide field microscope equipped with a 1.4 numerical aperture 63× Plan Apochromat oil objective, every 2 minutes, starting 10 minutes before EGF stimulation and ending 30 minutes after. Images were processed and FRET ratio determined as described previously (Aoki, 2009).

4.4.4 Mouse genetics, diet and husbandry

Animal use protocols were approved by the University Animal Care Committee of Texas A&M University and conformed to NIH guidelines. To generate an inducible colonic targeted oncogenic KRas mouse model, CDX2P-CreERT2 mice (Jackson Laboratory, Stock No: 022390) were crossed with LSL-K-ras G12D mice (Jackson Laboratory, Stock No: 008179). Mice were housed in cages in a temperature- and humidity-controlled animal facility with a 12 hour light/dark cycle and fed lab chow. For

in vivo diet studies, mice were fed experimental diets containing either n-6 (control) or n-3 PUFA for two weeks prior to tamoxifen injection (**Figure 3.1A**). Both diets contained 20% (w/w) casein, 42% sucrose, 22% cornstarch, 6% cellulose, 3.5% AIN-76 mineral mix, 1% AIN-76 vitamin mix, 0.3% methionine, 0.2% choline, and 0.02% t-butylhydroquinone (TBHQ). The n-6 diet contained 5% (w/w) corn oil (Dyets, Bethlehem, PA, #401150), and the n-3 diet contained 4% menhaden fish oil (Omega Pure, Houston, TX) and 1% corn oil. Diets were changed daily and contained TBHQ in order to prevent peroxidation (Fritsche and Johnston, 1988). At indicated times prior to termination, mice were injected once intraperitoneally (i.p.) with 200 mg/kg tamoxifen (Sigma-Aldrich, St. Louis, MO)(Feng et al., 2013) dissolved in corn oil or corn oil alone (control).

CHAPTER V

SUMMARY AND CONCLUSIONS

5.1 Summary

With respect to all human malignancies, 35% are linked directly to diet and an additional 14-20% to obesity (Coussens et al., 2013). Consistent with these data, cancer risk can be lowered by 36% when humans adhere to healthy dietary principles, e.g., high intake of fruits, vegetables, and whole grains and low meat consumption (Ford et al., 2009). Therefore, it is imperative that health professionals make sound dietary/lifestyle recommendations. However, even though there are many observational/epidemiological studies linking diet and cancer risk, the association cannot be easily explained mechanistically. Therefore, establishing a role for cancer dietary chemoprevention approaches that are generally free of safety problems intrinsic to drugs administered over long periods of time would have a major translational impact in cancer prevention and patient survivorship (Ford et al., 2009; Lien, 2009). In view of this need, our long-term goal is to better understand the molecular mechanisms modulating intestinal epithelial cell responses to MTDB's.

Notably, we have demonstrated that dietary n-3 PUFA modify colonocyte plasma membrane biophysical properties *in vitro* and *in vivo,* in a manner that is dependent on cytoskeletal interactions (**Figures 2.2 & 2.5**). In addition, a very similar phenotype was observed in activated $CD4^+$ T cells (**Figure 2.6**). Furthermore, we documented for the first time that membrane phase separation is induced following high dose n-3 PUFA in human $CD4^+$ T cell GPMVs (**Figure 2.6**).

We also documented the ability of n-3 PUFA to reshape the nanoscale architecture of Ras nanoclusters. Esterification of n-3 PUFA into plasma membrane phospholipids in vitro (**Table 3.3**) resulted in the formation of heterotypic mixed clusters of H- and KRas (**Figure 3.2 & 3.4**). These clusters signaled through ERK less efficiently (**Figure 3.3**), resulting in the attenuation of oncogenic Ras driven phenotypes in both murine (**Figure 3.1**) and *Drosophila* (**Figure 3.4**) models. Additionally, we found that a reduction in plasma membrane rigidity associated with n-3 PUFA incorporation (**Figure 4.2**) or cholesterol depletion (**Figure 4.3)**, attenuated colonic cell macropinocytosis. This is highly relevant because macropinocytosis has recently been identified as a dependency of oncogenic Ras driven tumors (Commisso et al., 2013). Using isogenic cell lines and *in vivo* mouse models, we then determined that oncogenic KRas increases plasma membrane rigidity via upregulation of plasma membrane free cholesterol levels (**Figure 4.5, 4.6, 4.8-4.10**). The ability of oncogenic KRas to increase macropinocytosis was dependent on the biophysical rigidification of the membrane imparted by the accumulation of cholesterol, as n-3 PUFA, which fluidized the membrane (**Figure 4.8**), attenuated macropinocytosis (**Figure 4.7**) but did not significantly alter cholesterol levels (**Figure 4.9**). These findings suggest that the dietary/pharmacological targeting of plasma membrane rigidity may suppress oncogenic KRas driven colonic tumors.

5.2 Future directions

The data presented herein contribute to the mechanistic understanding of how n-3 PUFA influence Ras mediated phenotypes, however many questions still remain regarding the precise impact of n-3 PUFA on cellular function. Furthermore, this research raises the question; are the chemoprotective effects attributed to other dietary MTDB's also linked to the modulation of plasma membrane hierarchical organization?

5.2.1 Plasma membrane cytoskeleton interaction

Our data demonstrate that the effect of n-3 PUFA on membrane organization is in part mediated by the actin cytoskeleton (**Figure 2.2 & 2.5**). Therefore, it is important to directly assess the effects on n-3 PUFA on the cytoskeleton. The cytoskeletal cortical actin mesh influences plasma membrane organization (Alvarez-Guaita et al., 2015; Dinic et al., 2013; Garcia-Parajo et al., 2014; Owen et al., 2012b). Importantly, this cortical actin mesh network structure is modulated at the sub-resolution scale (~1-20 nm), therefore conventional microscopy techniques may not provide sufficient resolution. Recent super-resolution techniques such as SIM (~50-100 nm) (Rego et al., 2012) are approaching the necessary resolution and others PALM/STORM (10-20 nm) (Xu et al., 2012) may achieve the resolution necessary to determine an effect of DHA on the cytoskeleton. Other techniques such as electron microscopy (~1 nm) provide sufficient resolution but require extensive experience in sample preparation (Henson et al., 2015; Morone, 2010; Morone et al., 2006).

Further insight into the precise mechanism of n-3 PUFA action can be elucidated through experiments involving pharmacological modulation of filamentous actin. As an example, the cytoskeletal stabilizing agent jasplakinolide has been shown to stabilize rigid membrane domains even after the addition of cholesterol disrupting agents (Chichili et al., 2010). Similar experiments can be performed with latrunculin B, however the interpretation is more difficult since disruption of f-actin can increase or decrease membrane order depending on the cell type (Alvarez-Guaita et al., 2015; Dinic et al., 2013).

What is the mechanism by which a membrane lipid containing n-3 PUFA inhibit the cytoskeleton? A possible explanation involves PIP_2, which is reduced by n-3 PUFA (Hou et al., 2012). This is mechanistically relevant because PIP_2 is highly enriched in lipid raft domains (Chierico et al., 2014; Zhou et al., 2014). In addition, sequestering

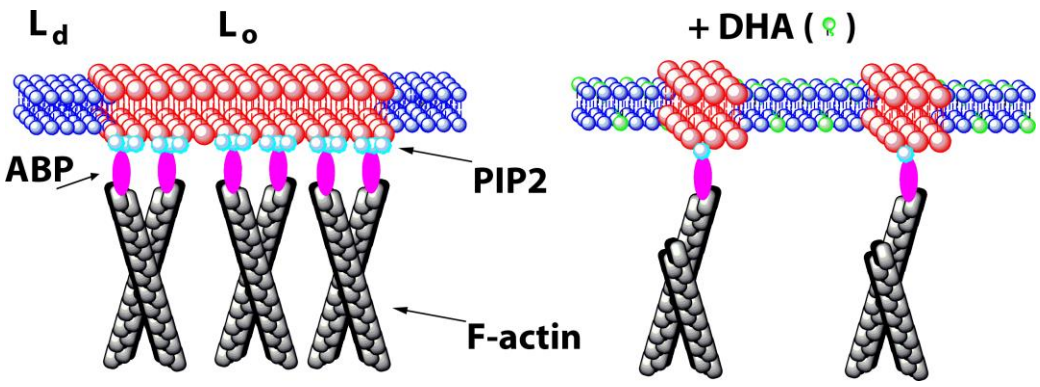

Figure 5.1. Putative model for the effect of DHA on membrane order. Actin-binding proteins (ABP) bind PIP_2 and F-actin, which stabilize membrane lipid order. DHA reduces levels of PIP_2, which reduces the interaction of filamentous actin with the plasma membrane, thereby reducing lipid order. Lo, liquid order; Ld, liquid disordered.

PIP_2 (using neomycin) reduces co-clustering of Liquid ordered (rigid) domain probes, indicating reduced membrane order (Chichili et al., 2010).

PIP_2 links to the cytoskeleton by the adaptor protein ezrin (Bosk et al., 2011; Logan and Mandato, 2006; Shabardina et al., 2016). Activated ezrin colocalizes with f-actin, acting as an adaptor protein linking the plasma membrane and cytoskeleton (Liu et al., 2013). Recently it was demonstrated the PIP_2 binding to ezrin increases membrane tension (Braunger et al., 2014) which is important for maintaining clustering of liquid ordered domains (Chichili et al., 2010). Since PIP_2 binding is a prerequisite for phosphorylation and activation of ezrin (Fievet et al., 2004), and PIP_2 levels are reduced in cells isolated from mice enriched with n-3 PUFA (Hou et al., 2012), we have hypothesized that DHA reduces membrane order by altering PIP_2 spatiotemporal dynamics, thereby modulating ezrin phosphorylation and reducing cytoskeletal attachment (**Figure 5.1**). This will be the subject of future experiments in the Chapkin lab.

5.2.2 Nanocluster mediating lipids

Our data indicate that n-3 PUFA modify the spatial organization of Ras nanoclusters, resulting in mixing of truncated forms of H- and KRas (**Figure 3.2G and Figure 3.4N**). However, the question regarding how n-3 PUFA mislocalize Ras nanoclusters still remains to be addressed. Insight to this question may be gained through monitoring the spatial organization of Ras isoforms in relation to specific lipid pools of phosphatidylserine (PS), phosphatidic acid (PA), and PIP_2. These lipids are key

structural components of Ras nanoclusters (Zhou and Hancock, 2017; Zhou et al., 2014). Specifically, the lateral segregation and heterotypic mixing of H- and KRas is dependent on PS levels in the plasma membrane, where only optimal levels produce segregated clusters (Zhou et al., 2014). In addition, future work will be necessary to determine if other dietary compounds that modify membrane organization (Fuentes et al., 2017) also modulate Ras cluster formation.

5.2.3 Cholesterol modulation by oncogenic Ras

We documented the ability of oncogenic Ras to rigidify the plasma membrane through increased plasma membrane free cholesterol (**Figure 4.5, 4.6, 4.8-4.10)**. Further work is necessary to determine the mechanism by which oncogenic Ras increases plasma membrane free cholesterol. A possible explanation for the increase in cholesterol may involve the cholesterol transporter ABCA1, who's down regulation by oncogenic Ras (Smith and Land, 2012) facilitates rapid tumor growth (Gabitova et al., 2015). ABCA1 expression results in a reduction of plasma membrane cholesterol which reduces the rigidity of the plasma membrane (Zarubica et al., 2009). In fact, the regulation of plasma membrane cholesterol and membrane order through ABCA1 is an intrinsic cell process utilized by crowded cells (Frechin et al., 2015).

5.2.4 Impact of other dietary bioactives on membrane organization

The two leaflets of the plasma membrane lipid bilayer each have unique interactions. The cytofacial (inner) leaflet interacts directly with the actin

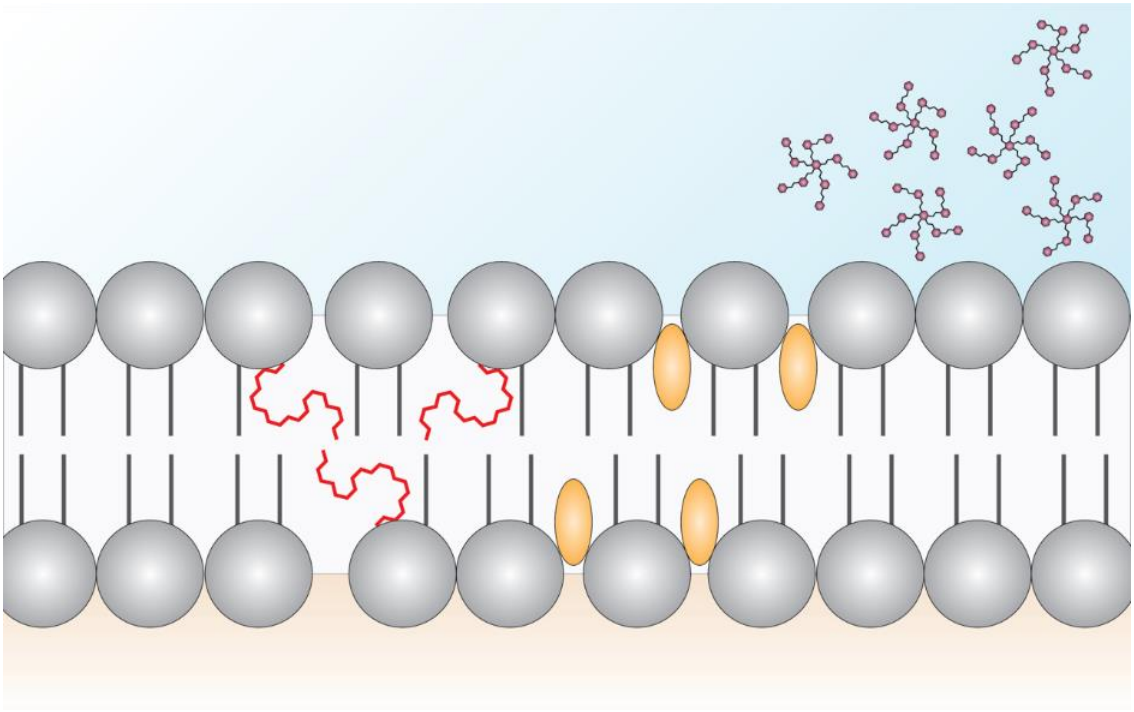

Figure 5.2. Putative mechanism by which bioactive dietary molecules interact with the plasma membrane. This model depicts plasma membrane structure with long-chain n-3 polyunsaturated fatty acids (PUFA) (red lines) incorporated into phospholipids, curcumin (yellow spheroids) intercalating between phospholipids and polyphenols (green shapes) interacting with the exofacial leaflet. The presence of either molecule may modulate plasma membrane-dependent cellular signaling by disrupting lipid-lipid and lipid-protein interactions.

cytoskeleton. The exofacial (outer) leaflet is the site for ligand-receptor interactions, as well as glycosylated protein interactions. Several classes of MTDBs, because of size, hydrophobic/hydrophilic interactions or steric hindrances, do not readily intercalate or incorporate into the phospholipid membrane. Examples, include high oligomer polyphenols, which do not penetrate the membrane but nevertheless alter membrane organization (Erlejman et al., 2004; Fuentes et al., 2017; Verstraeten et al., 2013) (**Figure 5.2**). For example, although intact procyanidins have some systemic

biological activity, they are poorly absorbed and pass into the distal intestine (colon) where they are further metabolized by gut microbes to generate monomeric catechin and epicatechin compounds along with other dimers-hexamer species (Choy et al., 2013; Verstraeten et al., 2015; Williamson and Manach, 2005). These microbial metabolites can interact with the apical membranes of colonic epithelial cells. Additional studies are needed to elucidate the mechanisms by which MTDBs and select drugs interact at the membrane level.

5.3 Conclusion

In regard to colon cancer, n-3 PUFA are believed to be chemoprotective. However, the mechanisms underlying the effects of these pleiotropic molecules have not been elucidated. By characterizing the effects of n-3 PUFA on plasma membrane protein/protein interactions, our research findings have contributed to the mechanistic understanding as to how biophysical alterations to plasma membrane organization can attenuate oncogenic Ras signaling and phenotypes.

REFERENCES

Adachi, S., Nagao, T., Ingolfsson, H.I., Maxfield, F.R., Andersen, O.S., Kopelovich, L., and Weinstein, I.B. (2007). The inhibitory effect of (-)-epigallocatechin gallate on activation of the epidermal growth factor receptor is associated with altered lipid order in HT29 colon cancer cells. Cancer Res *67*, 6493–6501.

Altenburg, J.D., Bieberich, A.A., Terry, C., Harvey, K.A., Vanhorn, J.F., Xu, Z., Jo Davisson, V., and Siddiqui, R.A. (2011). A synergistic antiproliferation effect of curcumin and docosahexaenoic acid in SK-BR-3 breast cancer cells: unique signaling not explained by the effects of either compound alone. BMC Cancer *11*, 149.

Alvarez-Guaita, A., Vil? de Muga, S., Owen, D.M., Williamson, D., Magenau, A., Garc?a-Melero, A., Reverter, M., Hoque, M., Cairns, R., Cornely, R., et al. (2015). Evidence for annexin A6-dependent plasma membrane remodelling of lipid domains. Br. J. Pharmacol. *172*, 1677–1690.

American Cancer Society (2015). Cancer Facts & Figures 2015 (Atlanta, Georgia: American Cancer Society).

Anti, M., Marra, G., Armelao, F., Bartoli, G.M., Ficarelli, R., Percesepe, A., De Vitis, I., Maria, G., Sofo, L., Rapaccini, G.L., et al. (1992). Effect of omega-3 fatty acids on rectal mucosal cell proliferation in subjects at risk for colon cancer. Gastroenterology *103*, 883–891.

Anti, M., Armelao, F., Marra, G., Percesepe, A., Bartoli, G.M., Palozza, P., Parrella, P.,

Canetta, C., Gentiloni, N., De Vitis, I., et al. (1994). Effects of different doses of fish oil on rectal cell proliferation in patients with sporadic colonic adenomas. Gastroenterology *107*, 1709–1718.

Ariotti, N., Fernández-Rojo, M.A., Zhou, Y., Hill, M.M., Rodkey, T.L., Inder, K.L., Tanner, L.B., Wenk, M.R., Hancock, J.F., Parton, R.G., et al. (2014). Caveolae regulate the nanoscale organization of the plasma membrane to remotely control Ras signaling. J Cell Biol *204*, 777–792.

Azzi, A., Brigelius-Flohe, R., Kelly, F., Lodge, J.K., Ozer, N., Packer, L., and Sies, H. (2005). On the opinion of the European Commission "Scientific Committee on Food" regarding the tolerable upper intake level of vitamin E (2003). Eur J Nutr *44*, 60–62.

Bar-Sagi, D., and Feramisco, J.R. (1986). Induction of membrane ruffling and fluid-phase pinocytosis in quiescent fibroblasts by ras proteins. Science *233*, 1061–1068.

Barman, S., and Nayak, D.P. (2007). Lipid raft disruption by cholesterol depletion enhances influenza A virus budding from MDCK cells. J Virol *81*, 12169–12178.

Baron, J.A., Sandler, R.S., Bresalier, R.S., Lanas, A., Morton, D.G., Riddell, R., Iverson, E.R., and Demets, D.L. (2008). Cardiovascular events associated with rofecoxib: final analysis of the APPROVe trial. Lancet *372*, 1756–1764.

Barrera, N.P., Zhou, M., and Robinson, C. V (2013). The role of lipids in defining membrane protein interactions: insights from mass spectrometry. Trends Cell Biol *23*, 1–8.

Bartram, H.P., Gostner, A., Scheppach, W., Reddy, B.S., Rao, C. V, Dusel, G., Richter, F., Richter, A., and Kasper, H. (1993). Effects of fish oil on rectal cell proliferation, mucosal fatty acids, and prostaglandin E2 release in healthy subjects. Gastroenterology *105*, 1317–1322.

Bell, G.A., Kantor, E.D., Lampe, J.W., Kristal, A.R., Heckbert, S.R., and White, E. (2014). Intake of long-chain omega-3 fatty acids from diet and supplements in relation to mortality. Am J Epidemiol *179*, 710–720.

Bene, L., Bodnar, A., Damjanovich, S., Vamosi, G., Bacso, Z., Aradi, J., Berta, A., and Damjanovich, J. (2004). Membrane topography of HLA I, HLA II, and ICAM-1 is affected by IFN-gamma in lipid rafts of uveal melanomas. Biochem Biophys Res Commun *322*, 678–683.

Beresford, S.A., Johnson, K.C., Ritenbaugh, C., Lasser, N.L., Snetselaar, L.G., Black, H.R., Anderson, G.L., Assaf, A.R., Bassford, T., Bowen, D., et al. (2006). Low-fat dietary pattern and risk of colorectal cancer: the Women's Health Initiative Randomized Controlled Dietary Modification Trial. JAMA *295*, 643–654.

Biteau, B., Hochmuth, C.E., and Jasper, H. (2011). Maintaining Tissue Homeostasis: Dynamic Control of Somatic Stem Cell Activity. Cell Stem Cell *9*, 402–411.

Bloch, K.E. (1983). Sterol structure and membrane function. CRC Crit Rev Biochem *14*, 47–92.

Bohdanowicz, M., and Grinstein, S. (2013). Role of phospholipids in endocytosis,

phagocytosis, and macropinocytosis. Physiol. Rev. *93*, 69–106.

Bosk, S., Braunger, J.A., Gerke, V., and Steinem, C. (2011). Activation of F-actin binding capacity of ezrin: synergism of PIP_2 interaction and phosphorylation. Biophys. J. *100*, 1708–1717.

Braunger, J.A., Brückner, B.R., Nehls, S., Pietuch, A., Gerke, V., Mey, I., Janshoff, A., and Steinem, C. (2014). Phosphatidylinositol 4,5-Bisphosphate Alters the Number of Attachment Sites between Ezrin and Actin Filaments. J. Biol. Chem. *289*, 9833–9843.

Browning, L.M., Walker, C.G., Mander, A.P., West, A.L., Madden, J., Gambell, J.M., Young, S., Wang, L., Jebb, S.A., and Calder, P.C. (2012). Incorporation of eicosapentaenoic and docosahexaenoic acids into lipid pools when given as supplements providing doses equivalent to typical intakes of oily fish. Am J Clin Nutr *96*, 748–758.

Bryant, K.L., Mancias, J.D., Kimmelman, A.C., and Der, C.J. (2014). KRAS: feeding pancreatic cancer proliferation. Trends Biochem. Sci. *39*, 91–100.

Buchon, N., Broderick, N.A., and Lemaitre, B. (2013). Gut homeostasis in a microbial world: insights from Drosophila melanogaster. Nat. Rev. Microbiol. *11*, 615–626.

Calder, P.C. (2015). Marine omega-3 fatty acids and inflammatory processes: Effects, mechanisms and clinical relevance. Biochim Biophys Acta *1851*, 469–484.

Caygill, C.P., Charlett, A., and Hill, M.J. (1996). Fat, fish, fish oil and cancer. Br J Cancer *74*, 159–164.

Chang, W.L., Chapkin, R.S., and Lupton, J.R. (1997). Fish Oil Blocks Azoxymethane-Induced Rat Colon Tumorigenesis by Increasing Cell Differentiation and Apoptosis Rather Than Decreasing Cell. J. Nutrtion *128*, 491–497.

Chapkin, R. (2007). Reappraisal of the Essential Fatty Acids. In Fatty Acids in Foods and Their Health Implications,Third Edition, (CRC Press), pp. 675–691.

Chapkin, R.S., and Carmichael, S.L. (1990). Effects of dietary n-3 and n-6 polyunsaturated fatty acids on macrophage phospholipid classes and subclasses. Lipids *25*, 827–834.

Chapkin, R.S., Akoh, C.C., and Miller, C.C. (1991). Influence of dietary n-3 fatty acids on macrophage glycerophospholipid molecular species and peptidoleukotriene synthesis. J Lipid Res *32*, 1205–1213.

Chapkin, R.S., McMurray, D.N., and Lupton, J.R. (2007). Colon cancer, fatty acids and anti-inflammatory compounds. Curr Opin Gastroenterol *23*, 48–54.

Chapkin, R.S., Seo, J., McMurray, D.N., and Lupton, J.R. (2008a). Mechanisms by which docosahexaenoic acid and related fatty acids reduce colon cancer risk and inflammatory disorders of the intestine. Chem Phys Lipids *153*, 14–23.

Chapkin, R.S., Wang, N., Fan, Y.-Y., Lupton, J.R., and Prior, I.A. (2008b). Docosahexaenoic acid alters the size and distribution of cell surface microdomains. Biochim. Biophys. Acta - Biomembr. *1778*, 466–471.

Chapkin, R.S., Kim, W., Lupton, J.R., and McMurray, D.N. (2009). Dietary

docosahexaenoic and eicosapentaenoic acid: emerging mediators of inflammation. Prostaglandins Leukot Essent Fat. Acids *81*, 187–191.

Chapkin, R.S., DeClercq, V., Kim, E., Fuentes, N.R., Fan, Y.-Y.Y., * Chapkin, R.S., DeClercq, V., Kim, E., Fuentes, R.N., and Fan, Y.-Y.Y. (2014). Mechanisms by Which Pleiotropic Amphiphilic n−3 PUFA Reduce Colon Cancer Risk. Curr Color. Cancer Rep *10*, 442–452.

Cheng, J., Ogawa, K., Kuriki, K., Yokoyama, Y., Kamiya, T., Seno, K., Okuyama, H., Wang, J., Luo, C., Fujii, T., et al. (2003). Increased intake of n-3 polyunsaturated fatty acids elevates the level of apoptosis in the normal sigmoid colon of patients polypectomized for adenomas/tumors. Cancer Lett *193*, 17–24.

Chichili, G.R., Westmuckett, A.D., and Rodgers, W. (2010). T Cell Signal Regulation by the Actin Cytoskeleton. J. Biol. Chem. *285*, 14737–14746.

Chierico, L., Joseph, A.S., Lewis, A.L., and Battaglia, G. (2014). Live cell imaging of membrane/cytoskeleton interactions and membrane topology. Sci. Rep. *4*, 6056.

Cho, K.-J.J.K., and Hancock, J.F.J.F. (2013). Ras nanoclusters: a new drug target? Small GTPases *4*, 57–60.

Choy, Y.Y., Jaggers, G.K., Oteiza, P.I., and Waterhouse, A.L. (2013). Bioavailability of intact proanthocyanidins in the rat colon after ingestion of grape seed extract. J. Agric. Food Chem. *61*, 121–127.

Cockbain, A.J., Toogood, G.J., and Hull, M.A. (2012). Omega-3 polyunsaturated fatty

acids for the treatment and prevention of colorectal cancer. Gut *61*, 135–149.

Cockbain, A.J., Volpato, M., Race, A.D., Munarini, A., Fazio, C., Belluzzi, A., Loadman, P.M., Toogood, G.J., and Hull, M. a (2014). Anticolorectal cancer activity of the omega-3 polyunsaturated fatty acid eicosapentaenoic acid. Gut *63*, 1760–1768.

Collett, E.D., Davidson, L.A., Fan, Y.Y., Lupton, J.R., and Chapkin, R.S. (2001). n-6 and n-3 polyunsaturated fatty acids differentially modulate oncogenic Ras activation in colonocytes. Am J Physiol Cell Physiol *280*, C1066-75.

Commisso, C., Davidson, S.M., Soydaner-Azeloglu, R.G., Parker, S.J., Kamphorst, J.J., Hackett, S., Grabocka, E., Nofal, M., Drebin, J.A., Thompson, C.B., et al. (2013). Macropinocytosis of protein is an amino acid supply route in Ras-transformed cells. Nature *497*, 633–637.

Commisso, C., Flinn, R.J., and Bar-Sagi, D. (2014). Determining the macropinocytic index of cells through a quantitative image-based assay. Nat Protoc *9*, 182–192.

Conquer, J.A., and Holub, B.J. (1998). Effect of supplementation with different doses of DHA on the levels of circulating DHA as non-esterified fatty acid in subjects of Asian Indian background. J Lipid Res *39*, 286–292.

Courtney, E.D., Matthews, S., Finlayson, C., Di Pierro, D., Belluzzi, A., Roda, E., Kang, J.Y., and Leicester, R.J. (2007). Eicosapentaenoic acid (EPA) reduces crypt cell proliferation and increases apoptosis in normal colonic mucosa in subjects with a history of colorectal adenomas. Int J Color. Dis *22*, 765–776.

Coussens, L.M., Zitvogel, L., and Palucka, A.K. (2013). Neutralizing tumor-promoting chronic inflammation: a magic bullet? Science (80-.). *339*, 286–291.

Cox, A.D., Fesik, S.W., Kimmelman, A.C., Luo, J., and Der, C.J. (2014). Drugging the undruggable RAS: Mission Possible? Nat. Rev. Drug Discov. *13*, 828–851.

D'Abaco, G.M., Whitehead, R.H., and Burgess, A.W. (1996). Synergy between Apc min and an activated ras mutation is sufficient to induce colon carcinomas. Mol. Cell. Biol. *16*, 884–891.

Delos Santos, R.C., Garay, C., and Antonescu, C.N. (2015). Charming neighborhoods on the cell surface: Plasma membrane microdomains regulate receptor tyrosine kinase signaling. Cell. Signal. *27*, 1963–1976.

Dinic, J., Ashrafzadeh, P., and Parmryd, I. (2013). Actin filaments attachment at the plasma membrane in live cells cause the formation of ordered lipid domains. Biochim. Biophys. Acta - Biomembr. *1828*, 1102–1111.

Downward, J. (2003). Targeting RAS signalling pathways in cancer therapy. Nat Rev Cancer *3*, 11–22.

Dragu, D.L., Necula, L.G., Bleotu, C., Diaconu, C.C., and Chivu-Economescu, M. (2015). Therapies targeting cancer stem cells: Current trends and future challenges. World J. Stem Cells *7*, 1185–1201.

Dunn, E.F., Iida, M., Myers, R.A., Campbell, D.A., Hintz, K.A., Armstrong, E.A., Li, C., and Wheeler, D.L. (2011). Dasatinib sensitizes KRAS mutant colorectal tumors to

cetuximab. Oncogene *30*, 561–574.

Eggeling, C., Ringemann, C., Medda, R., Schwarzmann, G., Sandhoff, K., Polyakova, S., Belov, V.N., Hein, B., von Middendorff, C., Schönle, A., et al. (2009). Direct observation of the nanoscale dynamics of membrane lipids in a living cell. Nature *457*, 1159–1162.

Eisenberg, S., Laude, A.J., Beckett, A.J., Mageean, C.J., Aran, V., Hernandez-Valladares, M., Henis, Y.I., and Prior, I. a (2013). The role of palmitoylation in regulating Ras localization and function. Biochem Soc Trans *41*, 79–83.

Elinav, E., Nowarski, R., Thaiss, C.A., Hu, B., Jin, C., and Flavell, R.A. (2013). Inflammation-induced cancer: crosstalk between tumours, immune cells and microorganisms. Nat Rev Cancer *13*, 759–771.

Erlejman, A.G., Verstraeten, S. V, Fraga, C.G., and Oteiza, P.I. (2004). The interaction of flavonoids with membranes: potential determinant of flavonoid antioxidant effects. Free Radic. Res. *38*, 1311–1320.

Escriba, P. V, Busquets, X., Inokuchi, J., Balogh, G., Torok, Z., Horvath, I., Harwood, J.L., and Vigh, L. (2015). Membrane lipid therapy: Modulation of the cell membrane composition and structure as a molecular base for drug discovery and new disease treatment. Prog Lipid Res *59*, 38–53.

Fan, Y.Y., McMurray, D.N., Ly, L.H., and Chapkin, R.S. (2003). Dietary (n-3) polyunsaturated fatty acids remodel mouse T-cell lipid rafts. J Nutr *133*, 1913–1920.

Fan, Y.Y., Davidson, L.A., Callaway, E.S., Goldsby, J.S., and Chapkin, R.S. (2014). Differential effects of 2- and 3-series E-prostaglandins on in vitro expansion of Lgr5+ colonic stem cells. Carcinogenesis *35*, 606–612.

Fasano, E., Serini, S., Piccioni, E., Toesca, A., Monego, G., Cittadini, A.R., Ranelletti, F.O., and Calviello, G. (2012). DHA induces apoptosis by altering the expression and cellular location of GRP78 in colon cancer cell lines. Biochim Biophys Acta *1822*, 1762–1772.

Fazio, C., and Ricciardiello, L. (2014). Components of the Mediterranean Diet with chemopreventive activity toward colorectal cancer. Phytochem. Rev. *13*, 867–879.

Fedida-Metula, S., Feldman, B., Koshelev, V., Levin-Gromiko, U., Voronov, E., and Fishman, D. (2012). Lipid rafts couple store-operated Ca2+ entry to constitutive activation of PKB/Akt in a Ca2+/calmodulin-, Src- and PP2A-mediated pathway and promote melanoma tumor growth. Carcinogenesis *33*, 740–750.

Feng, Y., Bommer, G.T., Zhao, J., Green, M., Sands, E., Zhai, Y., Brown, K., Burberry, A., Cho, K.R., and Fearon, E.R. (2011). Mutant KRAS promotes hyperplasia and alters differentiation in the colon epithelium but does not expand the presumptive stem cell pool. Gastroenterology *141*, 1003–1010.

Feng, Y., Sentani, K., Wiese, A., Sands, E., Green, M., Bommer, G.T., Cho, K.R., and Fearon, E.R. (2013). Sox9 induction, ectopic paneth cells, and mitotic spindle axis defects in mouse colon adenomatous epithelium arising from conditional biallelic Apc

inactivation. Am. J. Pathol. *183*, 493–503.

Fievet, B.T., Gautreau, A., Roy, C., Del Maestro, L., Mangeat, P., Louvard, D., and Arpin, M. (2004). Phosphoinositide binding and phosphorylation act sequentially in the activation mechanism of ezrin. J. Cell Biol. *164*, 653–659.

Ford, E.S., Bergmann, M.M., Kröger, J., Schienkiewitz, A., Weikert, C., Boeing, H., Kroger, J., Schienkiewitz, A., Weikert, C., and Boeing, H. (2009). Healthy living is the best revenge: findings from the European Prospective Investigation Into Cancer and Nutrition-Potsdam study. Arch Intern Med *169*, 1355–1362.

Frechin, M., Stoeger, T., Daetwyler, S., Gehin, C., Battich, N., Damm, E.-M., Stergiou, L., Riezman, H., and Pelkmans, L. (2015). Cell-intrinsic adaptation of lipid composition to local crowding drives social behaviour. Nature *523*, 88–91.

Frisz, J.F., Lou, K., Klitzing, H.A., Hanafin, W.P., Lizunov, V., Wilson, R.L., Carpenter, K.J., Kim, R., Hutcheon, I.D., Zimmerberg, J., et al. (2013). Direct chemical evidence for sphingolipid domains in the plasma membranes of fibroblasts. Proc Natl Acad Sci U S A *110*, E613-22.

Fritsche, K.L., and Johnston, P. V (1988). Rapid autoxidation of fish oil in diets without added antioxidants. J. Nutr. *118*, 425–426.

Fuentes, N.R., Salinas, M.L., Kim, E., and Chapkin, R.S. (2017). Emerging role of chemoprotective agents in the dynamic shaping of plasma membrane organization. Biochim. Biophys. Acta *1859*, 1668–1678.

Fujii, M., Kawai, K., Egami, Y., and Araki, N. (2013). Dissecting the roles of Rac1 activation and deactivation in macropinocytosis using microscopic photo-manipulation. Sci. Rep. *3*, 2385.

Fukano, T., Sawano, A., Ohba, Y., Matsuda, M., and Miyawaki, A. (2007). Differential Ras activation between caveolae/raft and non-raft microdomains. Cell Struct. Funct. *32*, 9–15.

Gabitova, L., Restifo, D., Gorin, A., Manocha, K., Handorf, E., Yang, D.H., Cai, K.Q., Klein-Szanto, A.J., Cunningham, D., Kratz, L.E., et al. (2015). Endogenous Sterol Metabolites Regulate Growth of EGFR/KRAS-Dependent Tumors via LXR. Cell Rep *12*, 1927–1938.

Garcia-Parajo, M.F., Cambi, A., Torreno-Pina, J.A., Thompson, N., and Jacobson, K. (2014). Nanoclustering as a dominant feature of plasma membrane organization. J Cell Sci *127*, 4995–5005.

George, K.S., and Wu, S. (2012). Lipid raft: A floating island of death or survival. Toxicol Appl Pharmacol *259*, 311–319.

Gerber, M. (2012). Omega-3 fatty acids and cancers: a systematic update review of epidemiological studies. Br J Nutr *107 Suppl*, S228-39.

Graham, D.J. (2006). COX-2 inhibitors, other NSAIDs, and cardiovascular risk: the seduction of common sense. JAMA *296*, 1653–1656.

Gray, E., Karslake, J., Machta, B.B., and Veatch, S.L. (2013). Liquid general anesthetics

lower critical temperatures in plasma membrane vesicles. Biophys. J. *105*, 2751–2759.

Gray, E.M., Díaz-Vázquez, G., Veatch, S.L.S., Holowka, D., Baird, B., Piccolo, N. Del, Placone, J., He, L., Agudelo, S., Hristova, K., et al. (2015). Growth Conditions and Cell Cycle Phase Modulate Phase Transition Temperatures in RBL-2H3 Derived Plasma Membrane Vesicles. PLoS One *10*, e0137741.

Griffié, J., Burn, G., and Owen, D.M. (2015). The Nanoscale Organization of Signaling Domains at the Plasma Membrane. In Current Topics in Membranes, pp. 125–165.

Grimmer, S., van Deurs, B., and Sandvig, K. (2002). Membrane ruffling and macropinocytosis in A431 cells require cholesterol. J. Cell Sci. *115*, 2953–2962.

Guzman, C., olman, M., Ligabue, A., Bla evit , O., Andrade, D.M., Reymond, L., Eggeling, C., and Abankwa, D. (2014). The Efficacy of Raf Kinase Recruitment to the GTPase H-ras Depends on H-ras Membrane Conformer-specific Nanoclustering. J. Biol. Chem. *289*, 9519–9533.

Haigis, K.M., Kendall, K.R., Wang, Y., Cheung, A., Haigis, M.C., Glickman, J.N., Niwa-Kawakita, M., Sweet-Cordero, A., Sebolt-Leopold, J., Shannon, K.M., et al. (2008). Differential effects of oncogenic K-Ras and N-Ras on proliferation, differentiation and tumor progression in the colon. Nat. Genet. *40*, 600–608.

Hall, M.N., Chavarro, J.E., Lee, I.-M.M., Willett, W.C., and Ma, J. (2008). A 22-year prospective study of fish, n-3 fatty acid intake, and colorectal cancer risk in men. Cancer Epidemiol Biomarkers Prev *17*, 1136–1143.

Hammond, D.E., Mageean, C.J., Rusilowicz, E. V, Wickenden, J.A., Clague, M.J., and Prior, I.A. (2015). Differential reprogramming of isogenic colorectal cancer cells by distinct activating K-Ras mutations. J Proteome Res *14*, 1535–1546.

Hancock, J.F. (2006). Lipid rafts: contentious only from simplistic standpoints. Nat Rev Mol Cell Biol *7*, 456–462.

Head, B.P., Patel, H.H., and Insel, P.A. (2014). Interaction of membrane/lipid rafts with the cytoskeleton: impact on signaling and function: membrane/lipid rafts, mediators of cytoskeletal arrangement and cell signaling. Biochim Biophys Acta *1838*, 532–545.

Hedlund, P.O., Johansson, R., Damber, J.E., Hagerman, I., Henriksson, P., Iversen, P., Klarskov, P., Mogensen, P., Rasmussen, F., Varenhorst, E., et al. (2011). Significance of pretreatment cardiovascular morbidity as a risk factor during treatment with parenteral oestrogen or combined androgen deprivation of 915 patients with metastasized prostate cancer: evaluation of cardiovascular events in a randomized trial. Scand J Urol Nephrol *45*, 346–353.

Henderson, M.M. (1992). International differences in diet and cancer incidence. J Natl Cancer Inst Monogr 59–63.

Henis, Y.I., Hancock, J.F., and Prior, I.A. (2009). Ras acylation, compartmentalization and signaling nanoclusters (Review). Mol. Membr. Biol. *26*, 80–92.

Henson, J.H., Yeterian, M., Weeks, R.M., Medrano, A.E., Brown, B.L., Geist, H.L., Pais, M.D., Oldenbourg, R., and Shuster, C.B. (2015). Arp2/3 complex inhibition

radically alters lamellipodial actin architecture, suspended cell shape, and the cell spreading process. Mol. Biol. Cell *26*, 887–900.

Herrmann, C. (2003). Ras-effector interactions: after one decade. Curr. Opin. Struct. Biol. *13*, 122–129.

Horejsi, V., and Hrdinka, M. (2014). Membrane microdomains in immunoreceptor signaling. FEBS Lett *588*, 2392–2397.

Hou, T.Y., Monk, J.M., Fan, Y.Y., Barhoumi, R., Chen, Y.Q., Rivera, G.M., McMurray, D.N., and Chapkin, R.S. (2012). n-3 polyunsaturated fatty acids suppress phosphatidylinositol 4,5-bisphosphate-dependent actin remodelling during CD4+ T-cell activation. Biochem J *443*, 27–37.

Hou, T.Y., Barhoumi, R., Fan, Y.-Y., Rivera, G.M., Hannoush, R.N., McMurray, D.N., and Chapkin, R.S. (2015). n-3 polyunsaturated fatty acids suppress CD4(+) T cell proliferation by altering phosphatidylinositol-(4,5)-bisphosphate [PI(4,5)P2] organization. Biochim. Biophys. Acta.

Hou, T.Y., Davidson, L.A., Kim, E., Fan, Y.-Y., Fuentes, N.R., Triff, K., and Chapkin, R.S. (2016). Nutrient-Gene Interaction in Colon Cancer, from the Membrane to Cellular Physiology. Annu. Rev. Nutr. *36*, 543–570.

Hryniewicz-Jankowska, A., Augoff, K., Biernatowska, A., Podkalicka, J., and Sikorski, A.F. (2014). Membrane rafts as a novel target in cancer therapy. Biochim Biophys Acta *1845*, 155–165.

Hudert, C.A., Weylandt, K.H., Lu, Y., Wang, J., Hong, S., Dignass, A., Serhan, C.N., and Kang, J.X. (2006). Transgenic mice rich in endogenous omega-3 fatty acids are protected from colitis. Proc. Natl. Acad. Sci. U. S. A. *103*, 11276–11281.

Hull, M. a, Sandell, A.C., Montgomery, A. a, Logan, R.F., Clifford, G.M., Rees, C.J., Loadman, P.M., and Whitham, D. (2013). A randomized controlled trial of eicosapentaenoic acid and/or aspirin for colorectal adenoma prevention during colonoscopic surveillance in the NHS Bowel Cancer Screening Programme (The seAFOod Polyp Prevention Trial): study protocol for a randomized cont. Trials *14*, 237.

Hung, W.-C.C., Chen, F.-Y.Y., Lee, C.-C.C., Sun, Y., Lee, M.-T.T., and Huang, H.W. (2008). Membrane-thinning effect of curcumin. Biophys J *94*, 4331–4338.

Iliev, A.I., Djannatian, J.R., Nau, R., Mitchell, T.J., and Wouters, F.S. (2007). Cholesterol-dependent actin remodeling via RhoA and Rac1 activation by the Streptococcus pneumoniae toxin pneumolysin. Proc. Natl. Acad. Sci. U. S. A. *104*, 2897–2902.

Imhoff, H., von Messling, V., Herrler, G., and Haas, L. (2007). Canine distemper virus infection requires cholesterol in the viral envelope. J Virol *81*, 4158–4165.

Ingolfsson, H.I., Koeppe, R.E., and Andersen, O.S. (2007). Curcumin is a Modulator of Bilayer Material Properties†. Biochemistry *46*, 10384–10391.

Inoue, N., Dong, R., Hirata, R.K., and Russell, D.W. (2001). Introduction of single base substitutions at homologous chromosomal sequences by adeno-associated virus vectors.

Mol Ther *3*, 526–530.

Irwin, M.E., Mueller, K.L., Bohin, N., Ge, Y., and Boerner, J.L. (2011). Lipid raft localization of EGFR alters the response of cancer cells to the EGFR tyrosine kinase inhibitor gefitinib. J Cell Physiol *226*, 2316–2328.

Jahn, K.A., Su, Y., and Braet, F. (2011). Multifaceted nature of membrane microdomains in colorectal cancer. World J Gastroenterol *17*, 681–690.

Janosi, L., Li, Z., Hancock, J.F., and Gorfe, A.A. (2012). Organization, dynamics, and segregation of Ras nanoclusters in membrane domains. Proc Natl Acad Sci U S A *109*, 8097–8102.

Jia, Q., Lupton, J.R., Smith, R., Weeks, B.R., Callaway, E., Davidson, L.A., Kim, W., Fan, Y.-Y.Y., Yang, P., Newman, R.A., et al. (2008). Reduced colitis-associated colon cancer in Fat-1 (n-3 fatty acid desaturase) transgenic mice. Cancer Res *68*, 3985–3991.

Jiang, H., and Edgar, B.A. (2009). EGFR signaling regulates the proliferation of Drosophila adult midgut progenitors. Development *136*, 483–493.

Jiang, H., Grenley, M.O., Bravo, M.-J., Blumhagen, R.Z., and Edgar, B.A. (2011). EGFR/Ras/MAPK signaling mediates adult midgut epithelial homeostasis and regeneration in Drosophila. Cell Stem Cell *8*, 84–95.

Kang, J.X. Fat-1 transgenic mice: a new model for omega-3 research. Prostaglandins. Leukot. Essent. Fatty Acids *77*, 263–267.

Kang, J.X., Wang, J., Wu, L., and Kang, Z.B. (2004). Transgenic mice: Fat-1 mice convert n-6 to n-3 fatty acids. Nature *427*, 504–504.

Kantor, E.D., Lampe, J.W., Peters, U., Vaughan, T.L., and White, E. (2014). Long-chain omega-3 polyunsaturated fatty acid intake and risk of colorectal cancer. Nutr Cancer *66*, 716–727.

Karpac, J., Biteau, B., and Jasper, H. (2013). Misregulation of an adaptive metabolic response contributes to the age-related disruption of lipid homeostasis in drosophila. Cell Rep. *4*, 1250–1261.

Katan, M.B., Deslypere, J.P., van Birgelen, A.P., Penders, M., and Zegwaard, M. (1997). Kinetics of the incorporation of dietary fatty acids into serum cholesteryl esters, erythrocyte membranes, and adipose tissue: an 18-month controlled study. J Lipid Res *38*, 2012–2022.

Kim, E., Davidson, L.A., Zoh, R.S., Hensel, M.E., Salinas, M.L., Patil, B.S., Jayaprakasha, G.K., Callaway, E.S., Allred, C.D., Turner, N.D., et al. (2016). Rapidly cycling Lgr5+ stem cells are exquisitely sensitive to extrinsic dietary factors that modulate colon cancer risk. Cell Death Dis. *7*, e2460.

Kim, J.A., Maxwell, K., Hajjar, D.P., and Berliner, J.A. (1991). Beta-VLDL increases endothelial cell plasma membrane cholesterol. J Lipid Res *32*, 1125–1131.

Kim, W., Fan, Y.-Y.Y., Barhoumi, R., Smith, R., McMurray, D.N., and Chapkin, R.S. (2008). n-3 polyunsaturated fatty acids suppress the localization and activation of

signaling proteins at the immunological synapse in murine CD4+ T cells by affecting lipid raft formation. J Immunol *181*, 6236–6243.

Kim, W., Khan, N.A., McMurray, D.N., Prior, I.A., Wang, N., and Chapkin, R.S. (2010). Regulatory activity of polyunsaturated fatty acids in T-cell signaling. Prog Lipid Res *49*, 250–261.

Kim, W., Barhoumi, R., McMurray, D.N., and Chapkin, R.S. (2014). Dietary fish oil and DHA down-regulate antigen-activated CD4+ T-cells while promoting the formation of liquid-ordered mesodomains. Br J Nutr *111*, 254–260.

Klymchenko, A.S., and Kreder, R. (2014). Fluorescent Probes for Lipid Rafts: From Model Membranes to Living Cells. Chem. Biol. *21*, 97–113.

Kohnke, M., Schmitt, S., Ariotti, N., Piggott, A.M., Parton, R.G., Lacey, E., Capon, R.J., Alexandrov, K., and Abankwa, D. (2012). Design and application of in vivo FRET biosensors to identify protein prenylation and nanoclustering inhibitors. Chem Biol *19*, 866–874.

Korzelius, J., Naumann, S.K., Loza-Coll, M.A., Chan, J.S., Dutta, D., Oberheim, J., Gläßer, C., Southall, T.D., Brand, A.H., Jones, D.L., et al. (2014). Escargot maintains stemness and suppresses differentiation in Drosophila intestinal stem cells. EMBO J. *33*, 2967–2982.

Kraft, M.L. (2013). Plasma membrane organization and function: moving past lipid rafts. Mol Biol Cell *24*, 2765–2768.

Kwiatek, J.M., Hinde, E., and Gaus, K. (2014). Microscopy approaches to investigate protein dynamics and lipid organization. Mol. Membr. Biol. *31*, 141–151.

Kwik, J., Boyle, S., Fooksman, D., Margolis, L., Sheetz, M.P., and Edidin, M. (2003). Membrane cholesterol, lateral mobility, and the phosphatidylinositol 4,5-bisphosphate-dependent organization of cell actin. Proc. Natl. Acad. Sci. U. S. A. *100*, 13964–13969.

Lacour, S., Hammann, A., Grazide, S., Lagadic-Gossmann, D., Athias, A., Sergent, O., Laurent, G., Gambert, P., Solary, E., and Dimanche-Boitrel, M.T. (2004). Cisplatin-induced CD95 redistribution into membrane lipid rafts of HT29 human colon cancer cells. Cancer Res *64*, 3593–3598.

Lange, Y., Swaisgood, M.H., Ramos, B. V, and Steck, T.L. (1989). Plasma membranes contain half the phospholipid and 90% of the cholesterol and sphingomyelin in cultured human fibroblasts. J Biol Chem *264*, 3786–3793.

Levental, I., and Veatch, S.L. (2016). The Continuing Mystery of Lipid Rafts. J. Mol. Biol. *428*, 4749–4764.

Levental, I., Byfield, F.J., Chowdhury, P., Gai, F., Baumgart, T., and Janmey, P.A. (2009). Cholesterol-dependent phase separation in cell-derived giant plasma-membrane vesicles. Biochem. J. *424*, 163–167.

Levental, K.R., Lorent, J.H., Lin, X., Skinkle, A.D., Surma, M.A., Stockenbojer, E.A., Gorfe, A.A., and Levental, I. (2016). Polyunsaturated Lipids Regulate Membrane Domain Stability by Tuning Membrane Order. Biophys. J. *110*, 1800–1810.

Levin, R., Grinstein, S., and Schlam, D. (2015). Phosphoinositides in phagocytosis and macropinocytosis. Biochim. Biophys. Acta *1851*, 805–823.

Li, Y., Zhang, X., and Cao, D. (2015). Nanoparticle hardness controls the internalization pathway for drug delivery. Nanoscale *7*, 2758–2769.

Li, Y.C., Park, M.J., Ye, S.K., Kim, C.W., and Kim, Y.N. (2006). Elevated levels of cholesterol-rich lipid rafts in cancer cells are correlated with apoptosis sensitivity induced by cholesterol-depleting agents. Am J Pathol *168*, 1105–1107.

Lien, E.L. (2009). Toxicology and safety of DHA. Prostaglandins Leukot Essent Fat. Acids *81*, 125–132.

Lim, J.P., and Gleeson, P.A. (2011). Macropinocytosis: an endocytic pathway for internalising large gulps. Immunol. Cell Biol. *89*, 836–843.

Lin, X., Lorent, J.H., Skinkle, A.D., Levental, K.R., Waxham, M.N., Gorfe, A.A., and Levental, I. (2016). Domain Stability in Biomimetic Membranes Driven by Lipid Polyunsaturation. J. Phys. Chem. B *120*, 11930–11941.

Lingwood, D., and Simons, K. (2010). Lipid rafts as a membrane-organizing principle. Science (80-.). *327*, 46–50.

Liu, H., Wu, Z., Shi, X., Li, W., Liu, C., Wang, D., Ye, X., Liu, L., Na, J., Cheng, H., et al. (2013). Atypical PKC, regulated by Rho GTPases and Mek/Erk, phosphorylates Ezrin during eight-cell embryocompaction. Dev. Biol. *375*, 13–22.

Liu, M., Zhou, L., Zhang, B., He, M., Dong, X., Lin, X., Jia, C., Bai, X., Dai, Y., Su, Y., et al. (2016). Elevation of n-3/n-6 PUFAs ratio suppresses mTORC1 and prevents colorectal carcinogenesis associated with APC mutation. Oncotarget *7*, 76944–76954.

Logan, M.R., and Mandato, C.A. (2006). Regulation of the actin cytoskeleton by PIP2 in cytokinesis. Biol. Cell *98*, 377–388.

Ma, D.W., Seo, J., Switzer, K.C., Fan, Y.Y., McMurray, D.N., Lupton, J.R., and Chapkin, R.S. (2004a). n-3 PUFA and membrane microdomains: a new frontier in bioactive lipid research. J Nutr Biochem *15*, 700–706.

Ma, D.W.L., Seo, J., Davidson, L. a, Callaway, E.S., Fan, Y.-Y.Y., Lupton, J.R., and Chapkin, R.S. (2004b). n-3 PUFA alter caveolae lipid composition and resident protein localization in mouse colon. FASEB J *18*, 1040–1042.

Machta, B.B., Gray, E., Nouri, M., McCarthy, N.L.C., Gray, E.M., Miller, A.L., Brooks, N.J., and Veatch, S.L. (2016). Stabilizing membrane domains antagonizes n-alcohol anesthesia.

MacLean, C.H., Newberry, S.J., Mojica, W. a, Khanna, P., Issa, A.M., Suttorp, M.J., Lim, Y.-W., Traina, S.B., Hilton, L., Garland, R., et al. (2006). Effects of omega-3 fatty acids on cancer risk: a systematic review. JAMA *295*, 403–415.

Maekawa, M., Terasaka, S., Mochizuki, Y., Kawai, K., Ikeda, Y., Araki, N., Skolnik, E.Y., Taguchi, T., and Arai, H. (2014). Sequential breakdown of 3-phosphorylated phosphoinositides is essential for the completion of macropinocytosis. Proc. Natl. Acad.

Sci. U. S. A. *111*, E978-87.

Magenau, A., Benzing, C., Proschogo, N., Don, A.S., Hejazi, L., Karunakaran, D., Jessup, W., and Gaus, K. (2011). Phagocytosis of IgG-coated polystyrene beads by macrophages induces and requires high membrane order. Traffic *12*, 1730–1743.

McDonald, G., Deepak, S., Miguel, L., Hall, C.J., Isenberg, D.A., Magee, A.I., Butters, T., and Jury, E.C. (2014). Normalizing glycosphingolipids restores function in CD4+ T cells from lupus patients. J Clin Invest *124*, 712–724.

McGranahan, N., Swanton, C., Zhang, J., Wedge, D.C., Song, X., Zhang, J., Seth, S., Chow, C.W., Cao, Y., Gumbs, C., et al. (2015). Biological and Therapeutic Impact of Intratumor Heterogeneity in Cancer Evolution. Cancer Cell *27*, 15–26.

Micchelli, C.A., and Perrimon, N. (2006). Evidence that stem cells reside in the adult Drosophila midgut epithelium. Nature *439*, 475–479.

Miguel, L., Owen, D.M., Lim, C., Liebig, C., Evans, J., Magee, A.I., and Jury, E.C. (2011). Primary human CD4+ T cells have diverse levels of membrane lipid order that correlate with their function. J. Immunol. *186*, 3505–3516.

Mochizuki, N., Yamashita, S., Kurokawa, K., Ohba, Y., Nagai, T., Miyawaki, A., and Matsuda, M. (2001). Spatio-temporal images of growth-factor-induced activation of Ras and Rap1. Nature *411*, 1065–1068.

Modest, D.P., Camaj, P., Heinemann, V., Schwarz, B., Jung, A., Laubender, R.P., Gamba, S., Haertl, C., Stintzing, S., Primo, S., et al. (2013). KRAS allel-specific activity

of sunitinib in an isogenic disease model of colorectal cancer. J Cancer Res Clin Oncol *139*, 953–961.

Mohammed, A., Janakiram, N.B., Brewer, M., Duff, A., Lightfoot, S., Brush, R.S., Anderson, R.E., and Rao, C. V (2012). Endogenous n-3 polyunsaturated fatty acids delay progression of pancreatic ductal adenocarcinoma in Fat-1-p48(Cre/+)-LSL-Kras(G12D/+) mice. Neoplasia *14*, 1249–1259.

Moissoglu, K., Kiessling, V., Wan, C., Hoffman, B.D., Norambuena, A., Tamm, L.K., and Schwartz, M.A. (2014). Regulation of Rac1 translocation and activation by membrane domains and their boundaries. J. Cell Sci. *127*, 2565–2576.

Monk, J.M., Turk, H.F., Fan, Y.-Y., Callaway, E., Weeks, B., Yang, P., McMurray, D.N., and Chapkin, R.S. (2014). Antagonizing Arachidonic Acid-Derived Eicosanoids Reduces Inflammatory Th17 and Th1 Cell-Mediated Inflammation and Colitis Severity. Mediators Inflamm. *2014*, 1–14.

Montero, J., Morales, A., Llacuna, L., Lluis, J.M., Terrones, O., Basanez, G., Antonsson, B., Prieto, J., Garcia-Ruiz, C., Colell, A., et al. (2008). Mitochondrial cholesterol contributes to chemotherapy resistance in hepatocellular carcinoma. Cancer Res *68*, 5246–5256.

Morone, N. (2010). Freeze-etch electron tomography for the plasma membrane interface. Methods Mol. Biol. *657*, 275–286.

Morone, N., Fujiwara, T., Murase, K., Kasai, R.S., Ike, H., Yuasa, S., Usukura, J., and

Kusumi, A. (2006). Three-dimensional reconstruction of the membrane skeleton at the plasma membrane interface by electron tomography. J. Cell Biol. *174*, 851–862.

Muller, P.Y., and Milton, M.N. (2012). The determination and interpretation of the therapeutic index in drug development. Nat. Rev. Drug Discov. *11*, 751–761.

Muratcioglu, S., Chavan, T.S., Freed, B.C., Jang, H., Khavrutskii, L., Freed, R.N., Dyba, M.A., Stefanisko, K., Tarasov, S.G., Gursoy, A., et al. (2015). GTP-Dependent K-Ras Dimerization. Structure *23*, 1325–1335.

Najumudeen, A.K., Jaiswal, A., Lectez, B., Oetken-Lindholm, C., Guzmán, C., Siljamäki, E., Posada, I.M.D., Lacey, E., Aittokallio, T., and Abankwa, D. (2016). Cancer stem cell drugs target K-ras signaling in a stemness context. Oncogene *35*, 5248–5262.

Nan, X., Tamgüney, T.M., Collisson, E.A., Lin, L.-J., Pitt, C., Galeas, J., Lewis, S., Gray, J.W., McCormick, F., and Chu, S. (2015). Ras-GTP dimers activate the Mitogen-Activated Protein Kinase (MAPK) pathway. Proc. Natl. Acad. Sci. U. S. A. *112*, 7996–8001.

Navarro-Lérida, I., Sánchez-Perales, S., Calvo, M., Rentero, C., Zheng, Y., Enrich, C., and Del Pozo, M.A. (2012). A palmitoylation switch mechanism regulates Rac1 function and membrane organization. EMBO J. *31*, 534–551.

Nielsen, J. (2009). Systems biology of lipid metabolism: from yeast to human. FEBS Lett *583*, 3905–3913.

Nussinov, R., Jang, H., and Tsai, C.-J. (2014). Oligomerization and nanocluster organization render specificity. Biol. Rev. Camb. Philos. Soc.

Ohlstein, B., and Spradling, A. (2006). The adult Drosophila posterior midgut is maintained by pluripotent stem cells. Nature *439*, 470–474.

Owen, D.M., Lanigan, P.M.P., Dunsby, C., Munro, I., Grant, D., Neil, M.A.A., French, P.M.W., and Magee, A.I. (2006). Fluorescence lifetime imaging provides enhanced contrast when imaging the phase-sensitive dye di-4-ANEPPDHQ in model membranes and live cells. Biophys. J. *90*, L80-2.

Owen, D.M., Rentero, C., Magenau, A., Abu-Siniyeh, A., and Gaus, K. (2012a). Quantitative imaging of membrane lipid order in cells and organisms. Nat. Protoc. *7*, 24–35.

Owen, D.M., Williamson, D.J., Magenau, A., and Gaus, K. (2012b). Sub-resolution lipid domains exist in the plasma membrane and regulate protein diffusion and distribution. Nat Commun *3*, 1256.

Pagler, T.A., Wang, M., Mondal, M., Murphy, A.J., Westerterp, M., Moore, K.J., Maxfield, F.R., and Tall, A.R. (2011). Deletion of ABCA1 and ABCG1 impairs macrophage migration because of increased Rac1 signaling. Circ. Res. *108*, 194–200.

Patra, S.K. (2008). Dissecting lipid raft facilitated cell signaling pathways in cancer. Biochim Biophys Acta *1785*, 182–206.

Pegorier, J.P., Le May, C., Girard, J., Pégorier, J.-P., Le May, C., and Girard, J. (2004).

Control of gene expression by fatty acids. J Nutr *134*, 2444S–2449S.

Phillips, R., Ursell, T., Wiggins, P., and Sens, P. (2009). Emerging roles for lipids in shaping membrane-protein function. Nature *459*, 379–385.

Phipps, A.I., Buchanan, D.D., Makar, K.W., Win, A.K., Baron, J.A., Lindor, N.M., Potter, J.D., and Newcomb, P.A. (2013). KRAS-mutation status in relation to colorectal cancer survival: the joint impact of correlated tumour markers. Br J Cancer *108*, 1757–1764.

Piazzi, G., D'Argenio, G., Prossomariti, A., Lembo, V., Mazzone, G., Candela, M., Biagi, E., Brigidi, P., Vitaglione, P., Fogliano, V., et al. (2014). Eicosapentaenoic acid free fatty acid prevents and suppresses colonic neoplasia in colitis-associated colorectal cancer acting on Notch signaling and gut microbiota. Int J Cancer *135*, 2004–2013.

Piper, M.D.W., Blanc, E., Leitão-Gonçalves, R., Yang, M., He, X., Linford, N.J., Hoddinott, M.P., Hopfen, C., Soultoukis, G. a, Niemeyer, C., et al. (2014). A holidic medium for Drosophila melanogaster. Nat. Methods *11*, 100–105.

Plowman, S.J., Muncke, C., Parton, R.G., and Hancock, J.F. (2005). H-ras, K-ras, and inner plasma membrane raft proteins operate in nanoclusters with differential dependence on the actin cytoskeleton. Proc Natl Acad Sci U S A *102*, 15500–15505.

Plowman, S.J., Berry, R.L., Bader, S.A., Luo, F., Arends, M.J., Harrison, D.J., Hooper, M.L., and Patek, C.E. (2006). K-ras 4A and 4B are co-expressed widely in human tissues, and their ratio is altered in sporadic colorectal cancer. J. Exp. Clin. Cancer Res.

25, 259–267.

Podkalicka, J., Biernatowska, A., Majkowski, M., Grzybek, M., and Sikorski, A.F. (2015). MPP1 as a Factor Regulating Phase Separation in Giant Plasma Membrane-Derived Vesicles. Biophys. J. *108*, 2201–2211.

Porat-Shliom, N., Kloog, Y., and Donaldson, J.G. (2007). A Unique Platform for H-Ras Signaling Involving Clathrin-independent Endocytosis. Mol. Biol. Cell *19*, 765–775.

Posada, I.M.D., Serulla, M., Zhou, Y., Oetken-Lindholm, C., Abankwa, D., and Lectez, B. (2016). ASPP2 Is a Novel Pan-Ras Nanocluster Scaffold. PLoS One *11*, e0159677.

Pot, G.K., Geelen, A., van Heijningen, E.M., Siezen, C.L., van Kranen, H.J., and Kampman, E. (2008). Opposing associations of serum n-3 and n-6 polyunsaturated fatty acids with colorectal adenoma risk: an endoscopy-based case-control study. Int J Cancer *123*, 1974–1977.

Pot, G.K., Majsak-Newman, G., Geelen, A., Harvey, L.J., Nagengast, F.M., Witteman, B.J.M., Meeberg, P.C. Van De, Timmer, R., Tan, A., Wahab, P.J., et al. (2009). Fish consumption and markers of colorectal cancer risk: a multicenter randomized controlled trial. Am J Clin Nutr *90*, 354–361.

Prentice, R.L., and Sheppard, L. (1990). Dietary fat and cancer: consistency of the epidemiologic data, and disease prevention that may follow from a practical reduction in fat consumption. Cancer Causes Control *1*, 81–109.

Prior, I.A., and Hancock, J.F. (2001). Compartmentalization of Ras proteins. J. Cell Sci.

114, 1603–1608.

Prior, I.A., and Hancock, J.F. (2012). Ras trafficking, localization and compartmentalized signalling. Semin. Cell Dev. Biol. *23*, 145–153.

Prior, I.A., Muncke, C., Parton, R.G., and Hancock, J.F. (2003). Direct visualization of Ras proteins in spatially distinct cell surface microdomains. J Cell Biol *160*, 165–170.

Prior, I.A., Lewis, P.D., and Mattos, C. (2012). A comprehensive survey of Ras mutations in cancer. Cancer Res *72*, 2457–2467.

Quail, D.F., and Joyce, J.A. (2013). Microenvironmental regulation of tumor progression and metastasis. Nat. Med. *19*, 1423–1437.

Raghavan, V., Vijayaraghavalu, S., Peetla, C., Yamada, M., Morisada, M., and Labhasetwar, V. (2015). Sustained Epigenetic Drug Delivery Depletes Cholesterol-Sphingomyelin Rafts from Resistant Breast Cancer Cells, Influencing Biophysical Characteristics of Membrane Lipids. Langmuir *31*, 11564–11573.

Raghunathan, K., Ahsan, A., Ray, D., Nyati, M.K., Veatch, S.L.S., Kelland, L., Gottesman, M., Kawaiz, K., Kamatani, N., George, E., et al. (2015). Membrane Transition Temperature Determines Cisplatin Response. PLoS One *10*, e0140925.

Rebillard, A., Tekpli, X., Meurette, O., Sergent, O., LeMoigne-Muller, G., Vernhet, L., Gorria, M., Chevanne, M., Christmann, M., Kaina, B., et al. (2007). Cisplatin-induced apoptosis involves membrane fluidification via inhibition of NHE1 in human colon cancer cells. Cancer Res *67*, 7865–7874.

Reddy, B.S., Burill, C., and Rigotty, J. (1991). Effect of diets high in omega-3 and omega-6 fatty acids on initiation and postinitiation stages of colon carcinogenesis. Cancer Res *51*, 487–491.

Reddy, B.S., Patlolla, J.M., Simi, B., Wang, S.H., and Rao, C. V (2005). Prevention of colon cancer by low doses of celecoxib, a cyclooxygenase inhibitor, administered in diet rich in omega-3 polyunsaturated fatty acids. Cancer Res *65*, 8022–8027.

Rees, D., Miles, E.A., Banerjee, T., Wells, S.J., Roynette, C.E., Wahle, K.W., and Calder, P.C. (2006). Dose-related effects of eicosapentaenoic acid on innate immune function in healthy humans: a comparison of young and older men. Am. J. Clin. Nutr. *83*, 331–342.

Rego, E.H., Shao, L., Macklin, J.J., Winoto, L., Johansson, G.A., Kamps-Hughes, N., Davidson, M.W., and Gustafsson, M.G.L. (2012). Nonlinear structured-illumination microscopy with a photoswitchable protein reveals cellular structures at 50-nm resolution. Proc. Natl. Acad. Sci. U. S. A. *109*, E135-43.

Rockett, B.D., Teague, H., Harris, M., Melton, M., Williams, J., Wassall, S.R., and Shaikh, S.R. (2012). Fish oil increases raft size and membrane order of B cells accompanied by differential effects on function. J Lipid Res *53*, 674–685.

Rogers, K.R., Kikawa, K.D., Mouradian, M., Hernandez, K., McKinnon, K.M., Ahwah, S.M., and Pardini, R.S. (2010). Docosahexaenoic acid alters epidermal growth factor receptor-related signaling by disrupting its lipid raft association. Carcinogenesis *31*,

1523–1530.

Rohrig, F., and Schulze, A. (2016). The multifaceted roles of fatty acid synthesis in cancer. Nat Rev Cancer *16*, 732–749.

Russell, D.W., Hirata, R.K., and Inoue, N. (2002). Validation of AAV-mediated gene targeting. Nat Biotechnol *20*, 658.

Sahl, S.J., Leutenegger, M., Hell, S.W., and Eggeling, C. (2014). High-Resolution Tracking of Single-Molecule Diffusion in Membranes by Confocalized and Spatially Differentiated Fluorescence Photon Stream Recording. ChemPhysChem *15*, 771–783.

Salloum, D., Mukhopadhyay, S., Tung, K., Polonetskaya, A., and Foster, D.A. (2014). Mutant ras elevates dependence on serum lipids and creates a synthetic lethality for rapamycin. Mol. Cancer Ther. *13*, 733–741.

Saw, C.L.L., Huang, Y., and Kong, A.-N.N. (2010). Synergistic anti-inflammatory effects of low doses of curcumin in combination with polyunsaturated fatty acids: docosahexaenoic acid or eicosapentaenoic acid. Biochem Pharmacol *79*, 421–430.

Schonberg, S.A., Lundemo, A.G., Fladvad, T., Holmgren, K., Bremseth, H., Nilsen, A., Gederaas, O., Tvedt, K.E., Egeberg, K.W., and Krokan, H.E. (2006). Closely related colon cancer cell lines display different sensitivity to polyunsaturated fatty acids, accumulate different lipid classes and downregulate sterol regulatory element-binding protein 1. FEBS J *273*, 2749–2765.

Seo, J., Barhoumi, R., Johnson, A.E., Lupton, J.R., and Chapkin, R.S. (2006).

Docosahexaenoic acid selectively inhibits plasma membrane targeting of lipidated proteins. FASEB J *20*, 770–772.

Serhan, C.N. (2014). Pro-resolving lipid mediators are leads for resolution physiology. Nature *510*, 92–101.

Sevcsik, E., and Schütz, G.J. (2015). With or without rafts? Alternative views on cell membranes. Bioessays.

Sezgin, E. (2017). Super-resolution optical microscopy for studying membrane structure and dynamics. J. Phys. Condens. Matter *29*, 273001.

Sezgin, E., Kaiser, H.-J.J., Baumgart, T., Schwille, P., Simons, K., and Levental, I. (2012). Elucidating membrane structure and protein behavior using giant plasma membrane vesicles. Nat Protoc *7*, 1042–1051.

Sezgin, E., Sadowski, T., and Simons, K. (2014). Measuring Lipid Packing of Model and Cellular Membranes with Environment Sensitive Probes. Langmuir *30*, 8160–8166.

Sezgin, E., Gutmann, T., Buhl, T., Dirkx, R., Grzybek, M., Coskun, Ü., Solimena, M., Simons, K., Levental, I., and Schwille, P. (2015). Adaptive lipid packing and bioactivity in membrane domains. PLoS One *10*, e0123930.

Sezgin, E., Levental, I., Mayor, S., and Eggeling, C. (2017). The mystery of membrane organization: composition, regulation and roles of lipid rafts. Nat. Rev. Mol. Cell Biol. *18*, 361–374.

Shabardina, V., Kramer, C., Gerdes, B., Braunger, J., Cordes, A., Schäfer, J., Mey, I., Grill, D., Gerke, V., and Steinem, C. (2016). Mode of Ezrin-Membrane Interaction as a Function of PIP 2 Binding and Pseudophosphorylation. Biophys. J. *110*, 2710–2719.

Shaikh, S.R., Dumaual, A.C., Castillo, A., LoCascio, D., Siddiqui, R.A., Stillwell, W., and Wassall, S.R. (2004). Oleic and docosahexaenoic acid differentially phase separate from lipid raft molecules: a comparative NMR, DSC, AFM, and detergent extraction study. Biophys J *87*, 1752–1766.

Shaikh, S.R., Locascio, D.S., Soni, S.P., Wassall, S.R., and Stillwell, W. (2009). Oleic- and docosahexaenoic acid-containing phosphatidylethanolamines differentially phase separate from sphingomyelin. Biochim Biophys Acta *1788*, 2421–2426.

Shira Neuman-Silberberg, F., Schejter, E., Michael Hoffmann, F., and Shilo, B.-Z. (1984). The drosophila ras oncogenes: Structure and nucleotide sequence. Cell *37*, 1027–1033.

Siddiqui, R.A., Harvey, K.A., Walker, C., Altenburg, J., Xu, Z., Terry, C., Camarillo, I., Jones-Hall, Y., and Mariash, C. (2013). Characterization of synergistic anti-cancer effects of docosahexaenoic acid and curcumin on DMBA-induced mammary tumorigenesis in mice. BMC Cancer *13*, 418.

Siegel, R.L., Miller, K.D., and Jemal, A. (2017). Cancer statistics, 2017. CA. Cancer J. Clin. *67*, 7–30.

Singh, P., Saxena, R., Srinivas, G., Pande, G., and Chattopadhyay, A. (2013).

Cholesterol biosynthesis and homeostasis in regulation of the cell cycle. PLoS One *8*, e58833.

Skarke, C., Alamuddin, N., Lawson, J.A., Ferguson, J.F., Reilly, M.P., and FitzGerald, G.A. (2015). Bioactive products formed in humans from fish oils. J. Lipid Res. *56*, 1808–1820.

Smith, B., and Land, H. (2012). Anticancer activity of the cholesterol exporter ABCA1 gene. Cell Rep *2*, 580–590.

Smith, G., Carey, F.A., Beattie, J., Wilkie, M.J. V., Lightfoot, T.J., Coxhead, J., Garner, R.C., Steele, R.J.C., and Wolf, C.R. (2002). Mutations in APC, Kirsten-ras, and p53--alternative genetic pathways to colorectal cancer. Proc. Natl. Acad. Sci. *99*, 9433–9438.

Sorensen, L.S., Rasmussen, H.H., Aardestrup, I. V, Thorlacius-Ussing, O., Lindorff-Larsen, K., Schmidt, E.B., and Calder, P.C. (2014). Rapid incorporation of omega-3 fatty acids into colonic tissue after oral supplementation in patients with colorectal cancer: a randomized, placebo-controlled intervention trial. JPEN J Parenter Enter. Nutr *38*, 617–624.

Sousa, T., Castro, R.E., Pinto, S.N., Coutinho, A., Lucas, S.D., Moreira, R., Rodrigues, C.M.P., Prieto, M., and Fernandes, F. (2015). Deoxycholic acid modulates cell death signaling through changes in mitochondrial membrane properties. J. Lipid Res. *56*, 2158–2171.

Spector, A.A., and Yorek, M.A. (1985). Membrane lipid composition and cellular

function. J. Lipid Res. *26*, 1015–1035.

Spite, M., Claria, J., Serhan, C.N., Clària, J., and Serhan, C.N. (2014). Resolvins, specialized proresolving lipid mediators, and their potential roles in metabolic diseases. Cell Metab *19*, 21–36.

Stephen, A.G., Esposito, D., Bagni, R.K., and McCormick, F. (2014). Dragging ras back in the ring. Cancer Cell *25*, 272–281.

Stillwell, W., and Wassall, S.R. (2003). Docosahexaenoic acid: Membrane properties of a unique fatty acid. Chem. Phys. Lipids *126*, 1–27.

Stolze, B., Reinhart, S., Bulllinger, L., Fröhling, S., and Scholl, C. (2015). Comparative analysis of KRAS codon 12, 13, 18, 61, and 117 mutations using human MCF10A isogenic cell lines. Sci. Rep. *5*, 8535.

Stone, M.B., Shelby, S.A., and Veatch, S.L. (2017). Super-Resolution Microscopy: Shedding Light on the Cellular Plasma Membrane. Chem. Rev. *117*.

Strobel, C., Jahreis, G., and Kuhnt, K. (2012). Survey of n-3 and n-6 polyunsaturated fatty acids in fish and fish products. Lipids Heal. Dis *11*, 144.

Strouch, M.J., Ding, Y., Salabat, M.R., Melstrom, L.G., Adrian, K., Quinn, C., Pelham, C., Rao, S., Adrian, T.E., Bentrem, D.J., et al. (2011). A high omega-3 fatty acid diet mitigates murine pancreatic precancer development. J Surg Res *165*, 75–81.

Tian, T., Harding, A., Inder, K., Plowman, S., Parton, R.G., and Hancock, J.F. (2007).

Plasma membrane nanoswitches generate high-fidelity Ras signal transduction. Nat Cell Biol *9*, 905–914.

Tisza, M.J., Zhao, W., Fuentes, J.S.R., Prijic, S., Chen, X., Levental, I., and Chang, J.T. (2014). Motility and stem cell properties induced by the epithelial-mesenchymal transition require destabilization of lipid rafts. Oncotarget.

Tsai, F.D., Lopes, M.S., Zhou, M., Court, H., Ponce, O., Fiordalisi, J.J., Gierut, J.J., Cox, A.D., Haigis, K.M., and Philips, M.R. (2015). K-Ras4A splice variant is widely expressed in cancer and uses a hybrid membrane-targeting motif. Proc. Natl. Acad. Sci. U. S. A. *112*, 779–784.

Turk, H.F., Barhoumi, R., and Chapkin, R.S. (2012). Alteration of EGFR spatiotemporal dynamics suppresses signal transduction. PLoS One *7*, e39682.

Turk, H.F., Monk, J.M., Fan, Y.-Y.Y., Callaway, E.S., Weeks, B., and Chapkin, R.S. (2013). Inhibitory effects of omega-3 fatty acids on injury-induced epidermal growth factor receptor transactivation contribute to delayed wound healing. Am J Physiol Cell Physiol *304*, C905-17.

Ueland, P.M., Refsum, H., Male, R., and Lillehaug, J.R. (1986). Disposition of endogenous homocysteine by mouse fibroblast C3H/10T1/2 Cl 8 and the chemically transformed C3H/10T1/2 MCA Cl 16 cells following methotrexate exposure. J Natl Cancer Inst *77*, 283–289.

Vargas, A.J., and Thompson, P.A. (2012). Diet and nutrient factors in colorectal cancer

risk. Nutr Clin Pr. *27*, 613–623.

Vartanian, S., Bentley, C., Brauer, M.J., Li, L., Shirasawa, S., Sasazuki, T., Kim, J.S., Haverty, P., Stawiski, E., Modrusan, Z., et al. (2013). Identification of mutant K-Ras-dependent phenotypes using a panel of isogenic cell lines. J Biol Chem *288*, 2403–2413.

Vasan, N., Boyer, J.L., and Herbst, R.S. (2014). A RAS renaissance: emerging targeted therapies for KRAS-mutated non-small cell lung cancer. Clin Cancer Res *20*, 3921–3930.

Vaughan, V.C., Hassing, M.R., and Lewandowski, P.A. (2013). Marine polyunsaturated fatty acids and cancer therapy. Br J Cancer *108*, 486–492.

Verstraeten, S. V, Jaggers, G.K., Fraga, C.G., and Oteiza, P.I. (2013). Procyanidins can interact with Caco-2 cell membrane lipid rafts: involvement of cholesterol. Biochim. Biophys. Acta *1828*, 2646–2653.

Verstraeten, S. V, Fraga, C.G., and Oteiza, P.I. (2015). Interactions of flavan-3-ols and procyanidins with membranes: mechanisms and the physiological relevance. Food Funct. *6*, 32–41.

Wallace, T.C., Blumberg, J.B., Johnson, E.J., and Shao, A. (2015). Dietary Bioactives : Establishing a Scienti fi c Framework for Recommended Intakes. Adv. Nutr. *6*, 1–4.

Walsh, A.B., and Bar-Sagi, D. (2001). Differential Activation of the Rac Pathway by Ha-Ras and K-Ras. J. Biol. Chem. *276*, 15609–15615.

Wang, C., Yu, Y., and Regen, S.L. (2017). Lipid Raft Formation: Key Role of Polyunsaturated Phospholipids. Angew. Chemie Int. Ed. *56*, 1639–1642.

Wang, Y.Y., Gao, J., Guo, X., Tong, T., Shi, X., Li, L., Qi, M., Wang, Y.Y., Cai, M., Jiang, J., et al. (2014). Regulation of EGFR nanocluster formation by ionic protein-lipid interaction. Cell Res *24*, 959–976.

Watson, A.J.M., and Collins, P.D. (2011). Colon cancer: a civilization disorder. Dig Dis *29*, 222–228.

Wei, Z., Wang, W., Chen, J., Yang, D., Yan, R., and Cai, Q. (2014). A prospective, randomized, controlled study of omega-3 fish oil fat emulsion-based parenteral nutrition for patients following surgical resection of gastric tumors. Nutr J *13*, 25.

West, N.J., Clark, S.K., Phillips, R.K.S., Hutchinson, J.M., Leicester, R.J., Belluzzi, A., and Hull, M.A. (2010). Eicosapentaenoic acid reduces rectal polyp number and size in familial adenomatous polyposis. Gut *59*, 918–925.

Whitehead, R.H., and Robinson, P.S. (2009). Establishment of conditionally immortalized epithelial cell lines from the intestinal tissue of adult normal and transgenic mice. Am J Physiol Gastrointest Liver Physiol *296*, G455-60.

Williams, J.A., Batten, S.E., Harris, M., Rockett, B.D., Shaikh, S.R., Stillwell, W., and Wassall, S.R. (2012). Docosahexaenoic and eicosapentaenoic acids segregate differently between raft and nonraft domains. Biophys J *103*, 228–237.

Williamson, G., and Manach, C. (2005). Bioavailability and bioefficacy of polyphenols

in humans. II. Review of 93 intervention studies. Am. J. Clin. Nutr. *81*, 243S–255S.

Wittinghofer, A., and Herrmann, C. (1995). Ras-effector interactions, the problem of specificity. FEBS Lett. *369*, 52–56.

Wu, S., Feng, B., Li, K., Zhu, X., Liang, S., Liu, X., Han, S., Wang, B., Wu, K., Miao, D., et al. (2012). Fish Consumption and Colorectal Cancer Risk in Humans: A Systematic Review and Meta-analysis. Am. J. Med. *125*, 551–559.e5.

Xu, K., Babcock, H.P., and Zhuang, X. (2012). Dual-objective STORM reveals three-dimensional filament organization in the actin cytoskeleton. Nat. Methods *9*, 185–188.

Yang, Y., Chaerkady, R., Beer, M.A., Mendell, J.T., and Pandey, A. (2009). Identification of miR-21 targets in breast cancer cells using a quantitative proteomic approach. Proteomics *9*, 1374–1384.

Yates, C.M., Calder, P.C., and Ed Rainger, G. (2014). Pharmacology and therapeutics of omega-3 polyunsaturated fatty acids in chronic inflammatory disease. Pharmacol Ther *141*, 272–282.

Yi, J.S., Mun, D.G., Lee, H., Park, J.S., Lee, J.W., Lee, J.S., Kim, S.J., Cho, B.R., Lee, S.W., and Ko, Y.G. (2013). PTRF/cavin-1 is essential for multidrug resistance in cancer cells. J Proteome Res *12*, 605–614.

Yog, R., Barhoumi, R., McMurray, D.N., and Chapkin, R.S. (2010). n-3 polyunsaturated fatty acids suppress mitochondrial translocation to the immunologic synapse and modulate calcium signaling in T cells. J. Immunol. *184*, 5865–5873.

Zalba, S., and ten Hagen, T.L.M. (2017). Cell membrane modulation as adjuvant in cancer therapy. Cancer Treat. Rev. *52*, 48–57.

Zarubica, A., Plazzo, A.P., Stöckl, M., Trombik, T., Hamon, Y., Müller, P., Pomorski, T., Herrmann, A., and Chimini, G. (2009). Functional implications of the influence of ABCA1 on lipid microenvironment at the plasma membrane: a biophysical study. FASEB J. *23*, 1775–1785.

Zech, T., Ejsing, C.S., Gaus, K., de Wet, B., Shevchenko, A., Simons, K., and Harder, T. (2009). Accumulation of raft lipids in T-cell plasma membrane domains engaged in TCR signalling. EMBO J *28*, 466–476.

Zhang, M.S., Sandouk, A., and Houtman, J.C.D. (2016). Glycerol Monolaurate (GML) inhibits human T cell signaling and function by disrupting lipid dynamics. Sci. Rep. *6*, 30225.

Zhou, Y., and Hancock, J.F. (2015). Ras nanoclusters: Versatile lipid-based signaling platforms. Biochim. Biophys. Acta *1853*, 841–849.

Zhou, Y., and Hancock, J.F. (2017). Chapter Two – Ras Proteolipid Nanoassemblies on the Plasma Membrane Sort Lipids With High Selectivity. In Advances in Biomembranes and Lipid Self-Assembly, pp. 41–62.

Zhou, Y., Plowman, S.J., Lichtenberger, L.M., and Hancock, J.F. (2010). The anti-inflammatory drug indomethacin alters nanoclustering in synthetic and cell plasma membranes. J. Biol. Chem. *285*, 35188–35195.

Zhou, Y., Cho, K.-J., Plowman, S.J., and Hancock, J.F. (2012). Nonsteroidal anti-inflammatory drugs alter the spatiotemporal organization of Ras proteins on the plasma membrane. J. Biol. Chem. *287*, 16586–16595.

Zhou, Y., Maxwell, K.N., Sezgin, E., Lu, M., Liang, H., Hancock, J.F., Dial, E.J., Lichtenberger, L.M., and Levental, I. (2013). Bile acids modulate signaling by functional perturbation of plasma membrane domains. J. Biol. Chem. *288*, 35660–35670.

Zhou, Y., Liang, H., Rodkey, T., Ariotti, N., Parton, R.G., and Hancock, J.F. (2014). Signal integration by lipid-mediated spatial cross talk between Ras nanoclusters. Mol Cell Biol *34*, 862–876.

Zhou, Y., Wong, C.-O., Cho, K., van der Hoeven, D., Liang, H., Thakur, D.P., Luo, J., Babic, M., Zinsmaier, K.E., Zhu, M.X., et al. (2015). SIGNAL TRANSDUCTION. Membrane potential modulates plasma membrane phospholipid dynamics and K-Ras signaling. Science *349*, 873–876.

Zhou, Y., Prakash, P., Liang, H., Cho, K.-J., Gorfe, A.A., and Hancock, J.F. (2017). Lipid-Sorting Specificity Encoded in K-Ras Membrane Anchor Regulates Signal Output. Cell *168*, 239–251.e16.

Zidovetzki, R., and Levitan, I. (2007). Use of cyclodextrins to manipulate plasma membrane cholesterol content: Evidence, misconceptions and control strategies. Biochim. Biophys. Acta - Biomembr. *1768*, 1311–1324.